Pesticides Research Nr. 66 2003
Bekæmpelsesmiddelforskning fra Miljøstyrelsen

Dry Deposition and Spray Drift of Pesticides to Nearby Water Bodies

Willem Asman and Andreas Jørgensen
National Environmental Research Institute

Peter Kryger Jensen
Danish Institute of Agricultural Sciences

Danish Environmental Protection Agency
Danish Ministry of the Environment

Table of contents

Preface

The integrated project

The project ”Model Based Tool for Evaluation of Exposure and Effects of Pesticides in Surface Water”, funded by the Danish Environmental Protection Agency (DEPA), was initiated in 1998. The aim of the project was:

> To develop a model-based tool (PestSurf) for evaluation of risk related to pesticide exposure of surface water. The tool must be directly applicable by the Danish Environmental Protection Agency in their approval procedure. As part of this goal, the project had to:

- Develop of guidelines for evaluation of mesocosm experiments based on a system-level perspective of the fresh water environment
- To develop models for deposition of pesticides on vegetation and soil.
- To estimate the deposition of pesticides from the air to the aquatic environment.

The project, called ”Pesticides in Surface Water”, consisted of seven subprojects with individual objectives. The sub-projects are listed in Table 1.

Table 1 Sub-projects of ”Pesticides in Surface Water”
Tabel 1 Oversigt over delprojekter i ”Pesticider i overfladevand”

	Title	Participating institutions
A	Development and validation of a model for evaluation of pesticide exposure	DHI Water & Environment (DHI)
B	Investigation of the importance of plant cover for the deposition of pesticides on soil	Danish Institute of Agricultural Sciences (DIAS)
C	Estimation of the airborne transport of pesticides to surface water by dry deposition and spray drift	National Environmental Research Institute (NERI) Danish Institute of Agricultural Sciences (DIAS)
D	Facilitated transport	DHI Water & Environment
E	Development of an operational and validated model for pesticide transport and fate in surface water	DHI Water & Environment National Environmental Research Institute
F	Mesocosm	DHI Water & Environment National Environmental Research Institute (NERI)
G	Importance of different transport routes in relation to occurrence and effects of pesticides in streams	National Environmental Research Institute (NERI) County of Funen County of Northern Jutland

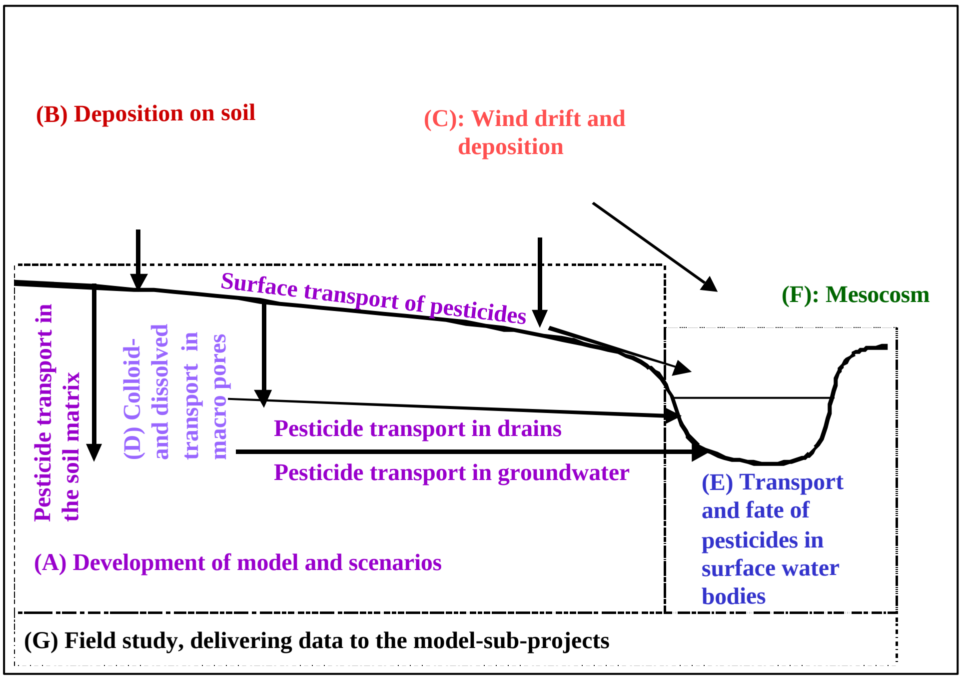

Figure 1. Links between the different sub-projects. The sub-projects are placed on a cross-section of the catchment to illustrate interactions
Figur 1. Sammenhæng mellem delprojekterne. Delprojekterne er placeret på et tværsnit af et opland for at illustrere interaktionerne

Figure 1 describes the relationship between the sub-projects. Sub-project 1 models the upland part of the catchment, while sub-project 5 models surface water bodies. Sub-project 8 delivers data to both modelling projects. Sub-project 2 and 3 develop process descriptions for spray drift, dry deposition and deposition onto soils. Sub-project 4 builds and tests a module for calculation of colloid transport of pesticide in soil. The module is an integrated part of the upland model. Sub-project 6 has mainly concentrated on interpretation of mesocosm-studies. However, it contains elements of possible links between exposure and biological effects.

The reports produced by the project are:

- Styczen, M., Petersen, S., Christensen, M., Jessen, O.Z., Rasmussen, D., Andersen, M.B. and Sørensen, P.B. (2002): Calibration of models describing pesticide fate and transport in Lillebæk and Odder Bæk Catchment. - Ministry of Environment, Danish Environmental Protection Agency, Pesticides Research No. 62.

- Styczen, M., Petersen, S. and Sørensen, P.B. (2002): Scenarios and model describing fate and transport of pesticides in surface water for Danish conditions. - Ministry of Environment, Danish Environmental Protection Agency, Pesticides Research No. 63.

- Styczen, M., Petersen, S., Olsen, N.K. and Andersen, M.B. (2002): Technical documentation of PestSurf, a model describing fate and transport of pesticides in surface water for Danish Conditions. - Ministry of Environment, Danish Environmental Protection Agency, Pesticides Research No. 64.

- Jensen, P.K. and Spliid, N.H. (2002): Deposition of pesticides on the soil surface. - Ministry of Environment, Danish Environmental Protection Agency, Pesticides Research No. 65.

- Asman, W.A.H., Jørgensen, A. and Jensen, P.K. (2002): Dry deposition and spray drift of pesticides to nearby water bodies. - Ministry of Environment, Danish Environmental Protection Agency, Pesticides Research No. 66.

- Holm, J., Petersen, C., and Koch, C. (2002): Facilitated transport of pesticides. - Ministry of Environment, Danish Environmental Protection Agency, Pesticides Research No. 67.

- Helweg, C., Mogensen, B.B., Sørensen, P.B., Madsen, T., Rasmussen, D. and Petersen, S. (2002): Fate of pesticides in surface waters, Laboratory and Field Experiments. Ministry of Environment, Danish Environmental Protection Agency, Pesticides Research No. 68.

- Møhlenberg, F., Petersen, S., Gustavson, K., Lauridsen, T. and Friberg, N. (2001): Guidelines for evaluating mesocosm experiments in connection with the approval procedure. - Ministry of Environment and Energy, Danish Environmental Protection Agency, Pesticides Research No. 56.

- Iversen, H.L., Kronvang, B., Vejrup, K., Mogensen, B.B., Hansen, A.M. and Hansen, L.B. (2002): Pesticides in streams and subsurface drainage water within two arable catchments in Denmark: Pesticide application, concentration, transport and fate. - Ministry of Environment, Danish Environmental Protection Agency, Pesticides Research No. 69.

The original thoughts behind the project are described in detail in the report ”Model Based Tool for Evaluation of Exposure and Effects of Pesticides in Surface Water”, Inception Report – J. nr. M 7041-0120, by DHI, VKI, NERI, DIAS and County of Funen, December, 1998.

The project was overseen by a steering committee. The members have made valuable contributions to the project. The committee consisted of:

- Inge Vibeke Hansen, Danish Environmental Protection Agency, chairman 1998-mid 2000.
- Jørn Kirkegaard, Danish Environmental Protection Agency (chairman mid-2000-2002).
- Christian Deibjerg Hansen, Danish Environmental Protection Agency
- Heidi Christiansen Barlebo, The Geological Survey of Denmark and Greenland.
- Mogens Erlandsen, University of Aarhus
- Karl Henrik Vestergaard, Syngenta Crop Protection A/S.
- Valery Forbes, Roskilde University
- Lars Stenvang Hansen, Danish Agricultural Advisory Centre (1998-2001).
- Poul-Henning Petersen, Danish Agricultural Advisory Centre (2002).
- Bitten Bolet, County of Ringkøbing (1988-1999)
- Stig Eggert Pedersen, County of Funen (1999-2002)

- Hanne Bach, The National Environmental Research Institute (1999-2002).

October 2002

Merete Styczen, project co-ordinator

This sub-project report

This report deals with the atmospheric pathway in the project. It describes the tools developed in the subproject “Estimering af tilførsel af pesticider til vandmiljøer via atmosfæren” (Estimation of the atmospheric input of pesticides to water bodies) the to estimate the atmospheric input (dry deposition, spray drift) to water bodies. Within the framework of this project the atmospheric transport model was further developed and all deposition processes were described in such a way that they could be incorporated easily in integrated decision tool.

The parameterisation of the uptake of pesticides by water bodies and the processes in the water bodies presented in this report was made within the framework of the project “Integreret monitering af pesticider i regnvand og luft” (integrated monitoring of pesticides in rainwater and air) which was financially supported by the Danish Parliament.

The parameterisation of the emission of pesticides used in this report was based on the work done by Smit et al. (1997) and Smit et al. (1998) at Alterra, Wageningen, The Netherlands. The incorporation of this part in the deposition model presented in this report was done within the framework of the project “Fordampning og atmosfærekemisk omdannelse” (volatilisation and atmospheric reaction) which was financially supported by the Danish Parliament.

We are grateful to Dr. Erik van den Berg, Alterra, Wageningen, The Netherlands to Ruwim Berkowicz, National Environmental Research Institute, Roskilde, Denmark and to Merete Styczen and Mette Thorsen (DHI Water & Environment, Hørsholm, Denmark) for their advice.

Sammenfatning og konklusioner

Beslutningsstøtteværktøj

Et beslutningsstøtteværktøj til Miljøstyrelsen til vurdering af risikoen for transport af pesticider til vandløb og søer er under udvikling (PestSurf). Udviklingen af PestSurf koordineres af DHI – Institut for Vand og Miljø. Nærværende rapport beskriver støtteværktøj til estimering af det atmosfæriske bidrag af pesticider til vandløb og søer forårsaget af sprøjtning på tilgrænsende marker. Der er taget højde for følgende processer:

- Tørdeposition af gasformige pesticider, som er fordampet fra markerne. Tørdeposition er stoftransport til overfladen ved hjælp af lufthvirvler (turbulens) og en efterfølgende optagelse i/på overfladen. For at tørdepositionen skal forekomme må pesticidet først fordampe fra det sprøjtede område og derefter blive transporteret til vandet med vinden. Fordampningen er størst lige efter sprøjtningen men kan foregå i mange dage efter (~10-20 dage)
- Afdrift af dråber, som dannes ved selve sprøjtningen. De skal også transporteres til vandet med luften . Afsætningen af dråberne forårsages hovedsagelig af tyngdekraften og ikke af turbulensen. Turbulensen spiller dog en rolle ved at holde en del af dråberne lidt længere i luften.

Der er udviklet en model til beregning af fordampning, atmosfærisk spredning og transport og af tørdeposition til vandløb og søer.

Fordampning

Fordampningen af pesticider fra afgrøder og jord er i denne model beskrevet ved empiriske relationer fremkommet ved sammenholdelse af forsøg med målinger af fordampning af et begrænset antal pesticider og deres fysik-kemiske egenskaber . Den empiriske relation for fordampning fra jord tager også højde for jordens egenskaber. Disse empiriske relationer er udviklet af Alterra, Wageningen, Holland (Smit et al., 1997; Smit et al., 1998). Relationen for afgrøder er en sammenhæng mellem fordampningen og pesticidets damptryk, mens fordampningen fra jorden afhænger af pesticidets koncentration i gasfasen i jorden. Disse empiriske relationer anvendes i modellen til at beregne fordampningen for alle pesticider.

Atmosfærisk transport og opblanding

I modellen tages højde for at et gasformigt pesticid transporteres vertikalt ved hjælp af lufthvirvler og i horisontal retning med vinden. Der tages også højde for, at vindhastigheden tiltager med højden.

Tørdeposition

Ved beskrivelse af tørdeposition i modellen tages højde for, at pesticidet er transporteret til vandoverfladen ved hjælp af turbulens og at diffusiviteten i gasfasen spiller en rolle i et tyndt lag lige over vandoverfladen. Optagelsen af pesticidet i vandet afhænger af opblandingen i den øverste del af vandet (masseoverførselskoeffcienten i vandfasen) og Henry’s lov konstant. Henry’s lov konstant er et mål for gassens opløselighed i vand og beskriver forholdet mellem koncentrationerne i gas- og vandfasen ved ligevægt. Opblandingen i den øverste del af vandet er forskellig for forskellige typer vandløb og søer.

I vandløb, som ikke er dybe, og hvor vandet strømmer med en rimelig hastighed er opblandingen i vandets øverste lag forårsaget af friktionen ved vandløbets bund. Opblandingen i vandet beskrives med empirisk bestemte masseoverførselskoefficienter for ilt, men der korrigeres for forskellen i diffusiviteten i vand mellem pesticidet og ilt. De empirisk bestemte masseoverførselskoefficienter afhænger af strømhastigheden, dybden og højdeforskelle i vandløbet.

I søer, langsomt strømmende og dybe vandløb samt i havet afhænger opblandingen i det øverste lag af vandet af vinden. Opblandingen beskrives her i modellen med empiriske relationer mellem målte masseoverførselskoefficienter for vandfasen og målt vindhastighed. Disse relationer er bestemt for forskellige gasser, men resultaterne normaliseres i forhold til opblandingen af CO_2 ved 20°C. I modellen er den normaliserede relation anvendt til af beregne masseoverførselskoefficienten for pesticidet i vandfasen, men der korrigeres for effekten af forskelle i diffusiviteten for pesticidet og CO_2. Masseoverførselskoefficienten for vandfasen tiltager i disse tilfælde med vindhastigheden.

For de fleste pesticider bestemmes tørdeposition af modstanden for transport i atmosfæren og ikke af opblanding i vandet.

Afdrift

Afdrift ved marksprøjtning påvirkes af en række faktorer. Der kan skelnes mellem teknisk/agronomiske faktorer som sprøjteføreren kan påvirke samt de klimatiske forhold på sprøjtetidspunktet. Følgende faktorer er væsentlige for afdriftens omfang:

1. Dråbestørrelse (dysevalg)
2. Bomhøjde
3. Kørehastighed
4. Luftledsagelse, skærmning af sprøjteudstyr
5. Dosering
6. Afgrødeudvikling, naboafgrøde, læbælter
7. Vindhastighed
8. Temperatur og luftfugtighed

De første 5 punkter vedrører den anvendte teknik og her er dråbestørrelsen den væsentligste faktor af betydning for afdriftspotentialet fra traditionelle marksprøjter. Dråbestørrelsen påvirkes gennem valg af dyse og tryk. Når der ved marksprøjtning ofte anvendes en dyse og dermed dråbestørrelse med et relativt stort afdriftspotentiale skyldes det, at opnåelse af en høj biologisk effekt, til en række planteværnsopgaver er afhængig af en fin til medium dråbekvalitet. Anvendes derimod en grov forstøvning som er karakteristisk for afdriftsreducerende dyser opnås en dårligere effekt. Det betyder, at der skal anvendes højere dosering med afdriftsreducerende dyser for at opnå samme effektniveau som med finere forstøvende afdriftsfølsomme dyser. Såfremt bomhøjden hæves over det anbefalede øges afdriftspotentialet mærkbart fordi de små dråber er længere tid om at nå målet. Tilsvarende øges afdriftspotentialet når kørehastigheden øges fordi sprøjtedouchen påvirkes af en større modvind der trækker små dråber ud af douchen. Der er udviklet udstyr som reducerer afdriften fra traditionelle marksprøjter. Det mest udbredte system er såkaldt luftledsagelse som har den funktion at sprøjtedouchen ledsages af et lufttæppe ned mod målet. Det sikrer at den forekommende vind eller fartvinden forårsaget af kørehastigheden ikke kan føre dråber ud af sprøjtedouchen. Det såkaldte Twin system har i forsøg dokumenteret en afdriftsreduktion på ca 2/3 i forhold til en tilsvarende behandling med samme dråbestørrelse uden luftledsagelse. I forhold til biologisk effekt er Twin systemet neutralt til positivt afhængigt af opgavetype. Sprøjter med forskellige former for afskærmning for at begrænse afdriften har begrænset betydning til traditionelle marksprøjter, men finder anvendelse ved sprøjter i træ- og buskfrugt (tunnelsprøjter) samt ved båndsprøjtning.

Vindhastigheden på sprøjtetidspunktet er meget afgørende for omfanget af afdrift. Temperatur og luftfugtighed skønnes ligeledes at være væsentlige faktorer for afdrift ved at påvirke fordampning fra dråber under transporten. Dermed mindskes dråbestørrelsen og afdriftspotentialet øges. Betydningen af de 2 faktorer er ikke velkvantificeret under markforhold. Med hensyn til betydningen af vindhastighed skønnes det at afdriften stiger lineært ved vindhastigheder på over 1 m s^{-1}. Det bedste bud på hvordan afdriftsværdier kan normaliseres til samme vindhastighed er ved at dividere afdriften med den målte vindhastighed – 1 m s^{-1}. Det betyder eksempelvis at afdriften fordobles når vindhastigheden øges fra to til tre m s^{-1}. Danmark er geografisk placeret i et kystklima som er karakteriseret ved større vindhastigheder end under kontinentale klimaforhold. Det skønnes derfor at Ganzelmeier et al.'s (1995) 95 percentil værdier for afdrift er mere repræsentative for gennemsnitlige danske sprøjteforhold end de middelværdier der er fundet under tyske klimaforhold.

Beskrivelse af processer for afdrift

Rapporten giver også information om de processer, som er nødvendige for at kunne udforme modeller for afdrift, men der er ikke udviklet en model for afdrift. De værdier, der betegnes som 95% percentil værdier for afdrift under tyske forhold af Ganzelmeier et al. (1995), anses som værende repræsentative gennemsnitsværdier for afdrift under danske vindforhold. Det er disse afdriftsværdier der anvendes i PestSurf.

Sammenligning af tørdeposition og afdrift

I den sidste del af rapporten er bidragene fra tørdeposition og fra afdrift sammenlignet. Sammenligningen viser, at bidraget fra tørdeposition potentielt kan være større end bidraget fra afdrift for de gasformige pesticider, som er letopløselige i vand (defineret ved en Henry's lov konstant: koncentration i luft (kg m^{-3})/koncentration i vand (kg m^{-3})) for vandløb og søer med en stor opblanding i det øverste lag. Med "potentiel" menes i det tilfælde næsten 100% af pesticidet fordamper. For flygtige pesticider som fenpropimorph, pendimethalin og bentazon er tørdeposition ofte vigtigere end afdrift. Hvis kun en lille brøkdel af pesticidet fordamper (et par %) bliver bidraget fra afdrift større end tørdepositionsbidraget. Afdriften aftager relativt hurtig med afstanden til markkanten mens tørdeposition aftager langsommere.

Summary and conclusions

Decision tool

A decision tool is being developed for the Danish Environmental Protection Agency to evaluate the risk of transport of pesticides to water bodies such as streams and lakes (PestSurf). The development of PestSurf is co-ordinated by DHI Water & Environment. In this report the tools to estimate the atmospheric contribution from the application of pesticides to fields close to water bodies are presented that will become part of the decision tool. The following processes are taken into account:

- Dry deposition of gaseous pesticides that are volatilised from the field mainly after application. Dry deposition is transport to the surface by whirls in the air (turbulence). In order to get dry deposition to the water body the pesticide should volatilise first then be transported by the wind to the water body. Although volatilisation is usually highest just after application, it will continue for many days (~10-20 days).
- Spray drift, i.e. transport of pesticides in drops generated during the spraying operation. Also in this case the droplets have to be transported to the water body by the wind. The deposition of these droplets to the water body is in this case mainly caused by gravitation and not by turbulence. Turbulence, however, plays a role in keeping a fraction of the drops somewhat longer in the atmosphere.

A model has been developed to describe the volatilisation of pesticides, the atmospheric transport/mixing and the dry deposition to water bodies.

Volatilisation

The volatilisation of pesticides from crops and fallow soil in this model is described by empirical relationships between the measured volatilisation of pesticides and their physico-chemical properties for a limited number of pesticides. The relationship for volatilisation from fallow soil also includes soil properties. These relationships were developed by Alterra, Wageningen, The Netherlands (Smit et al., 1997; Smit et al., 1998). They state that the volatilisation from crops is a function of the vapour pressure of the pesticide and that the volatilisation from fallow soil is a function of the fraction of the pesticide that is in the gas phase in the soil. These relationships are in the model used for all pesticides.

Atmospheric transport and mixing

The atmospheric transport and mixing in the model takes into account that the gaseous pesticide released at low heights is mixed up by whirls in the air (turbulence) and that the wind speed increases with height.

Dry deposition

The dry deposition in the model takes into account that the pesticide is transported downward towards the water surface by whirls (turbulence) and that the gas phase diffusivity plays a role in a thin layer close to the surface. The uptake of the pesticide by the water surface depends on the mixing in the upper part of the water body (aqueous phase mass transfer coefficient) and the Henry's law coefficient. The Henry's law coefficient is a measure of the solubility of the gas that describes the relation between the concentration of the pesticide in the gas phase and the concentration in the aqueous phase at equilibrium. The mixing in the upper part of the water body is different for different types of water bodies.

In rapidly running shallow waters the mixing in the upper part of the water body is created by friction at the river bottom. The mixing in the upper part of this type of water body in the model is described using empirically determined mass transfer coefficients for oxygen. A correction is applied to these coefficients to take into account the difference in diffusivity of the pesticide and oxygen in the aqueous phase. The empirically determined mass transfer coefficients are also function of the average velocity of the stream, its average depth and the slope (metre change in height per metre horizontal distance).

In lakes, slowly running or deep waters and the sea, mixing in the upper part of the water body is caused by the wind. The mixing in the upper part of these water bodies is described with empirical relationships between measured mass transfer coefficients and measured wind speed. These relationships are established for different gases, but the results are normalised to the exchange of CO_2 at 20°C. In the model these normalised relationship is then used to calculate the aqueous mass transfer coefficient of the pesticide. Corrections are then made to take into account the difference in diffusivity of the pesticide and CO_2 in water. These experimentally determined mass transfer coefficients increase with wind speed.

For most pesticides the resistance to transport in the atmosphere limits the dry deposition and not the resistance to transport in the water body.

Spray drift

Spray drift during field spraying is influenced by a number of factors. One can divide these into technical/agronomic factors, which can be influenced by the farmer and climatic conditions at the time of application. The following factors are influencing the spray drift potential:

1. Droplet size (nozzle choice)
2. Boom height
3. Driving speed
4. Air-assistance, shielding
5. Dose rate
6. Crop development, neighbour crop, shelter belt
7. Wind speed
8. Temperature and humidity

The first 5 points relate to the technique used and the droplet size is the most influential factor concerning spray drift from traditional field sprayers. The

droplet size is influenced through the choice of nozzle and spray pressure. When fine atomising nozzles with a high drift potential are preferred for some applications then it is because a high biological efficacy is dependent on the use of fine or medium atomising nozzles. If a coarse drift reducing droplet size is used a reduced efficacy can be the result. This means that for some applications an increased dose rate might be needed in order to retain biological efficacy if drift-reducing nozzles are used for the application. Raising the boom height above the recommended level increases the drift potential considerably because the travelling time of the small droplets increases significantly. The drift potential is correspondingly increased when the driving speed is increased due to the increased wind speed experienced by the spray swath. Different types of drift reducing equipment have been developed for traditional field sprayers. Probably the most widespread system is air-assistance. The system creates an air-stream parallel to the spray swath, which helps keeping the droplets in the spray cloud until they reach the target. One of the air-assistance systems, the Twin system, has documented a drift reduction of approximately 2/3 compared to the use of the same droplet size without air-assistance. Concerning biological efficacy, a neutral or positive influence of air-assistance is seen dependent on the type of application. Different types of shielding devices for traditional field sprayers has been developed but shielding devices are at the moment primarily used for orchard sprayers (tunnel sprayers) and for band sprayers.
The wind speed at the time of spraying is one of the most important factors influencing spray drift. Temperature and humidity influences spray drift through their effect on evaporation from the droplets during their travel to the target. In this way droplet size is reduced and spray drift potential increases. The effect of temperature and humidity on spray drift is not quantified under field conditions. At wind speeds above 1 m s^{-1} spray drift increases more or less linearly with wind speed. The best estimate to normalise spray drift values to the same wind speed is by dividing the actual found drift values with the measured wind speed – 1 m s^{-1}. This means as an example that spray drift is doubled when the wind speed is raised from two to three m s^{-1}. The coastal climate in Denmark is characterised with more windy conditions than found in a continental climate. From this reason it seems that the 95 percentile Ganzelmeier values (Ganzelmeier.et al., 1995) are more representative for spray drift under average Danish conditions than the mean values found under German wind conditions.

Description of spray drift processes

The report gives also information on the processes necessary to model spray drift, but no spray drift model has been developed. The 95% percentile values for spray drift described in Ganzelmeier et al. (1995) is regarded as being representative of mean values for spray drift under Danish wind conditions. These values are being used to describe spray drift in PestSurf.

Conclusions: comparison of dry deposition and spray drift

In the last part of the report the contribution from dry deposition and from spray drift are compared. The comparison shows that the contribution from dry deposition potentially can be larger than from spray drift for those gaseous pesticides that are highly soluble (defined by having a small Henry's law coefficient, which is here defined as: concentration in air (kg m^{-3})/concentration in water (kg m^{-3})) for waters with a high mixing rate in the upper layer. With potentially it is meant in the case that almost 100% of the applied pesticides volatilises. For pesticides that are rather volatile such as fenpropimorph, pendimethalin, bentazone the dry deposition is often more important than spray drift. If only a small fraction of the pesticide (a few %) volatilises spray drift becomes relatively more important. Spray drift decreases rather fast as a function of the downwind distance from the edge of the field, whereas dry deposition decreases much more slowly.

1 Introduction

This report treats the following subjects:

- Theory and development of a model for deposition of pesticides to water bodies (rivers, lakes and seas) as a function of the distance to a nearby field onto which pesticides are applied.
- Evaluation of spray drift experiments and selection of information that can be used to estimate the spray drift as a function of the distance to a nearby field onto which pesticides are applied.
- Theory on spray drift.
- Discussion and conclusions where the (potential) contribution from dry deposition and spray drift to various water bodies are compared.

It should be noted that it was not planned to develop a model for spray drift within the framework of this (sub)project; only the basic processes are described that are needed to model spray drift. This project does not cover the contribution of pesticides to water bodies by wind erosion or the contribution from more distant sources.

A special version of the model for deposition to water bodies was made, so that it could be incorporated in the integrated decision tool that includes the contribution from all pathways to water bodies. The number of parameters that can be chosen by the user of this version of the model is restricted. A documentation of this model version and an overview of the parameter values chosen in this version are reported in Appendix G.

2 Modelling dry deposition of to water bodies

2.1 Introduction

A model called PESTDEP was developed that can be used to estimate the (maximum) dry deposition of gaseous pesticides to a water body adjacent to a field onto which a pesticide is applied. The water body can be a stream, a lake or a sea area. The basic situation that the model describes is given in Figure 1a.

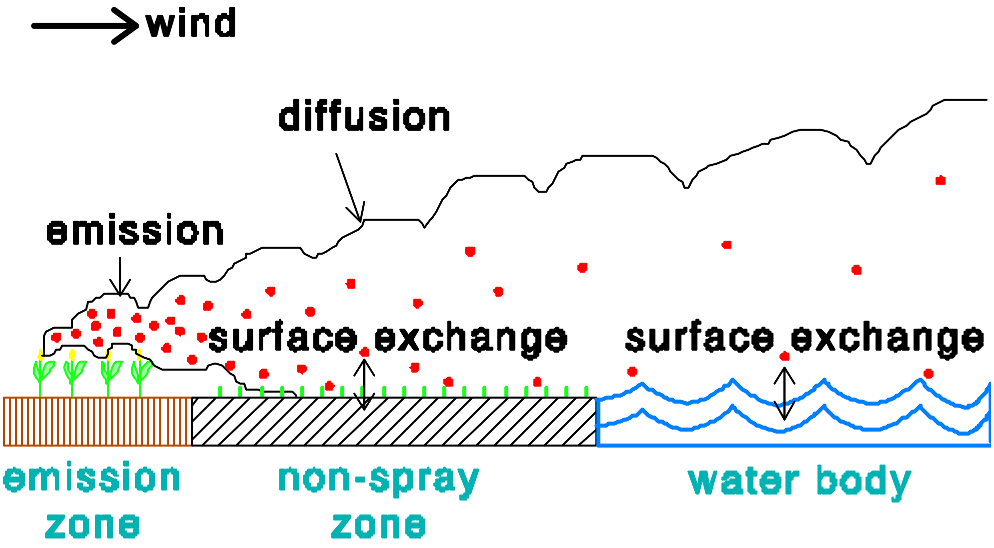

Figure 1a. Set-up of PESTDEP.
Figur 1a. Opsætning af PESTDEP

A pesticide is applied to a field. Part of the pesticide volatilises and is transported first over a non-spray zone ("buffer zone") and then over a water body. The pesticide is then transported further away, but that process is not described by this version of PESTDEP. The pesticide can be exchanged between the air and the surface (non-spray zone or water body). If the concentration in the air is higher than the concentration in the air that is in equilibrium with the concentration in the surface (e.g. water), the net flux will be downward. In that case dry deposition is occurring. In the opposite case the emission occurs.

A special version of PESTDEP will be used in a decision tool (PestSurf) in the approval procedure for pesticides. This means that the model should be able to describe a general situation. For that reason it was chosen to develop a

2-dimensional model with a distance x in the downwind direction and a height z as the dimensions. This type of model gives the same results as a 3-dimensional model with an indefinitely long field, indefinitely long non-spray zone and indefinitely long water body in the y direction. To simplify the results and to get an estimate of the maximum deposition of the pesticide to the water body, it is assumed that the wind is always blowing from the direction of the field to the water body. This is, in fact, not correct. However, it should be kept in mind that there are also fields at the other side of the water body and when the wind direction is opposite these fields will then contribute to the deposition to the water body. Corrections can be made, taking into account the frequencies of the wind directions and the position of the water body, but this is difficult to generalise. In the version of PESTDEP that is integrated in PestSurf no corrections are made so that an estimate of the maximum deposition is obtained.

The model should describe the following processes:

a) Volatilisation of pesticide applied to a field without or with crops.
b) Atmospheric transport and diffusion of the emitted pesticide.
c) Exchange of pesticide between the air and the vegetation of the non-spray zone (dry deposition or emission).
d) Exchange of pesticide between the air and the water body (dry deposition or emission).
e) Wet deposition. This process is not yet incorporated in the model because the emission rate as a function of time is not known (see section 2.2).
f) Reaction of the pesticide in the air, e.g. by photolysis. The transport time from the nearby field to the water body is so short that the pesticide has almost not reacted. For that reason reaction is not taken into account in PESTDEP.

2.2 Emission

The emission rate of pesticides to crops and fallow soil depends on many factors, e.g.:

- Chemical and physical properties of the pesticide.
- Chemical and physical properties of the soil or crops.
- Processes in the soil or in crops (e.g. water and heat transport in the soil, uptake through the stomata or in the cuticles in plants etc.).
- Meteorological conditions (e.g. wind speed, atmospheric stability, temperature, relative humidity, and precipitation).

At present there are no models available that simulate the emission rate of pesticides applied to crops as a function of time, but only the accumulated emission as a percentage of the applied dose (Smit et al., 1998). There are some models available that simulate the emission of pesticides applied to fallow soil as a function of time (see e.g. Jury, 1983). Most of the pesticides are applied to crops. As for this type of application no model was available that gives the emission as a function of the time, it was decided to use models that calculate the accumulated emission as a percentage of the applied dose, both for application to the soil and to crops.

It was decided to use the models of Smit et al. (1997) and Smit et al. (1998) to calculate the accumulated emission after application. These models are based on statistical correlation of the observed accumulated emission published in the literature with physical and chemical parameters that are likely to play an important role in the volatilisation process. The relations found were based on pesticides that do not photolyse or hydrolyse. For that reason these methods cannot be applied for pesticides that show a noticeable photolysis or hydrolysis. Sometimes these methods lead to extremely high volatilisations, e.g. 80-100%. Such high numbers indicate that the compound is highly volatile, but they can in that case not be used as a quantitative measure.

Smit et al. (1998) found the following statistical relation for the accumulated emission of pesticides during 7 days after application to crops that fully cover the soil in the field and in climate chambers (see also Fig. 2):

$$^{10}\log(CV_7) = 1.528 + 0.466\ ^{10}\log(VP); \quad \text{for VP} \leq 10.3 \text{ mPa} \qquad (1)$$

where:

CV_7 = accumulated emission during 7 days after application (% of dosage of active ingredient).

VP = vapour pressure (mPa).

This relation is based on 14 field and climate chamber experiments with 13 pesticides. It should be noted that this relation cannot be used for the emission of pesticides incorporated in the soil.

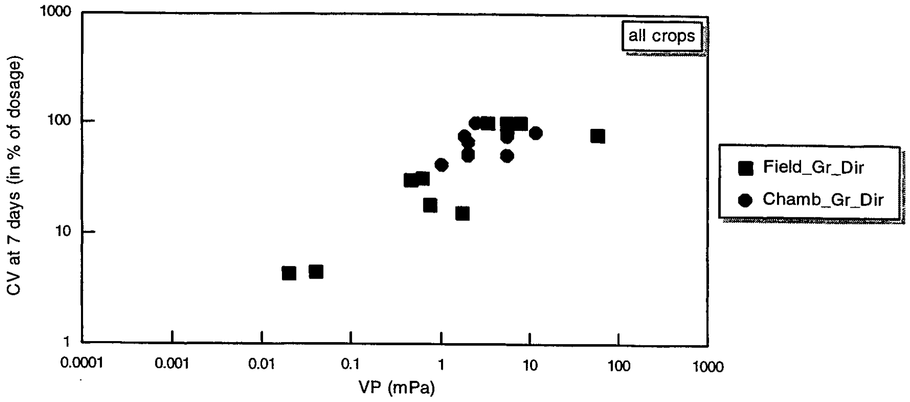

Figure 2. Accumulated emission during 7 days after application of the pesticide to the crop vs. vapour pressure of the pesticide (Smit et al., 1998).

Figur 2. Akkumuleret emission af pesticidet de første 7 dage efter udsprøjtning over afgrøden i relation til. pesticidets damptryk (Smit et al., 1998).

Smit et al. (1997) found the following statistical relation for the accumulated emission of pesticides during 21 days after application to normal moist fallow soil (see also Fig. 3):

$$CV_{21} = 71.9 + 11.6\ ^{10}\log(100\,FP_{gas}); \quad \text{for } 6.33\times10^{-9} < FP_{gas} \leq 1 \qquad (2)$$

where:

CV = accumulated emission during 21 days after application (% of dosage of active ingredient).

FP = fraction of the pesticide in the gas phase in the soil.

Note that the accumulated emission CV_{21} cannot be calculated if FP_{gas} falls outside the range indicated in equation (2). The maximum accumulated emission during 21 days using this equation is 95.1%. This relation was based on 14 field studies with 31 pesticides.

In Appendix A information is presented on how FP_{gas} can be calculated from soil and pesticide properties.

Experiments show that the emission rate is high in the beginning and shows diurnal variations that are connected to variations in meteorological variables: temperature and turbulence. Moreover, the emission rate is affected by precipitation.

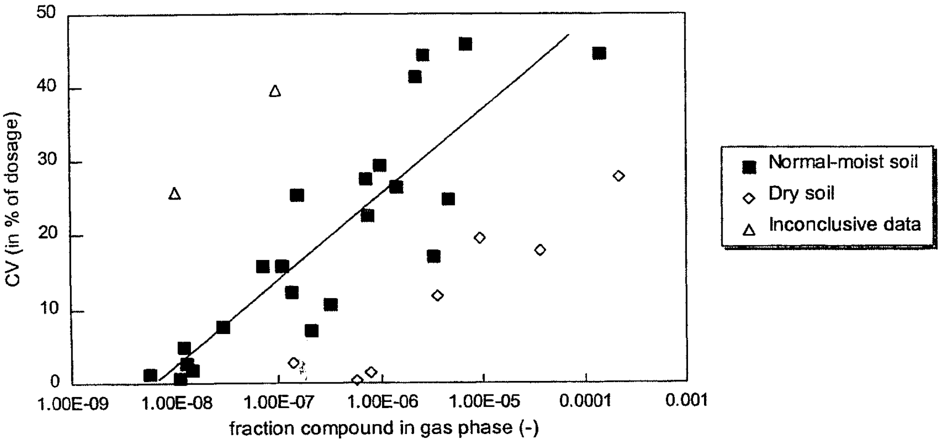

Figure 3. Accumulated emission 21 days after application of the pesticide to fallow soil vs. the fraction of the pesticide in the gas phase in the soil (Smit et al., 1997).
Figur 3. Akkumuleret emission de første 21 dage efter udsprøjtning af pesticid på jorden vs. fraktionen af pesticidet som er i gasfasen i jorden (Smit et al., 1997).

The fact that only accumulated emissions are available for periods of 7 or 21 days has some consequences for the modelling. This would mean that it is only possible to model removal by precipitation for rain events that last 7 or 21 days. These events occur only in the Bible and are less relevant to the problem treated here. As the emission rate is highly variable during the periods of 7 and 21 days it is difficult to model the removal by precipitation. Model experiments (Asman, 2001) showed that the contribution of the emission from the field to the wet deposition is usually not so important compared to the contribution from dry deposition. The reason for this is that the pesticide plume relatively close to the field has not yet reached the cloud base. This means that uptake of pesticides can only occur by raindrops and not by cloud droplets. Raindrops have a high fall speed. Moreover, they are relatively large which means that they have not so much surface area where uptake can occur per volume. So they are only during a short time in the plume and do not take up the gas very efficiently. For this reason it was decided not to take removal by precipitation into account in this version of PESTDEP.

Removal of pesticides by precipitation can be an important pathway, but only if the more efficient in-cloud processes that play a role. Cloud droplets have a residence time of maybe 20 minutes or longer in clouds and their surface to volume ratio is such that they reach equilibrium with the surrounding air in the cloud within a few seconds.

2.3 Atmospheric diffusion

A steady-state atmospheric diffusion model was developed that describes the diffusion in the x direction (horizontal, downwind) and the z direction (vertical). In the model the atmosphere is described by a number of logarithmically spaced layers (Fig. 4). Within each layer there is a constant horizontal wind speed. The vertical wind speed is neglected because it is usually rather small. Only turbulent vertical exchange between the layers is taken into account. Diffusion in the x direction is also not taken into account because it can also be neglected for more or a less stationary source as is the case here. As the model is only two-dimensional in the x, z plane, diffusion perpendicular to the wind direction (y direction) is not taken into account. So, the only diffusion taken into account is the diffusion in the vertical direction (z direction).

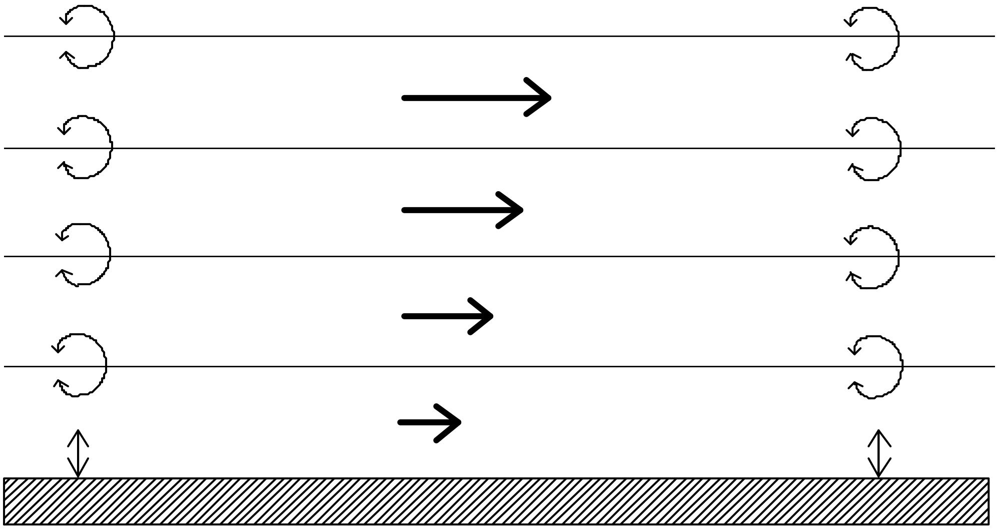

Figure 4. Set-up of the model: layers, wind speed (symbolised by arrows), exchange between layers by eddy diffusivity (symbolised by whirls) and exchange between the air and the surface (symbolised by double arrows). It should be noted that emission is a form of exchange between the atmosphere and the surface.
Figur 4. Modellens opsætning: lag, vindhastighed (symboliseret ved pile), udveksling mellem lag ved eddy diffusion (symboliseret ved hvirvler) og udveksling mellem atmosfæren og overfladen (symboliseret ved dobbelte pile). Det skal bemærkes, at emission er en form af udveksling mellem atmosfæren og overfladen.

The average wind speed within a layer is calculated from the wind speed at 100 regularly spaced vertical points within the layer using the following relation (Arya, 1988):

$$u(z) = \frac{u_*}{k} \ln\left(\frac{z}{z_{0m}} \right) \qquad (3)$$

where:
u(z) = wind speed at height z (m s^{-1})
u_* = friction velocity (m s^{-1}); this is a measure of turbulence. The larger u_* the larger the turbulence, an as can be seen from (3) also the larger the wind speed.
κ = von Karman's constant (0.4; dimensionless)
z = height (m)
z_{0m} = surface roughness length for momentum (m); this is a measure of the surface roughness, it is of the order of 1/10th of the height of obstacles.

From (3) it can be seen that the wind speed increases with height. Moreover, it can been seen that the wind speed at height z_{0m} is zero. In reality (3) is not valid at heights close to z_{0m} and there will be some wind at height z_{0m}. Relation (3) is valid for a neutral atmosphere, i.e. an atmosphere where the turbulence is generated mechanically. For a stable or an unstable atmosphere the relation is somewhat more complicated (Arya, 1988). The atmosphere is neutral most of the time. As a generalised model should be made it was therefore decided only to model diffusion for neutral atmospheric conditions.

The exchange of material between two adjacent layers in the model is described by an eddy diffusivity (diffusivity by whirls) coefficient. This coefficient is the same for material as for heat. For neutral atmospheric conditions it is given by (Arya, 1988):

$$K_{Heat}(z) = k \; u_* \, z \qquad (4)$$

where:
$K_{Heat}(z)$ = eddy diffusivity at height z (m^2 s^{-1}).

Equation (4) shows that the eddy diffusivity increases with turbulence and height. For stable or unstable conditions there are more complicated expressions (Arya, 1988).

A more detailed discussion of atmospheric diffusion can e.g. be found in Asman (2001).

The vertical diffusion part of the model was tested against the results of a tracer experiment in the U.S.A., where the tracer was released from a low-level source. The emission height is representative of the height from which pesticides are released after application to a field. The general problem with testing the diffusion part of models is that there are only done a very few diffusion experiments because they are so expensive.

In the experiment sulphur dioxide was released from a 0.46 m high point source (van Ulden, 1978). The concentrations were measured at a height of 1.5 m at distances of 50, 200 and 800 m from the source. The surface roughness length was 0.008 m. The diffusion using (3) and (4) lead to an underprediction of the concentration at 50 m by 9%, an overprediction at 200 m by 7% and an overprediction at 800 m by 23%. This phenomenon was also observed for other diffusion models (Gryning et al., 1983; Brown et al., 1993). They guess that part of the observed differences can be explained by the fact that sulphur dioxide is dry depositing to a minor extent. They come also up with other explanations.

Based on the comparison it was somewhat arbitrarily decided to increase the vertical diffusivity $K_{Heat}(z)$ in PESTDEP by 30%, so that somewhat better agreement was obtained (Note: this change in K_{Heat} has an effect on the concentrations that is usually less than 30%). There is, however, no theoretical justification for this correction. Fig. 5 shows the modelled vs. measured ratio of crosswind-integrated concentration/source strength $\bar{c}/Q$ as a function of 3 distances from the source for both a neutral, stable and unstable atmospheres. The ratio $\bar{c}/Q$ is a measure of dilution due to vertical diffusion. Taking into account the uncertainty in the measured concentrations this is a very reasonable result.

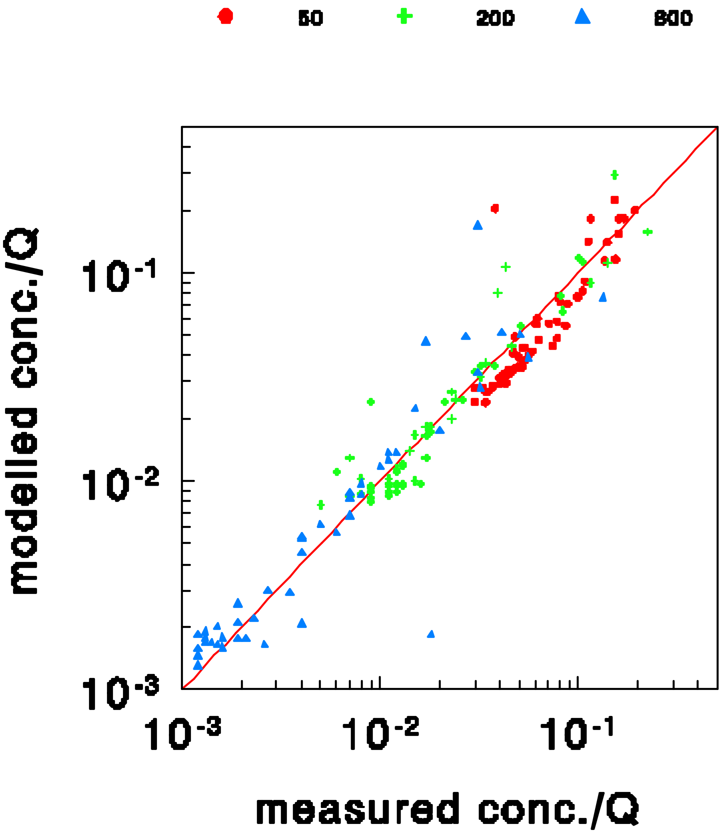

Figure 5. Modelled vs. measured ratio crosswind-integrated concentration/source strength (this is a measure for dilution caused by vertical diffusion) for 3 downwind distances: 50, 200 and 800 m. The line indicates the curve that would be obtained if the modelled values were equal to the measured values.
Figur 5. Modelleret vs. målt koncentration på tværs af vinden divideret med kildestyrken (det er et mål for fortynding pga. vertikal diffusion) for 3 nedstrøms afstande: 50, 200 and 800 m. Den optrukne linie viser forholdet når de modellerede værdier er lig med de målte værdier.

2.4 Exchange between the air and the surface: general principles

In the model a description of the exchange between the air and the surface is needed for the non-spray area and the water body. The following model can be used to calculate the exchange (Fig. 6; see also Appendix C). It consists of different resistances to transport. It should be noted that the resistances in the model are in series because a molecule must subsequently pass these barriers before reaching the surface or the atmosphere (analogous to the principle of electrical resistance).

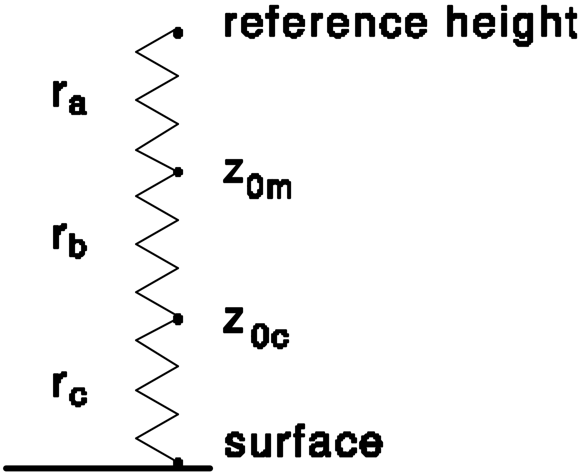

Figure. 6. Model for resistance to exchange between the atmosphere and a surface (soil, vegetation, water body).
Figur 6. Model for modstand mod udveksling mellem atmosfæren og overfladen (jord, vegetation, vandløb eller sø).

These resistances should be overcome during both the dry deposition as well as the emission process. The description for both processes is the same.

The flux between the atmosphere and the surface is described by:

$$F = -K_g \left(c_{g,r} - c_{g,surface} \right) \quad (5)$$

where :
F = flux (kg m^{-2} s^{-1}). The flux is here defined as negative when material is
removed from the atmosphere.
K_g = overall gas phase mass transfer coefficient (m s^{-1})
$c_{g,r}$ = gas phase concentration at a reference height (kg m^{-3})
$c_{g,surface}$ = gas phase concentration that is in equilibrium with the concentration in
the liquid phase (kg m^{-3}). It is necessary that the concentration in the
liquid phase (plant tissue, water) is expressed in a gas phase
concentration, because only concentrations in the same phase can be
compared.

K_g can be expressed as:

$$K_g = \frac{1}{r_a + r_b + r_c} \tag{6}$$

where:
r_a = aerodynamic resistance (s m^{-1})
r_b = laminar boundary layer resistance (s m^{-1})
r_c = surface resistance (s m^{-1})

In the model there is a resistance to transport in the air (r_a, called "aerodynamic resistance") from a certain reference height to surface roughness length z_{0m}, i.e. the height at which the wind speed is zero. It is the eddy diffusivity, the turbulence that is taking care of this transport. The aerodynamic resistance can be found by integrating (4) between those heights, which leads to the following expression for r_a neutral atmospheric conditions:

$$r_a = \frac{1}{k u_*} \ln\left(\frac{z_r}{z_{0m}}\right) \tag{7}$$

The units in which r_a is expressed is s m^{-1}; this is just the inverse of a speed. In this equation z_r is a reference height (m). In PESTDEP z_r is the height of the centre of the lowest layer. The aerodynamic resistance is the same for all gases, i.e. it does not depend on the properties of the gas and depends only on the turbulence and the roughness of the surface for momentum.

Then there is a layer, which is usually called the laminar boundary layer. This is a stagnant or intermittently mixed layer in the air close to the surface (≈ 1 mm) through which the transport is mainly thought to occur through molecular diffusion, which is much less efficient than turbulent diffusion. Molecular diffusion varies with the size of the molecules. Larger molecules such as pesticides do not diffuse as fast as small ones. Thus for pesticides the laminar boundary layer resistance will be larger than for lighter molecules. The laminar boundary layer resistance does not only depend on the properties of the gas, it also depends on the properties of the surface. As a result r_b is different for vegetation and water bodies. The laminar boundary layer resistance r_b is defined by:

$$r_b = \frac{1}{k u_*} \ln\left(\frac{z_{0m}}{z_{0c}}\right) \tag{8}$$

where z_{0c} is the surface roughness length for concentration (m) and z_{0c} is the surface roughness length for concentration. From this equation it can be seen that r_b decreases with turbulence. The reason for this is that when there is more turbulence the layer becomes thinner and the molecules do not have to diffuse such a long way.

The surface resistance r_c (s m^{-1}) is the resistance for the uptake into the surface. If it is small the gas will be taken up very well by the surface and the dry deposition velocity will be relatively large. If the surface is resistance is large almost no gas is taken up and the dry deposition velocity will be low. In surfaces there is often some water present. For the more polar pesticides that are soluble in water it could be reasonable to expect r_c to decrease with the solubility of the gas in water. For non-polar solubility in e.g. wax layers on plants or on organic matter in the soil could determine the surface resistance. In the model r_c should be known for the emission zone and the non-spray zone.

In section 2.5 the parameterisation of r_b and r_c for vegetation is discussed, whereas the parameterisation of r_b and r_c for water bodies is discussed in section 2.6.

2.5 Exchange between the air and the surface: vegetation

In general there will be vegetation in the non-spray zone. The amount of gaseous pesticide removed in the non-spray zone cannot be dry deposited to the water body and it is therefore important to know it. It should be noted, however, that only a relatively small fraction of the total airborne mass of pesticides is deposited to a non-spray zone if it is only a few metres wide.

For vegetation r_b is often parameterised as follows (Hicks et al., 1987):

$$r_b = \frac{2\left(\frac{Sc_g}{Pr}\right)^{\frac{2}{3}}}{k u_*} \qquad (9)$$

where:
Pr is the Prandtl number (dimensionless; value: 0.72) and Sc_g is the Schmidt number in the gas phase Sc_g is defined by:

$$Sc_g = \frac{\nu_a}{D_g} \qquad (10)$$

where:
ν_a = kinematic viscosity of the air ($m^2\ s^{-1}$); information on the ν_a can be found in Appendix B.
D_g = diffusivity of the gas in the gas phase ($m^2\ s^{-1}$); information on D_g for gaseous pesticides can be found in Appendix B.

From (10) it can be seen that r_b decreases with turbulence and increases with the molecular mass of the gas, which in the equation is “hidden” in Sc_g.

Also a value of r_c for the non-spray zone should be chosen. The problem, however, is that there are no values known in the literature for pesticides. Moreover, vegetation seems to have a limited capacity to absorb pesticide, which depends on the concentration of the pesticide in the air (Deinum et al., 1995; Duyzer and van Oss, 1997). If the concentration in the air decreases even emission of deposited pesticide from vegetation could occur. There are different options to choose extreme values for r_c for the non-spray zone. One is setting r_c to zero which leads to a maximum possible dry deposition in the non-spray zone (all pesticide that reaches the surface is taken up). The other one is setting r_c to indefinite (no pesticide at all is taken up), which leads to the maximum possible dry deposition to the water body. In the version of PESTDEP that is integrated in PestSurf, the r_c in the non-spray area is set to indefinite (dry deposition velocity is zero). This is done to obtain an estimate of the maximum deposition to the water body.

2.6 Exchange between the air and the surface: water

In this section the exchange between the atmosphere and the surface is discussed. First information on the laminar boundary layer resistance r_b is presented and then information on the surface resistance r_c. These resistances are different for different types of water bodies and depend in general on meteorological conditions and sometimes on the flow characteristics (rapidly running shallow rivers).

- Within the framework of this subproject a model for dry deposition to water bodies was developed. As with many other models also this model is based on an “ideal situation”, which often does not occur in practise. Some examples of non-ideal situations:
- There are often bushes or trees along a water body that may the air flow (e.g. direction, turbulence).
- Some streams are situated in a “canyon”. Differences in height may again influence the airflow.
- The temperature of the water in the water body will often be different from the air temperature. This can also have consequences for the exchange between the atmosphere and the water body.

One should, however, keep in mind that the purpose of the model is to evaluate the risk of pesticides relative to each other. The dry deposition of pesticides will in most cases be influenced by these factors in the same fashion. In that way they will have little relevance. It should be noted that the uptake of pesticides in principle also depends on the mass accommodation coefficient and a possibility of the pesticide to react in water (see Appendix C). In the following it is, however, assumed that these processes will not have any influence on the uptake rate.

2.6.1 Laminar boundary layer resistance for water

The laminar boundary layer resistance r_b for water can be parameterised for smooth surfaces and rough surfaces (surfaces with waves). There is no parameterisation for the transition area between smooth and rough surfaces.

2.6.1.1 Rivers and small lakes

Denmead et al. (1992) did an experiment in a shallow freshwater pond 300×100 m wide with an average depth of 0.22 m. They spread urea fertiliser in this pond by aircraft. The urea hydrolysed and ammonia was formed. They measured the emission flux of ammonia from this pond. Ammonia is highly soluble gas and has a very limited resistance for uptake in the water (surface resistance). This means that the emission flux is mainly a function of the aerodynamic resistance r_a and the laminar boundary layer resistance r_b. This is important as their measurements for that reason give a strong indication which parameterisation of r_b should be used for this type of waters. They found that the parameterisation of r_b made by Deacon (1977) gave reasonable results: it overestimated the emission flux by about 25% for wind speeds up to 8 m s^{-1} at 1.1 m height over the surface of the pond. Deacon parameterises not only the laminar boundary resistance, but also the surface resistance in case it is determined by interaction of the water surface with the wind (i.e. not for rapidly running waters where mixing is generated by friction at the river

bottom). Raupach et al. (2001a; 2001b) used also the Deacon parameterisation in a study where the transport of endosulfan to waterways was modelled.
It was therefore to adopt the Deacon parameterisation for r_b for rivers and small lakes because there surface is similar to the surface in Denmeads experiment (smooth):

$$r_b = \frac{1}{0.066 Sc_g^{-0.61} u_*} \tag{11}$$

This equation shows that r_b decreases with the friction velocity u_* (i.e. r_b decreases with wind speed). Equation (11) and (10) show that r_b will increase with the molecular weight, but this increase is rather moderate: r_b for a compound with a molecular weight of 400 g mol^{-1} is only 30% larger than r_b for a compound with a molecular weight of 200 g mol^{-1}.

Not to far from land u_* will still be about the same as on land. For that reason it is reasonable to assume that the value of u_* from land can be applied in equation (11) to find r_b for streams and small lakes.

In the version of PESTDEP that is integrated in PestSurf two values for u_* are used that are representative for average Danish conditions: for areas with crops $u_* = 0.386$ m s^{-1} and for area with fallow soil $u_* = 0.284$ m s^{-1} (see Appendix G for details). This leads to r_b values of 79 s m^{-1} for areas with crops and 107 s m^{-1} for areas with fallow soil if a molecular mass of 300 g mol^{-1} is assumed.

As there are not many experiments where r_b for smooth water surfaces is measured there is still a considerable uncertainty in the parameterisation used here. If the surface were rough in stead of smooth and the parameterisation of r_b for the sea were used (see next section) r_b would be 33 s m^{-1} in stead of 79 s m^{-1}.

2.6.1.2 *Sea*

In the following parameterisation of r_b for a smooth and rough sea surface is discussed.

The laminar boundary layer resistance r_b was previously defined by equation (8), where both the roughness length for momentum (z_{0m}) and the roughness length for concentration (z_{0c}) need to be known.

The ratio z_{0m}/z_{0c} used here for all water surfaces is given by Brutsaert (1975) with a slight modification by Lindfors et al. (1991).

For a smooth surface, i.e. for streams (for all Reynolds numbers) and for large water bodies which are smooth (for Reynolds numbers Re < 0.15):

$$\frac{z_{0m}}{z_{0c}} = \frac{1}{\frac{30}{Re} e^{\left(-13.6 k \ Sc^{\frac{2}{3}}\right)}} \tag{12a}$$

For large water bodies with waves so that they are rough (for Reynolds numbers $Re \geq 0.15$):

$$\frac{z_{0m}}{z_{0c}} = \frac{1}{20e^{\left(-7.3\,k\,Re^{\frac{1}{4}}\,Sc^{\frac{1}{2}}\right)}} \qquad (12b)$$

In this case the thickness of the laminar boundary layer increases with u_*.

The Reynolds number is defined by:

$$Re = \frac{u_* z_{0m}}{n}$$

(12c)

The wind generates waves on larger water bodies the wave height increases with wind speed for speeds larger than about 2 m s^{-1} and so does the roughness length. The surface roughness length at sea is (Joffre, 1988):

$$z_{0m} = \frac{an}{u_*} + \frac{bu_*^2}{g} \qquad (13)$$

where:

a = a constant (0.13)

b = a constant (0.0144); values between 0.012 and 0.035 are reported (Garratt,1992 cited in Heikinheimo et al., 1999)

g = acceleration due to gravity (9.80665 m s^{-2})

According to (13) z_{0m} decreases with u_* for wind speeds up to about 2 m s^{-1}. For larger wind speeds z_{0m} increases with u_* due to wave formation. A typical value for z_{0m} is 1×10^{-4} m.

Fig. 7 shows how r_b varies with u_* based on (12a) and (12b). This is a strange function which shows a ”jump” near a value of 0.06 m s^{-1} for u_* where the change from the parameterisation of the smooth to the rough surface occurs. For that reason it was felt that a further examination was needed. The curve is apparently based on wind tunnel experiments with thorium-B (^{222}Pb) vapour made by Chamberlain (1968). For rough surfaces measurements have only been made for roughness Reynolds numbers greater than 0.3, which is equivalent to u_* values greater than 0.12 m s^{-1}. Further it is known that for very low roughness Reynolds numbers the value of r_b becomes very large. The middle part of the curve is a form of interpolation that is maybe correct for water vapour, but apparently not for molecules with much higher molecular mass such as pesticides. There are apparently no data for this range. The nice thing is that Pb has a molecular mass of 207, which is representative of the molecular mass of pesticides. It was decided to use only the parameterisation of (z_{0m}/z_{0c}) for rough surfaces for the sea, as the sea is rough most of the time. If the friction velocity u_* becomes smaller than 0.12 m s^{-1} (Re = 0.3) in PESTDEP r_b is automatically set to the value for u_* = 0.12 m s^{-1}. Fig. 7 shows that r_b varies little with u_* for u_* values greater than 0.12 m s^{-1} (from 18 to 34 s m^{-1}).

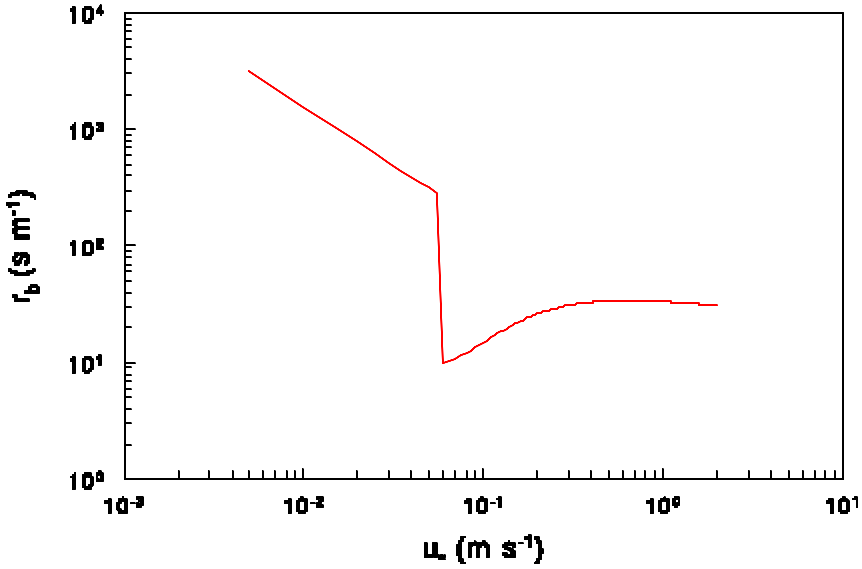

Figure 7. The laminar boundary layer resistance r_b for water as a function of the friction velocity u_* (molecular mass 300 g mol^{-1} and a temperature of 15°C).
Figur 7. Den laminære grænselagsmodstand r_b for vand som funktion af friktionshastigheden u_* (molekylmasse 300 g mol^{-1} og en temperatur på 15°C) .

As the sea is large it cannot be assumed that the friction velocity u_* at sea is the same as on land. For that reason u_* has to be corrected, e.g. by assuming that the wind speed at some height (e.g. 50 m) is the same as over land. With equation (3) this wind speed can be calculated knowing u_* and z_{0m} for land. The same equation can then be used to find u_* and z_{0m} for the sea from the wind speed at e.g. 50 m using equation (13) for z_{0m} in an iterative process.
In the version of PESTDEP that is integrated in PestSurf no deposition to the sea can be calculated.

2.6.2 Surface resistance for water

The surface resistance r_c for water is (see Appendix C):

$$r_c = \frac{K_H}{k_w} \tag{14}$$

where:
K_H = Henry's law coefficient (dimensionless); this is a measure of the solubility of the gas.
k_w = aqueous phase mass transfer coefficient (m s^{-1}); this is a measure of the transport velocity of the gas in water, which is a function of the mixing rate in the upper part of the water body.

Henry’s law coefficient is defined by:

$$K_H = \frac{equilibrium\ conc.\ in\ gas\ phase\ \left(kg\ m^{-3}\right)}{equilibrium\ conc.\ in\ aqueous\ phase\ \left(kg\ m^{-3}\right)} \qquad (15)$$

It should be noted here, that there are numerous definitions of Henry’s law coefficients, having different units and even different senses.

Equation (14) shows that the resistance for uptake decreases (the dry deposition velocity increases) with a decrease in K_H and an increase in k_w.

The mass transfer in the aqueous phase depends on the turbulence of the upper part of the water body. This turbulence is caused by the water currents and by the influence of the wind and by raindrops that are deposited onto the water (Banks and Herrera, 1977). Wind not only creates currents in the water, but can also lead to the formation of waves and air bubbles, that influence the mass transfer in the water phase. The waves depend in a complicated way on the wind speed, the fetch and surface contamination (affecting the surface tension of the water). It should be noted here, that in principle it is the wind speed relative to the flow velocity of the water (as vectors) that causes the part of the turbulence created by the wind.

Different mechanisms play a role in the mass transfer in the aqueous phase. For that reason we will in the following sections differentiate between:

- Rapidly running shallow waters like, shallow streams and rivers where the turbulence in the water is mainly created by the interaction of the current with rapidly varying depths and rocks and logs.
- Slowly running waters that are fairly deep or stagnant waters, where the turbulence in the water is mainly determined by the friction of the wind and related effects. These waters are e.g. slowly flowing rivers, lakes estuaries, and seas.

2.6.2.1 Mass transfer in the water phase in rapidly running shallow waters

The mass transfer in the aqueous phase is caused by turbulence at the water surface. In a rapidly running river turbulence is created by friction at the river bottom. The turbulence at the surface decreases for that reason with the depth of the river (O’Connor and Dobbins 1958). It should be noted that for that reason rivers with different bottoms have different turbulence at the surface if all other parameters are the same. The exchange is often expressed as in experimentally determined functions of the slope (the difference in water level between two points at the river, m m^{-1}), the flow velocity and the depth.

Schwarzenbach et al. (1993) came up with an expression for the mass transfer coefficient k_w (m s^{-1}) in the water phase using the surface renewal model (Danckwerts, 1951) and taking into account that the transfer decreases with the depth of the water:

$$k_w = \left(\frac{D_w u_w}{d_w}\right)^{\frac{1}{2}} \qquad (16)$$

where:

D_w = diffusivity of the gas in water ($m^2 s^{-1}$)
u_w = average water velocity ($m s^{-1}$)
d_w = average depth (m)

It should be noted that in this equation k_w increases with $D_w^{½}$.

Schwarzenbach et al. (1993) compared this expression with the measured rates of volatilisation of organic chemicals from streams and rivers and found that (16) underpredicts the measured volatilisation by a factor 2 or 3. They note that this is more than adequate having in mind that this equation does not take into account wind effects and effects of waterfalls. The weak point of this equation is, however, that k_w is not a function of the slope, which is a very important parameter which should be taken into account in this type of equations (Moog and Jirka, 1998). In principle the slope could be added to this equation, but in PESTDEP another method will be used.

The method used in PESTDEP is based on information on the exchange of oxygen between the atmosphere and the water (reaeration). Oxygen is a slightly soluble gas, and for slightly soluble gases the overall mass transfer (exchange between air and water) is dominated by the aqueous phase mass transfer. This means that for oxygen the mass transfer in the aqueous phase can be determined from experiments where the overall gas transfer is measured. This is an advantage as it is much easier to measure the overall gas transfer than the mass transfer in the aqueous phase. Moreover, there have been made so many reaeration measurements in rivers with different properties that it has been possible to generalise the results in experimentally determined functions for all types of rivers. For other gases experimental data are only available for a few rivers (Rathburn and Tai, 1982; Wanninkhof et al., 1990; Genereux and Hemond, 1992; Chapra and Wilcock, 2000), but not so many as for oxygen and they are more difficult to generalise.

For that reason it was decided to model the mass transfer of pesticides in the aqueous phase in rivers the same way as the mass transfer of oxygen taking into account that pesticides and oxygen have different diffusivities in water (see also Brumley and Jirka, 1988).

The relation between the mass transfer coefficients of a slightly soluble gas and that of oxygen is given by:

$$k_w(\text{compound}) = k_w(O_2)\left(\frac{D_w(\text{compound})}{D_w(O_2)}\right)^n \tag{17}$$

The stagnant two film model suggests that n = 1 whereas the surface renewal model suggests n = 0.5 (Genereux and Hemond, 1992). Smith et al. (1980) suggest a value of n of 0.6 based on laboratory measurements. Other experiments mentioned by Genereux and Hemond (1992) point to a value of 0.7. Genereux and Hemond (1992) mention also that the value of n is rather uncertain. In PESTDEP value of n is 0.5 is chosen, which is also used by Mackay and Yeun (1983), Cirpka et al. (1993) and Hibbs et al. (1998).

The relation between the mass transfer rate in the water phase and the reaeration coefficient is (Moog and Jirka, 1998):

$$k_w = K_{2s} d_w \tag{18}$$

where K_{2s} is the reaeration coefficient (s^{-1}).

Usually, however, this K_{2s} coefficient is given in day^{-1}. If it is now assumed k_w that is a function of $D_w^{½}$ the following relation can be found:

$$k_w(compound) = 1.16\times10^{-5} d_w K_{2d} \left(\frac{D_w(compound)}{D_w(O_2)} \right)^{\frac{1}{2}} \tag{19}$$

In this equation is K_{2d} the reaeration coefficient (day^{-1}), whereas k_w is in m s^{-1}. It should be noted that K_{2d} is usually given for a temperature of 20°C. This means that the diffusivities at 20 °C should be used in this equation. The diffusivity of O_2 in water at 20°C can be calculated from the diffusivity at 25°C (value: 2.20×10^{-9} m^2 s^{-1} given by Ferrell and Himmelblau, 1967). With the relations in Appendix B then a value of the diffusivity of O_2 of 1.92×10^{-9} m^2 s^{-1} at 20°C is found.

The reaeration coefficient is a function of the temperature, which reflects that the diffusivity of O_2 in water increases with temperature. The general relationship is:

$$\mathrm{K_{2d}(t) = K(20)}q^{(\mathrm{t}-20)} \tag{20}$$

where t is the temperature(°C) and θ is a temperature coefficient (dimensionless).
In the literature different experimentally values for θ presented. Churchill et al. (1962) found a value of 1.024 and Tsivouglou et al. (1972) determined a value of 1.022. It should be noted that if K_{2d} would be a function of the square root of the diffusivity only (which is a function of the temperature and the viscosity of water, see Appendix B) θ would be about 1.016 (for temperature range 0-20°C). In PESTDEP a value of 1.024 is used. The final expression of the mass transfer coefficient in water is found from (19), (20) and the diffusivity of O_2 in water at 20 °C:

$$\mathrm{k_w(t) = 0.265 d_w K_{2d} D_w(gas)^{½}}q^{(\mathrm{t}-20)} \tag{21}$$

It should be noted that in this equation the units of k_w in this equation are in m s^{-1} whereas the units of K_{2d} are in day^{-1}. This is done because they are usually given in these units.

In the literature numerous parameterisations of reaeration coefficients can be found. This reflects partly the variety of streams that can be found. Moog and Jirka (1998) compared various proposed parameterisations with different experimental data sets and found that the slope should be included in the parameterisations to obtain a good result. For low slope streams (slope < 0.0004 m m^{-1}) the predictive relationships were not adequate and suggest that K_{2d} may be controlled by other variables such as bed type, roughness, wind shear or surfactants. For this group of streams the geometric average value of the measured K_{2d} (1.8 day^{-1}) did describe the reaeration better than any predictive equation.

They also noted that the relationships of O'Connor and Dobbins (1958) and of Churchill et al. (1962) that are among the most frequently applied, but do not include the slope, have little or no predictive value for streams of all types of slopes. One of the relationships that showed the most reasonable agreement with measured data for all slopes was of Cadwallader and McDonnell (1969):

$$K_{2d} = 186(u_w I)^{0.5} d_w^{-1} \tag{22}$$

where I = slope (m m^{-1}).

As the relationships of O'Connor and Dobbins (1958) and Churchill et al. (1962) are among the most known they will be given below, but they should preferably not be used, because they do not contain information on the slope. The relationship of O'Connor and Dobbins (1958) is often used for ordinary rivers and is given by:

$$K_{2d} = 3.9\, u_w^{0.5} d_w^{-1.5} \tag{23}$$

The relationship of Churchill et al. (1962) is often used for rivers with high flow velocities and is given by:

$$K_{2d} = 5.01 u_w^{0.969} d_w^{-1.673} \tag{24}$$

In Denmark streams are small and are in most cases dominated by macrophytes. For this type of streams Thyssen and Erlandsen (1987) derived the following expression for K_{2d} based on measurements with different methods using 144 measurements:

$$K_{2d} = 8784 u_w^{0.734} d_w^{-0.420} I^{0.930} \tag{25}$$

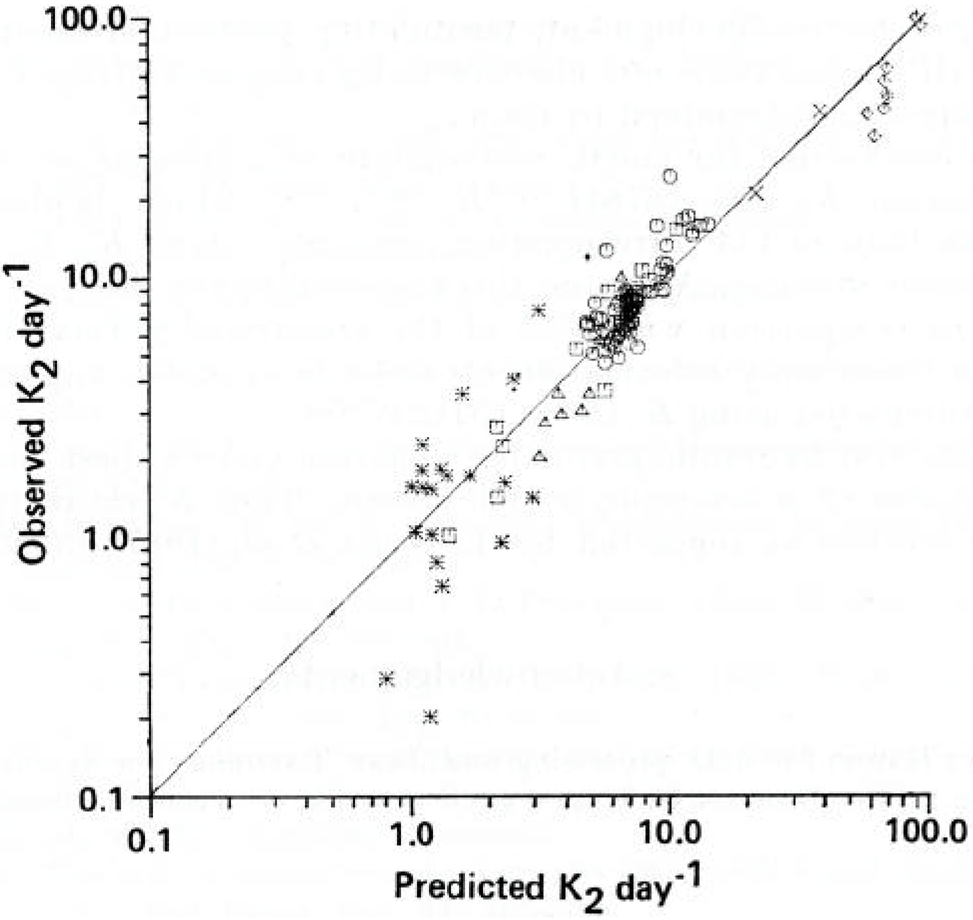

Figure 8. Predicted vs. observed K_{2d} for Danish streams (Thyssen and Erlandsen, 1987).
Figur 8. Modellerede vs. målte K_{2d} for danske vandløb (Thyssen and Erlandsen, 1987).

It should be noted here that this relationship includes information on the slope that according to Moog and Jirka (1998) is very important in general. Thyssen's relationship was based on streams with the characteristics presented in Table 1a.

Table 1a. Minimum and maximum parameter values used in the reaeration model of Thyssen and Erlandsen (1987).
Table 1a. Minimum og maksimum parameter værdier anvendt i Thyssen og Erlandsens (1987) iltningsmodel.

Parameter	Minimum value	Maximum value
Flow velocity (m s^{-1})	0.06	0.52
Depth (m)	0.12	1.37
Slope (m m^{-1})	3×10^{-4}	7.4×10^{-3}

Fig. 8. shows that the predicted values for K_{2d} for the Thyssen and Erlandsen parameterisation agree well with the measurements for the range from 3-15 day^{-1}, but that the model does not predict K_{2d} well for low (< 3 day^{-1}) and high (> 30 day^{-1}) reaeration rates.

It should be noted here that the gas exchange in rivers can be strongly influenced by hydraulic controls such as weirs, falls, or even cascades. In such a situation the gas exchange is strongly dominated by the entrainment of air bubbles, at least for compounds with smaller Henry's law coefficients (Cirpka et al., 1993).

In PESTDEP it is possible to choose one of the parameterisations of K_{2d} that is presented in this section. In the version of PESTDEP that is integrated in PestSurf no choice can be made and only the Thyssen and Erlandsen parameterisation is used because this tool is applied for Danish conditions.

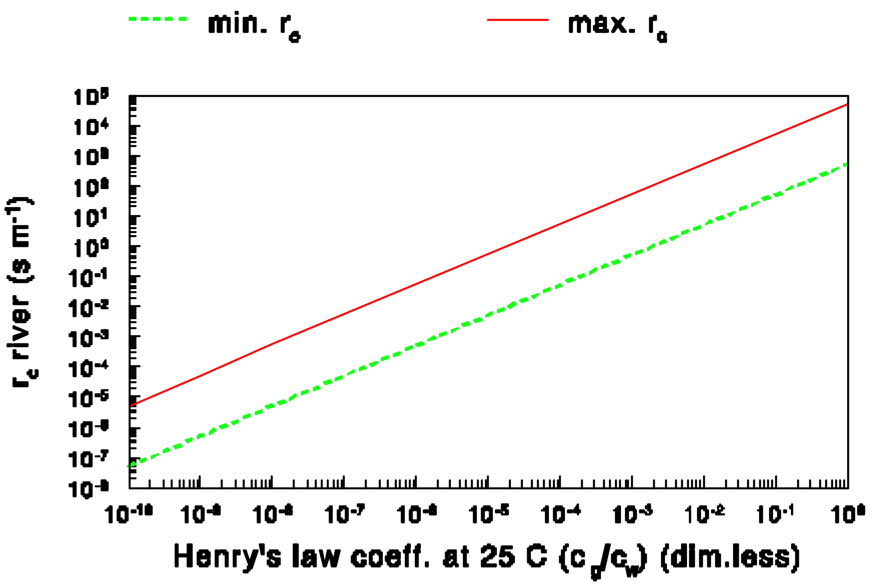

Figure 9. The surface resistance r_c for streams at 15°C as a function of Henry's law coefficient at 25°C for K_{2d} values of 1 and 100 day^{-1}, which is a representative range for Danish streams.
Figur 9. Overflademodstanden r_c for vandløb ved 15°C som funktion af Henry's lov konstant ved 25°C for K_{2d} værdier på 1 og 100 dag^{-1}, som er repræsentative for danske vandløb.

Fig. 9 shows how r_c depends on the Henry's law coefficient for typical range of values of K_{2d} measured by Thyssen and Erlandsen (1987) (1 and 100 day^{-1}). The calculations were made for a temperature of 15°C and a water depth of 1.37 m. As Henry's law coefficient K_H is usually only known for 25°C it was decided to plot r_c as a function of K_H at this temperature. In order to find Henry's law coefficient at 15°C a correction for the difference in temperature was made assuming at heat of dissolution of –68000 J mol^{-1} (see Appendix A).

It should be noted, that the Lillebæk stream on the island of Funen, for which the pesticide input is modelled within the integrated project is a shallow stream with a very steep slope and a high flow velocity, which often are outside the range for which the Thyssen and Erlandsen (1987) relation is valid. A K_{2d} value of the order of 300 day^{-1} is often calculated for this stream.

In the version of PESTDEP that is integrated in PestSurf K_H at 15°C is used which is calculated from K_H at 25 °C assuming a heat of dissolution of –68000 J mol^{-1} (see Appendix A and G).
Fig. 9. shows that there can be up to a factor of 100 difference in r_c or k_w for Danish streams due to variations in K_{2d} that are cause by variations in the flow velocity, depth and slope.

2.6.2.2 Mass transfer in the water phase in lakes and slowly running waters

The aqueous phase mass transfer coefficient for situations for which the turbulence is mainly caused by the wind is proportional to Sc_w^{-n}, where Sc_w is the Schmidt number in the water phase:

$$\mathrm{Sc_w} = \frac{\nu_w}{\mathrm{D_w}} \tag{26}$$

where:
ν_w = kinematic viscosity of water (m^2 s^{-1})
D_w = diffusivity of the gas in the water phase (m^2 s^{-1}) (see Appendix B)

Jähne et al. (1987) found that at low wind speed n = 2/3 and at higher wind speed n = 1/2. Csanady (1990) showed that a value of n = 2/3 is correct when the flow is adjacent to a solid boundary and a value of n = 1/2 is correct when the flow is adjacent to a fluid boundary. Field experiments show that in most cases n = 1/2 is appropriate (MacIntyre et al., 1995). This relation holds for lakes, estuaries and seas.

An empirical relationship is used to describe the aqueous phase mass transfer coefficient for lakes, based on experimental data for 5 lakes (MacIntyre, 1995):

$$k(600) = 1.25\times10^{-6} k_4 u(10)^{1.6} \tag{27}$$

where:
k(600) = the aqueous phase mass transfer coefficient of CO_2 at 20°C in freshwater (m s^{-1})
k_4 = constant necessary to obtain the right dimensions. Its value is 1.0 and its dimension is s$^{1.6}$ m$^{-1.6}$.
u(10) = wind speed at 10 m height (m s^{-1}); the wind speed has usually measured on land near to the lake.

The reason to use k(600) in this equation is that the aqueous phase mass transfer coefficient is often normalised to Sc_w = 600, which is the Schmidt number of CO_2 at 20°C in freshwater. By normalising the results of exchange experiments for different gases can be easily compared. The aqueous phase mass transfer coefficient for other gases can be easily calculated from k(600) with the following relation:

$$\mathrm{k_w} = \mathrm{k}(600)\left(\frac{600}{\mathrm{Sc_w}}\right)^{1/2} \tag{28}$$

where k_w is the aqueous mass transfer coefficient of the gas (m s^{-1}).

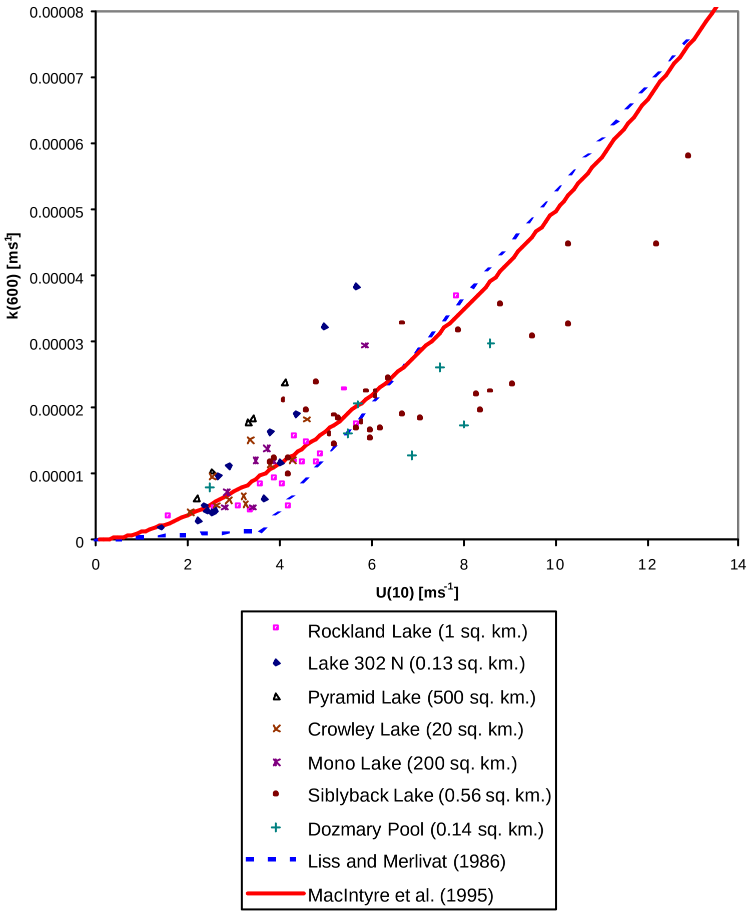

Figure 10. k(600) as a function of wind speed at 10 m height for lakes and functional relationships given by MacIntyre et al. (1995) and Liss and Merlivat (1986).
Figur 10. k(600) som funktion af vindhastigheden i 10 m højde for søer samt funktionel sammenhæng givet af MacIntyre et al. (1995) og Liss og Merlivat (1986).

There are a few more measurements of k(600) for lakes than MacIntyre et al., 1995) have used to find their experimental relation between k(600) and and u(10). Figure 10 includes all measurements and shows that the relation of MacIntyre et al. (1995) also gives a reasonable description of k(600) for the additional experiments (Siblyback Lake and Dozmary Pool). For that reason the relation of MacIntyre was adopted to model k(600) for lakes. It shows that the uncertainty in k(600) is often a factor of 2-3. According to MacIntyre (1995) the average value of k(600) for the duration of each experiment (1-3 months) shows that there is a tendency that k(600) increases with lake size. All references and data can be found in Appendix D.

In Fig. 10 also the relation of Liss and Merlivat (1986) is given, which has not only been used for seas but also for lakes. It is given by:

$$\begin{aligned}
&k(600) = 4.72\times10^{-7}\ u(10) && \text{for } u(10) \le 3.6 \\
&k(600) = 7.92\times10^{-6}\ u(10) - 2.68\times10^{-5} && \text{for } 3.6 < u(10) \le 13 \qquad (29) \\
&k(600) = 1.64\times10^{-5}\ u(10) - 1.37\times10^{-4} && \text{for } u(10) > 13
\end{aligned}$$

In this equation k(600) and u(10) are in m s^{-1}.

MacIntyre et al. (1995) suggest that the Liss and Merlivat (1986) relation underestimates gas transfer on lakes at low wind speeds and overestimates it at higher wind speeds.

Fig. 11 shows r_c as a function of Henry's law coefficient K_H for different wind speeds. It can be seen that r_c increases with K_H and decreases with wind speed.

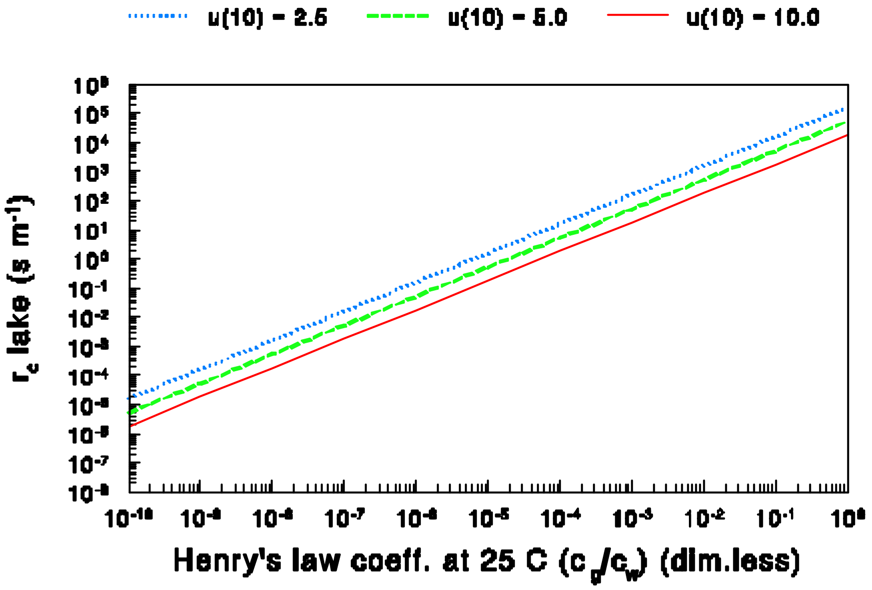

Figure 11. The surface resistance r_c for lakes at 15°C as a function of Henry's law coefficient at 25°C for different wind speeds

Figur 11. Overflademodstanden r_c *for søer ved 15°C som funktion af Henry's lov konstant ved 25°C for forskellige vindhastigheder.*

2.6.2.3 Mass transfer in the water phase in sea areas

Experimental information on the relation between k(600) and u(10) for sea areas was collected and is presented in Appendix D. All references and data used can be found there. Fig.12 summarises these data. It shows that there is a large scatter and that there are almost no measurements at wind speeds less than 5 m s^{-1}. The Liss and Merlivat (1986) relation between k(600) and u(10) gives a reasonable description. There is, however, a tendency, that it underestimates the more recent measurements (Southern North Sea, Equatorial Pacific Ocean). Also here there is an uncertainty of a factor of 2-3. So to start with the relation of Liss and Merlivat can be used to describe the mass transfer coefficient in the aqueous phase.

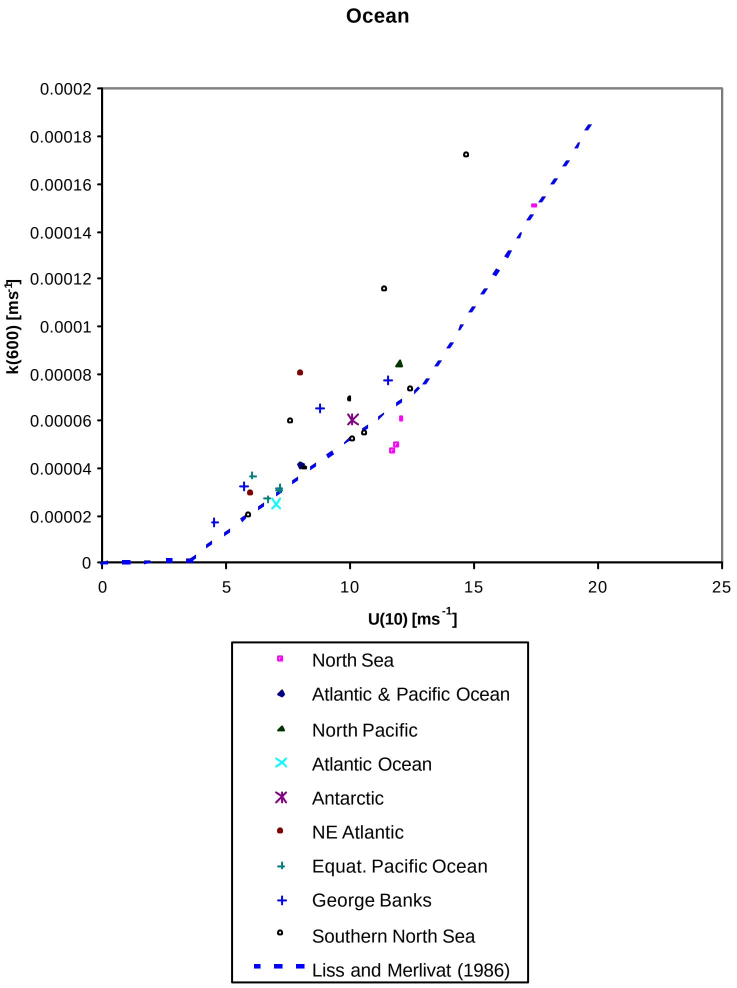

Figure 12. k(600) as a function of wind speed at 10 m height for sea areas and the relation of Liss and Merlivat (1986).
Figur 12. k(600) som funktion af vindhastigheden i 10 m højde for havområder og Liss og Merlivats (1986) funktion.

Fig. 13 shows r_c as a function of Henry's law coefficient K_H for different wind speeds. The surface resistance r_c increases with K_H and decreases with wind speed.

In PestSurf only deposition of pesticides to streams and lakes is included. For that reason the version of PESTDEP that is integrated in PestSurf does not include the parameterization of the deposition of pesticides to the sea that is presented here.

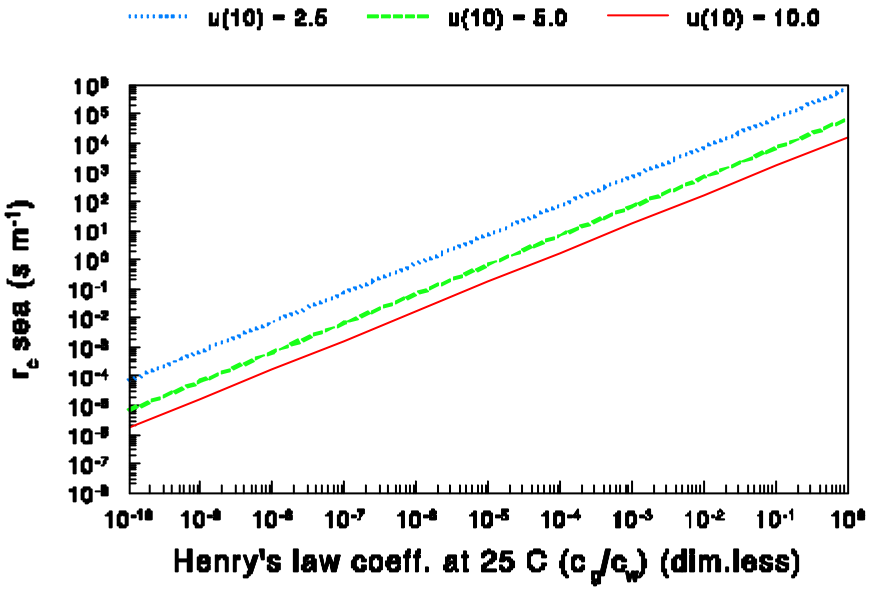

Figure 13. The surface resistance r_c for seas at 15°C as a function of Henry's law coefficient at 25°C for different wind speeds.
Figur 13. Overflademodstanden r_c for havområder ved 15°C som funktion af Henry's lov konstant ved 25°C for forskellige vindhastigheder.

2.6.2.4 Comparison of r_c for different water bodies

Fig. 14 shows r_c as a function of K_H for different water bodies. It summarises (parts of) the Figs. 9 and 11. For rivers values representative values for the minimum and maximum r_c are given for Danish streams (for a K_{2d} of 100 respectively 1
day^{-1} and a water depth of 1.37 m). The function of r_c for lakes for a wind speed of 5 m s^{-1} is also given and has about the same value as the maximum r_c for rivers. This means that under the same conditions the dry deposition to small lakes will be less than to rivers. It can therefore be concluded that the turbulence generated by the interaction of the current with the bottom in streams is apparently larger than the turbulence by the wind. The values of r_c for seas is about the same as for lakes and is for that reason not shown in Fig 14. A wind speed of 5 m s^{-1} represents approximately the average situation in Denmark.

2.6.2.5 Comparison of r_c and r_b for water bodies

If r_c is larger than r_b the dry deposition is limited by mixing in the water phase. If r_c is much larger than r_b the dry deposition will always be limited by mixing in the water phase and almost not be influenced by meteorological conditions. If r_b is larger than r_c the dry deposition will be limited by the laminar boundary layer resistance and will be highly dependent on meteorological conditions.

In the version of PESTDEP that is integrated in PestSurf r_b values of 79 (area with crops) and 107 s m^{-1} are used (fallow soil). These values are representative of average Danish conditions (see Appendix G how the friction velocity u_* used in the equation (11) is derived). In Fig. 14 r_b for average Danish conditions is indicated as well (a value of 93 s m^{-1} is presented, being the average of 79 and 107 s m^{-1}). This figure shows that dry deposition is limited by mixing in the water phase for K_H values larger than about 2×10^{-3} (for rivers with a maximum r_c and small lakes) or 0.2 (rivers with a minimum r_c). It should be mentioned here, that for some water bodies the value may be lower than 2×10^{-3}, depending on the combination of flow, slope and depth.

It should be noted here, that Denmark consists of a peninsula and islands and that one is never far from the sea, which leads to a rather windy climate. In central Europe e.g. the average wind speed would be more of the order of 2 m s^{-1} (in stead of 5 m s^{-1}). This would lead to both higher values of r_c for lakes (but not necessarily for rivers) and also to higher values for r_b than for Denmark. It should also be mentioned here, that a reduced wind speed in principle also will lead to a lower emission, a phenomenon that cannot be modelled with the empirical equations that are used to estimate the accumulated emission in this report.

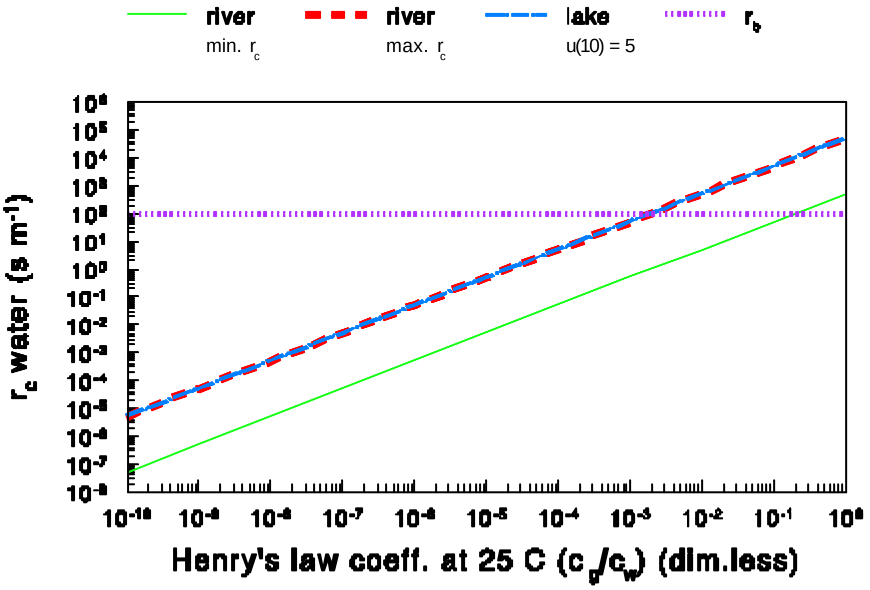

Figure 14. The surface resistance r_c for different water bodies at 15°C as a function of Henry's law coefficient (K_H) at 25°C and a laminar boundary layer resistance r_b representative of average Danish conditions. Note that r_c is a function of Henry's law coefficient, but r_b is not.

Figur. 14. Overfladемodstanden r_c for forskellige vandtyper ved 15°C som funktion af Henry's lov konstant (K_H) ved 25°C og en laminære grænselagsmodstand r_b, som er repræsentativ for danske forhold. Bemærk at r_c er en funktion af Henry's lov konstant, mens r_b ikke er.

To know whether the dry deposition is limited by r_b or r_c the Henry's law coefficient for 316 often used pesticides was examined (Fig. 15). These data were mainly taken from Smit et al. (1998). These pesticides are the same for which calculations are presented in Appendix E. The distribution of Henry's law coefficients shows that most pesticides have a Henry's law coefficient less than 2×10^{-3}. This means that in general r_b will be larger than r_c, i.e. the resistance dry deposition of pesticides to water bodies will in general be limited by the laminar boundary layer resistance, i.e. by the transport in the air and not by uptake by the water. It should be noted that it is assumed that the mass accommodation coefficient of these pesticides is so large that it does not influence the uptake and that no reaction in water occurs (see Appendix C for a discussion). Occurrence of a fast reaction in water will lead to smaller r_c values.

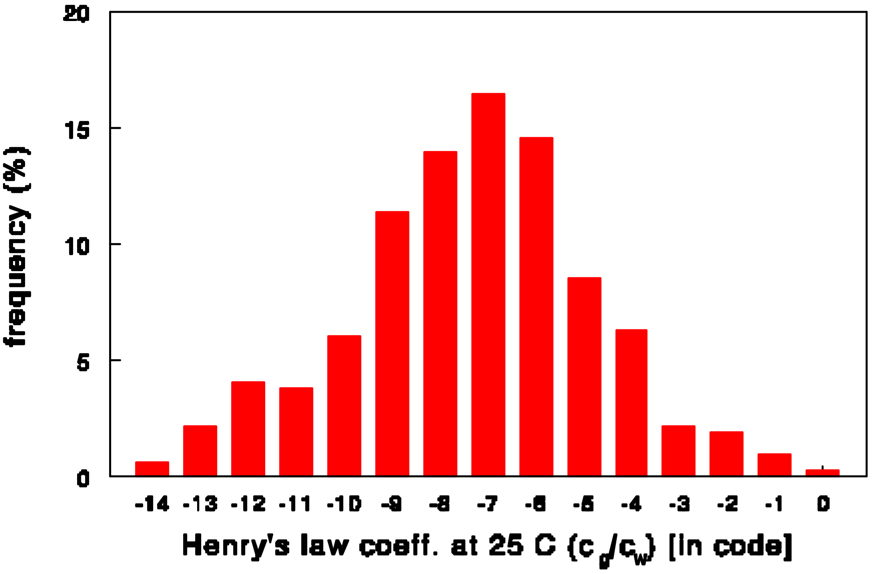

Figure 15. Frequency distribution of Henry's laws coefficients for 316 pesticides, mainly from Smit et al. (1998). Code: -14 = from 1×10^{-14} to 10×10^{-14} (=1×10^{-13}), -13 = from 1×10^{-13} to 10×10^{-13} (=1×10^{-12}) etc.
Figur 15. Frekvensfordelingen af Henry's lov konstant for 316 pesticider, hovedsagelig fra Smit et al. (1998). Kode: -14 = fra 1´10^{-14} til 10´10^{-14} (=1´10^{-13}), -13 = fra 1´10^{-13} til 10´10^{-13} (=1´10^{-12}) osv.

Table 2. Sales statistics and physico-chemical properties of pesticides that were sold in the year 2000 in Denmark in the large quantities.
Tabel 2. Salgsstatistik og fysisk-kemiske egenskaber for pesticider, som i 2000 blev solgt i større mængder i Danmark.

Compound	Sales in 2000 (kg act. ingr.)	Molecular weight (g mol^{-1})	Vap. press. (mPa) 20-25°C	Sol. (mg l^{-1}) 20-25°C	K_H (c_g/c_w) 20-25°C
bentazone	47773	240.3	4.6×10^{-1}	570	7.96×10^{-8}
bromoxynil	42327	276.9	1	130	1.05×10^{-6}
dimethoate	26610	229.2	1.1	23800	2.25×10^{-9}
diuron	30500	233.1	9.2×10^{-3}	42	1.30×10^{-8}
fenpropimorph	118648	303.5	2.3	4.3	6.66×10^{-5}
ioxynil	39468	370.9	1	50	3.66×10^{-6}
MCPA	146514	200.6	2.3×10^{-2}	734	3.1×10^{-9}

metamitron	100065	202.2	8.6×10^{-4}	1700	4.2×10^{-11}
pendimethalin	243256	281.3	4	0.3	7.96×10^{-4}
propiconazole	29847	342.2	5.6×10^{-2}	110	3.7×10^{-8}
terbutylazine	59263	229.7	1.5×10^{-1}	8.5	8.6×10^{-7}

In Table 2 the properties of all pesticides that were sold in the large quantities in Denmark in the year 2000 are presented (values from Smit et al., 1998). These results show that the Henry's law coefficient K_H is less than 2×10^{-3} for all these pesticides. This means that for all these pesticides the dry deposition to water bodies is limited by the laminar boundary layer resistance (transport in the air). The only compound for which a small but notable resistance in the water can be expected in some cases is pendimethalin and to a minor extent fenpropimorph.

2.7 Results for example situations

Example runs were made to calculate the dry deposition of 316 pesticides to different water bodies for a situation where the emission originated from application of pesticides to crops and to fallow soil. The details of these calculations are given in Appendix E.

It was assumed here that the mass accommodation coefficient of the pesticide is so large that it does not have an influence on the uptake and that no fast reaction occurs in the water phase. If such a reaction occurs the uptake rate increases (this e.g. the case for bentazone).

Here follows a short summary for those pesticides that were sold in large quantities in Denmark in the year 2000 (Table 3). It was assumed here, that all pesticides were applied to crops, which is true in most cases. But some pesticides may be applied in early growth stages of the plants and for that reason the parameterisation for crops may be less appropriate.

The water bodies were:

- A stream for which the surface resistance r_c is small. A flow velocity of 0.52 m s^{-1}, a depth of 1.37 m and a slope of 7.4×10^{-3} m m^{-1} was adopted. This gives a reaeration coefficient K_{2d} of about 44 day^{-1} with the Thyssen and Erlandsen (1987) parameterisation. This is a rather large value and this leads to a rather small surface resistance, leading to an upper estimate of the dry deposition to the river. The width of the non-spray zone is 1.5 m (FOCUS scenario for winter cereals) and the width of the stream is also 1.5 m.
- A stream for which the surface resistance r_c is large. A flow velocity of 0.06 m s^{-1}, a depth of 0.12 m and a slope of 3×10^{-4} m m^{-1} were adopted. This gives a reaeration coefficient K_{2d} of about 1 day^{-1} with the Thyssen and Erlandsen (1987) parameterisation. This is a rather low value and this leads to a rather high surface resistance, leading to a lower estimate of the dry deposition to the stream. The width of the non-spray zone is 1.5 m (FOCUS scenario for winter cereals) and the width of the stream is also 1.5 m.
- A situation for a pond with a wind speed at 10 m height of about 5 m s^{-1}. The width of the non-spray zone is 3.5 m (FOCUS scenario for winter cereals) and the width of the pond is 30 m.

- A situation for a ditch with a wind speed at 10 m height of about 5 m s^{-1}. The width of the non-spray zone is 1 m (FOCUS scenario for winter cereals) and the width of the ditch is 1 m.

Table 3 gives the following information:

1. Name of the compound.
2. Accumulated emission of the pesticide (in % of the dose).
3. Accumulated flux of the pesticide (kg m^{-2}) to the water body expressed as a percentage of the dose flux (kg m^{-2}). This is the average flux over the whole width of the river. This number can be compared directly to the spray drift flux.

Table 3 shows e.g. that if 10^{-4} kg m^{-2} bentazone is applied, 2.07 % of that amount has been dry deposited per m^{-2} of water surface in a stream with a small r_c , i.e. 10^{-4} 2.07×10^{-2} kg m^{-2} = 2.07×10^{-6} kg m^{-2}.

Table 3. Sales in 2000 in Denmark, accumulated emission flux and accumulated flux to water body expressed as a function of the dose for the pesticides that are sold in large quantities in Denmark. It is assumed here that the pesticides are applied to crops. Note: the numbers are given much more accurately than they actually are known.

Tabel 3. Salgsstatistik for 2000 for Danmark samt akkumulerede emissionsfluks og akkumulerede fluks til vand som funktion af dosen for pesticider, som blev solgt i større mængder. Bemærkning: tallene er gengivet mere nøjagtigt end de er kendt i virkeligheden.

Compound	Sales in 2000 (kg active ingr.)	% of the dose that volatilises	Accumulated flux to water as % of the dose			
			stream small r_c	stream large r_c	pond u(10)= 5 m s^{-1}	ditch u(10)= 5 m s^{-1}
bentazone	47773	17.14	2.07	2.07	1.09	2.18
bromoxynil	42327	24.61	2.84	2.82	1.50	2.99
dimethoate	26610	18.97	2.33	2.33	1.23	2.45
diuron	30500	2.04	0.25	0.25	0.13	0.26
fenpropimorph	118648	36.28	4.06	2.56	2.01	3.95
ioxynil	39468	24.61	2.58	2.52	1.37	2.71
MCPA	146514	4.24	0.54	0.54	0.29	0.57
metamitron	100065	0.92	0.12	0.12	0.06	0.12
pendimethalin	243256	24.62	3.92	0.60	1.22	2.35
propiconazole	29847	4.74	0.51	0.51	0.27	0.54
terbutylazine	59263	7.50	0.92	0.91	0.48	0.97

It can be concluded that the accumulated dry deposition flux averaged over the whole width of the water body varies from 0.1 to 4% of the dose. For most pesticides the accumulated flux is the same for a stream with a small and a large surface resistance (r_c). This is cause by the fact, that the dry deposition flux for those pesticides is mainly determined by the laminar boundary resistance in the air (r_b) and not by the surface resistance of the stream which is a function of the flow, slope and depth of the water body. The accumulated dry deposition flux to a pond averaged over the whole width of the pond is

about half the accumulated dry deposition flux to a ditch. This is cause by the following:
The non-spray zone near the pond is larger (3.5 m) than near the ditch (1 m). The width of the pond (30 m) is larger than the width of the ditch (1 m). At a larger distance from the field where the emission occurs the concentrations in the air will be lower due to vertical mixing. This leads to a lower deposition flux.

2.8 Possibilities for generalisation

For most pesticides the laminar boundary layer resistance (r_b) limits the dry deposition flux to the water body. This means that the dry deposition flux does not depend on the properties of the water body. The laminar boundary layer resistance only shows a limited variation with the molecular weight of the pesticide (30% over the range 200 g mol^{-1} to 400 g mol^{-1}). Assuming a molecular weight of 300 g mol^{-1} would therefore lead to a very reasonable guess for r_b that can be used for all pesticides for which the flux does not depend on the properties of the water body. For the same meteorological conditions, the same width of the non-spray zone and the same width of the water body it is then possible to generalise the results: they then only depend on the accumulated emission flux.

2.9 Dependence on the wind speed

If it is assumed that the surface resistance r_c is low, which is the case for most pesticides, then the deposition to a water body is limited by the surface resistance r_b (see section 2.8). A reduction in wind speed by a factor two will in principle lead to a doubling of the concentration, if the emission rate remains constant and the atmospheric stability does not change. Such a reduction will also lead to a doubling of r_b, i.e. reducing the dry deposition by a factor of two. The net result of this is that a reduction of the wind speed will not have any effect on the dry deposition to water bodies provided the emission rate is constant. So the ratio dry deposition to a water body/emission does not depend on wind speed for the same atmospheric stability. This last result was also confirmed by a test-run with the model PESTDEP.

In reality the emission rate itself is not constant, but increases with wind speed. With the same amount of pesticide on the crop a reduction of the wind speed by a factor two is likely to lead to a reduction in the emission rate of a factor two. But if the wind speed is lower for a longer period other (loss) processes than volatilisation may play a role that may have an influence on the emission rate. We are currently unable to model the effects of changes in wind speed on the accumulated emission.

2.10 Effect of the upwind field length

Spray drift is transport of pesticides in drops generated during spraying. Just as with dry deposition of gaseous pesticides the compound has to be transported to the water body by the wind. The main difference is that the transport to the surface of spray droplets is mainly caused by gravitation. The droplets fall down with a reasonably high speed and for that reason almost all have reached the surface within 30 m distance of the point of release. This means that only pesticide applied within 30 m upwind distance lead to measurable spray drift. Gaseous pesticides are transported to the surface by atmospheric turbulence, which occurs at a lower speed. For that reason gaseous pesticides are airborne for a much longer time and can be transported over much longer distances than spray drift droplets. This means that the upwind length of the field onto which a pesticide is applied has a large influence on the deposition to a water body, whereas this is unimportant for spray drift.

In this section the influence of the upwind length of the field onto which a pesticides is applied is discussed. This is done for a highly soluble pesticide for which the surface resistance r_c is negligible compared to the laminar boundary layer resistance r_b (this holds for many pesticides). The resistance r_b has the same value for all types of water bodies (streams, ditches, lakes) for the same meteorological conditions. This makes it possible to generalize the results. The dry deposition to the water body as function to the upwind edge of the water body was calculated for different upwind field lengths. This was done for the following conditions: a neutral atmosphere, a surface roughness of 0.1 m, a mixing height of 500 m, no non-spray zone, a gaseous pesticide with a molecular weight of 300, the same uniform emission density all over the field in all cases. The accumulated dry deposition per m^{-2} of water is divided by the accumulated emission per m^{-2} surface of the field onto which the pesticide is applied. This ratio is independent of the wind speed (see section 2.9). It should be noted that the absolute amount of pesticide that is released increases in these calculations linearly with the length of the field and that for that reason the dry deposition per m^{-2} of water increases with the field length (the emission m^{-2} is the same everywhere in the field). It is assumed that no net dry deposition occurs on the field.

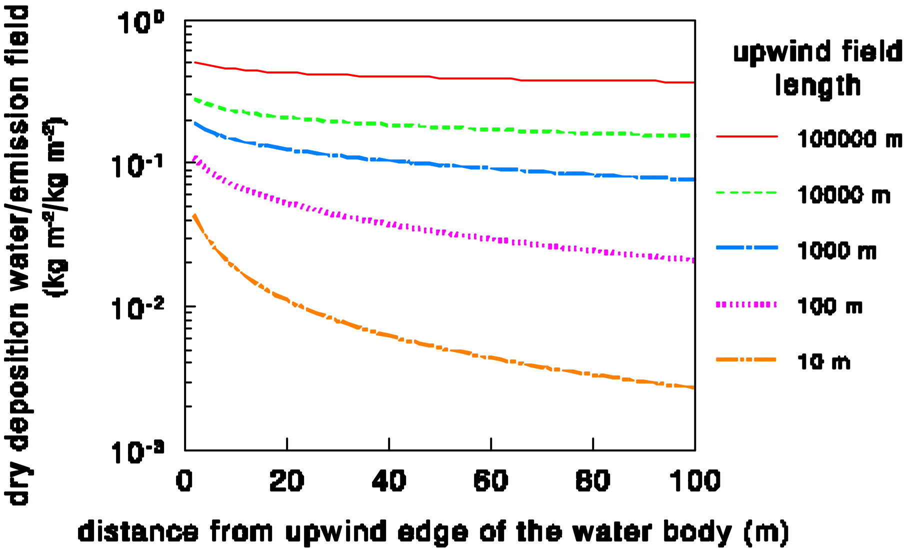

Figure 16. Ratio accumulated dry deposition m^2 water body/accumulated emission m^2 field as a function of the distance to the upwind edge of the water body for highly soluble pesticides (r_c << r_b) and different upwind lengths of the emission field. The situation

is without any non-spray zone. The first point in the graph is at 2 m distance from the edge.

Figur 16. Forholdet akkumuleret tørdeposition m^{2} vandløb eller sø/akkumuleret emission m^{-2} på marken som funktion af den vindopstrøms længde af vandløbet/søen for letopløselige pesticider ($r_c << r_b$) og marker med emission med forskellig vindopstrøms længde. Der findes ikke en sprøjtefri zone. Det første punkt i grafen er på 2 m's afstand fra bredden.

Fig,.16 shows that the deposition increases with the upwind length of the field with a uniform emission density (emission m^{-2}). As the scale on the y-axis is logarithmic the curves should be parallel if the ratio between the values would not change with the distance. This is not the case. The reason for this is that if the field length is short, the pesticide concentration in the air decreases rapidly with distance due to vertical mixing in the air. For long field lengths the pesticide is vertically well mixed and its concentration decreases slowly with distance.

It should be noted that for these calculations, as for all other calculations presented in this report the theoretical value of the eddy diffusivity was increased by 30% to match the results of the experiment mentioned in section 2.3. This means that the dry deposition presented here could be somewhat underestimated.

2.11 Effect of the length of the non-spray zone

In this section the effect of varying upwind lengths of the non-spray zone is discussed. The calculations were made for the same conditions as mentioned in 2.10 (but with a non-spray zone of course). To make the results comparable the upwind length of the field on which the emission occurred was set to 100 m for all cases. This means that the absolute emission is the same for all lengths of the non-spray zone.

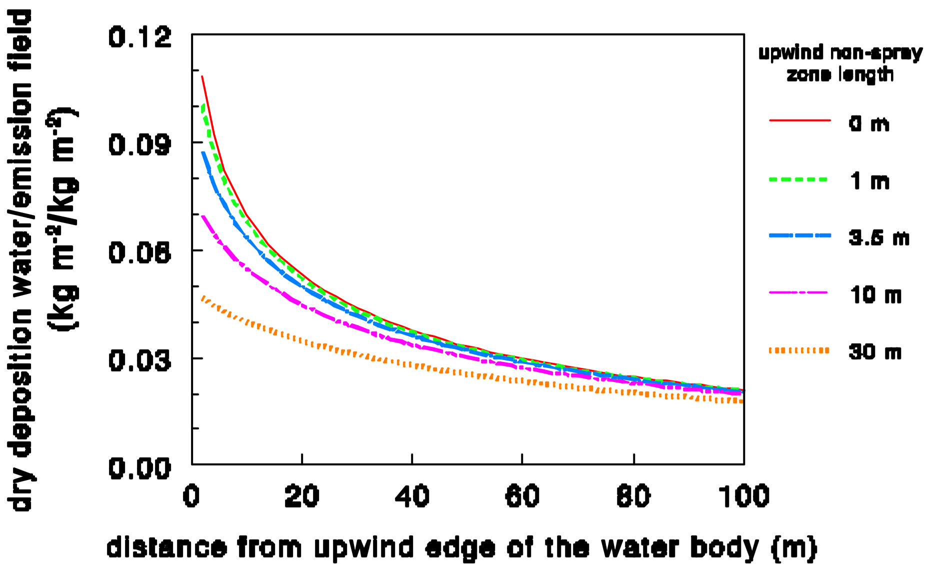

Figure 17. Ratio accumulated dry deposition m^2 water body/accumulated emission m^2 field as a function of the distance to the upwind edge of the water body for highly soluble pesticides ($r_c << r_b$) and different upwind lengths of the non-spray zone. The upwind length of the emission field is 100 m in all cases. The first point in the graph is at 2 m distance from the edge.
Figur 17. Forholdet akkumuleret tørdeposition m^2 vandløb eller sø/akkumuleret emission m^2 på marken som funktion af den vindopstrøms længde af vandløbet/søen for letopløselige pesticider ($r_c << r_b$) og marker med emission med forskellig længde af sprøjtefrie zone. Vindopstrømslængden af marken med emissioner er 100 m i alle tilfælde. Det første punkt i grafen er på 2 m's afstand fra bredden.

Fig. 17 shows that the presence of non-spray zones of 1-3.5 m as used in the FOCUS scenario's has limited influence on the dry deposition of pesticides to water bodies; this in contrary to the influence on spray drift (see section 3.1.10). This is caused by the fact that gaseous pesticides are transported further away than spray drift. For larger upwind field lengths than 100 m this difference becomes even less. The dry deposition to the water body at 2 m from the upwind edge with non-spray zones of 1, 1.5, and 3.5 m are respectively 8, 11 and 20% less than in the case without a non-spray zone.

2.12 Parameter choice in the decision tool PestSurf

In the decision tool PestSurf that is being developed for the Danish Environmental Protection Agency to evaluate the risk of transport of pesticides to water bodies a special version of PESTDEP is used. In that version the user can only choose a limited number of parameters. The other parameters are set so that they reflect average Danish conditions. The selection of the parameters that are fixed is documented in Appendix G.

3 Spray drift

3.1 Spray properties

3.1.1 Equipment

Pesticides are applied in dose rates ranging from a few grams formulated product per hectare. Such small amounts cannot be applied with the equipment normally used for pesticide application.

Before pesticides are applied they are generally diluted with water in order to obtain a liquid amount that can be distributed evenly on the sprayed area/crop with the aimed dose of pesticide.

Pesticide application under field conditions is generally carried out with different types of tractor-mounted or self-propelled sprayers. Boom sprayers are used in annual crops with a limited height and in perennial crops in the establishment stages. This includes all agricultural crops, field grown vegetables, plantations of bush fruit and Christmas trees. Boom sprayers consist of a vertical boom placed perpendicular to the driving direction. The boom is equipped with atomisers along it which have two functions.

1) To atomise the spray liquid into droplets that can effectively be transferred and deposited on the spray target, and
2) To distribute the spray liquid evenly below the boom.

The hydraulic nozzle is by far the most common atomiser type on the Danish market. Different designs exist. The design decides the spray angle, the droplet size distribution and the droplet speed. These characteristics all influence the potential spray drift during an application as discussed later.

When the spray liquid under pressure passes the nozzle orifice a liquid sheet is created. The actual droplet formation takes place outside/below the nozzle where the liquid sheet is broken up into individual droplets. The normal nozzle orientation is with the outlet facing vertically downwards.

Different boom sprayers with alternative atomiser systems such as the air-sprayer from Danfoil and the Twin-fluid nozzles have a small percentage of the market. The droplet characteristics from these systems are somewhat different than that from hydraulic nozzles, and also the initial droplet velocity may deviate.

3.1.2 Drop size distribution

Due to the construction of the hydraulic nozzles a mixture of different droplet sizes are produced. The droplet size or more correct droplet sizes can be characterised by different methods. As a minimum, the VMD (Volume Median Diameter) is normally given. VMD for a nozzle at a given pressure indicates the droplet size dividing the spray liquid in such a way that 50% of the liquid volume will atomise into droplets smaller than the VMD, and 50% will atomise into droplets larger than the VMD. VMD is often denoted D50. Additional values describing the variation in droplet sizes are D10 and D90, which denotes the droplet sizes dividing the spray liquid in such a way that 10% of the liquid amount will atomise into droplets smaller than D10 or larger than D90. In spray drift studies a close correlation between droplet size and spray drift is seen and a big proportion of this correlation can be explained by the fraction of droplets with a diameter below 100 µm (Hobson et al., 1993) (Lagerfelt, 1988). Because of this, the percentage of the spray liquid atomised into droplets below this size is often given. Another classification system, which describes the droplet size distribution with a single notation into five categories has been developed (Doble et al., 1985), (Southcombe et al., 1997). The classification divides the hydraulic nozzles into the categories very fine, fine, medium, coarse and very coarse (Fig. 18).

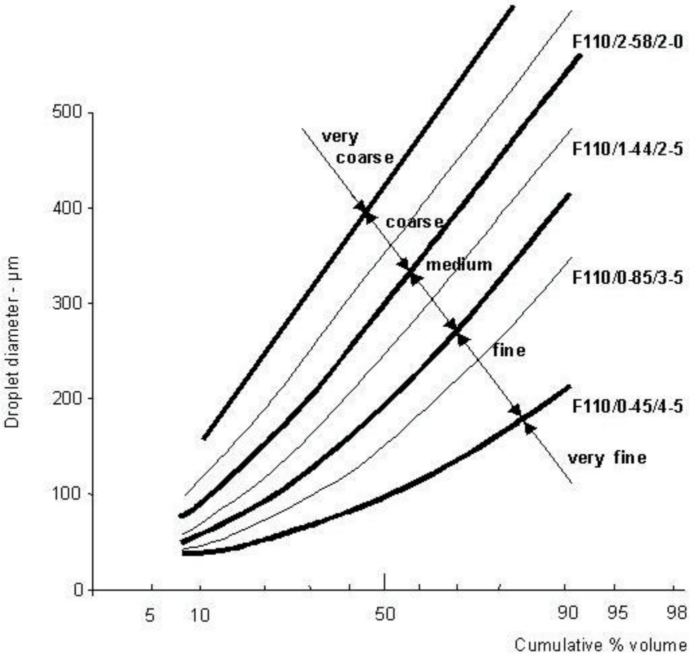

Figure 18. Droplet size distribution of nozzles according to the BCPC classification.
Figur 18. Dråbestørrelsesfordeling fra forskellige dyser ifølge BCPC klassificeringen.

This is possible because a change in droplet size (MVD), generally, doesn’t change the shape of the droplet size distribution. A change in droplet size moves the distribution of droplets towards another size class. Droplet size measurements are dependent on the technique used for the measurement. In order to eliminate this problem, the BCPC classification includes seven reference nozzles. Four of these are threshold nozzles describing the border between the five categories, and three describes characteristic “Fine”, “Medium” and “Coarse” nozzles. The commonly used hydraulic flat fan nozzles fit well into this classification, whereas some special nozzles do not.

3.1.3 Droplet velocity

When the spray liquid leaves the nozzle the typical velocity is approximately 20 m s^{-1} according to Elliott and Wilson (1983). This initial velocity is lost after a distance due to air resistance. Depending on the size, the droplets then reach the sedimentation velocity, in different distances from the nozzle. The sedimentation velocity is the velocity due to gravitation and air resistance. The sedimentation velocity of different droplet sizes is shown in Table 4.

Table 4. Sedimentation velocity and stop distance of water droplets (After Elliott and Wilson, 1983).

Tabel 4. Sedimenteringshastighed og stopafstand for vanddråber (Efter Elliott and Wilson, 1983).

Diameter (µm)	Sedimentation velocity (m s^{-1})	Stop distance (m)
10	0.0030	0.0004
20	0.012	0.012
50	0.072	0.065
100	0.25	0.20
200	0.70	-
500	2.0	-

The table also includes the corresponding stop distance of the smallest droplet sizes. The stop distance is defined as the distance the droplet travels if it is projected horizontally with an initial velocity of 20 m s^{-1}. During application with field sprayers, the spray is normally emitted vertically downward from the boom/nozzle. At a distance below the nozzle approximately equal to the stop distance, the droplet will approach its sedimentation velocity. Droplets with a small diameter have a relatively low weight in proportion to their surface and air resistance therefore exerts a greater influence than on larger droplets. As a result small droplets loose their initial velocity fast and the sedimentation velocity of these droplets are low. The consequence is that small droplets are influenced by wind and turbulence in the field for a much longer period than larger droplets. The difference between different droplet sizes is, however, more limited than the figures in Table 4 indicate. This is due to the fact that when the spray leaves the nozzle, a downward pointing air current is created.

Another aspect discussed by Reichard et al. (1992) is the influence of humidity and wind on droplet size during the travel from nozzle to target. Some results of simulations from this work are shown in Table 5.

Table 5. Mean droplet diameter at impact when droplets are directed downward with initial velocity of 20 m s^{-1} toward a target 0.5 m below point of discharge and through air with various wind velocities and relative humidities. (From Reichard et al, 1992)

Tabel 5. Gennemsnitlig dråbediameter ved nedslag for 0.5 m under udgangspunktet for dråber med en begyndelseshastighed på 20 m s^{-1} ved forskellig vindhastighed og relativ fugtighed.

Initial Droplet Size (µm)	Wind velocity (m s^{-1})	Final mean droplet diameter (µm)			
		Relative humidity (%)			
		20	40	60	80
60	0.5	*	*	41	53
60	1.0	*	**	37	52
80	0.5	63	69	74	77
80	1.0	62	68	73	77
80	2.0	61	68	73	77
100	0.5	92	95	97	98
100	1.0	92	94	97	98
100	2.0	92	94	97	98

100	4.0	92	94	97	98
200	0.5	200	200	200	200
200	1.0	200	200	200	200
200	2.0	200	200	200	200
200	4.0	200	200	200	200

* droplets totally evaporated ; ** drift distance longer than 6.0 m

The simulations indicate a much greater change between initial and final droplet sizes during the flight for droplets with an initial small droplet size. A water droplet with an initial size of 60 µm was only 37 µm in diameter when it reached the target after travelling through wind with a velocity of 1 m s^{-1} and 60% relative humidity. This change in droplet size corresponds to a much larger change in volume as 76.6% of the initial volume was lost. For the same conditions 100 and 200 µm diameter droplets lost 8.7 and 0% respectively, of their initial volumes during flight. Smaller droplets lose a greater proportion of their volume faster due to evaporation because they have larger surface area to volume ratios than larger droplets. The smaller droplets are therefore potentially more driftable due to different factors. This is also reflected in a number of spray drift investigations, where a close relationship between percentage of droplets with a diameter below 100 µm and measured spray drift is shown (Hobson et al., 1993) (Lagerfelt, 1988).

The droplet velocity is dependent on pressure and low-drift nozzles, which are developed to reduce spray drift by creating a coarser atomisation, have a pre-orifice, which reduces pressure at the outlet. Measurements has shown that the droplet velocity from low-drift nozzles is reduced compared to standard flat fan nozzles (Miller, 1999). This means that the potential spray drift reduction from low-drift nozzles is less than would be expected only by considering the droplet size distribution from the low-drift nozzle and the standard flat fan nozzle.

Some alternative atomiser systems exist, where the droplet velocity at the nozzle outlet deviates from the approximate 20 m s^{-1} of standard flat fan nozzles. These include the Danfoil air-sprayer where air-pressure is involved in droplet formation giving the droplets a higher velocity than from standard flat fan nozzles (Lund, 1997).

3.1.4 Droplet movement

After the spray liquid has left the nozzle and the droplets have been formed they are subject to different forces before they reach the target. Gravitation and air resistance are discussed elsewhere. The droplets are, however subject to other forces before they reach the target. During the atomisation, the spray liquid is projected vertically downwards, but at the same time the field sprayer is moving forwards typically with a driving speed close to 2 m s^{-1}. When the spray liquid leaves the nozzle, the movement of the spray cloud accelerates the air surrounding it into a motion parallel to the spray cloud. The induced downward aircurrent creates a vacuum around the nozzle. At the front side of the nozzle the depression is filled by air coming in when the boom is moved in the driving direction. The vacuum behind the nozzle is compensated by air being sucked up from behind the spray cloud to maintain a pressure equilibrium (Fig. 19).

The droplets on their way to the target experience the forward speed as wind coming in from the front. Depending on their momentum they are deflected more or less from their vertical trajectory. The smaller the momentum the more is the direction bent towards the rear of the spray cloud. The droplets which are sucked out of the spray cloud in this manner are caught by the upward directed air current behind the nozzle forming trailing vortices of primarily small droplets behind the nozzle. By this process a proportion of the primarily small droplets will be placed above the height where they were released from the nozzle. The aerodynamic properties of the spraying nozzle itself can therefore be an important factor influencing the spray drift potential.

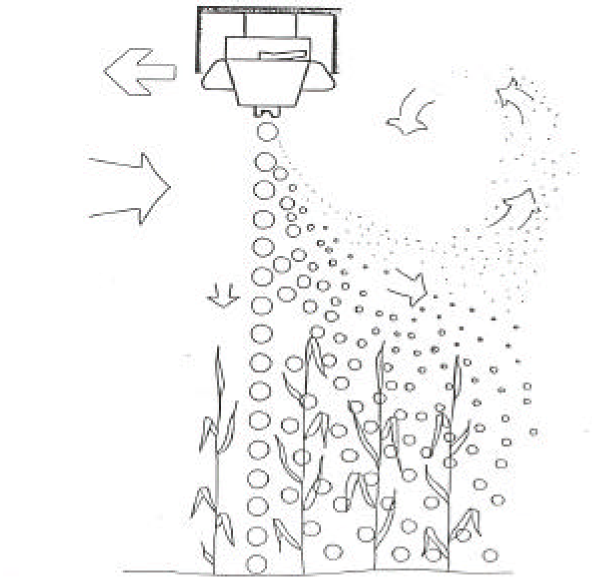

Figure 19. Droplet movement.
Figur 19. Dråbebevægelse.

3.1.5 Boom height

From Table 5 it appears indirectly that boom height has a major influence on the drift potential. When the sprayer is equipped with hydraulic flat fan nozzles with a spray angle of 110^0 the recommended boom height is 40-50 cm. Using this boom height, droplets with a diameter larger than 200 µm will reach the spray target with some of their initial velocity retained. The time used to pass from nozzle outlet to target is then limited. Small droplets with a diameter below 50 µm on the other hand loose their initial velocity a few centimetres below the nozzle outlet. With the very low sedimentation velocity of droplets in this size class, the time interval these droplets spend on their way to the target is long and this makes them very susceptible to wind drift. Droplets with diameters ranging from 50-200 µm are transferred a part of the way from nozzle to target before they reach their sedimentation velocity. An increased boom height means that the smallest droplets below 50 µm are influenced by the natural wind conditions for a longer time period. Increasing the boom height also means that an increasing proportion of the droplets in the medium size class 50-200 µm looses their initial velocity farther away from the target and becomes potentially drift prone. In a paper by Reichard et al (1994) examples of the influence of changes in boom height on the transport of different droplets sizes are calculated. From these it appears that it is primarily the drift potential of droplets in the group below 100 µm that are influenced by changes in boom height. From an actual spray drift measurement a doubling of the drift values were found when the boom height was raised from 50 to 70 cm (Miller, 1988). When using hydraulic flat fan nozzles a double spray pattern overlap is desired in order to obtain a good distribution. Nozzles with a wide spray angle achieve the double overlap of the spray pattern at lower boom height than those with a narrow spray angle. With a 110° spray angle double overlap is achieved at 35 cm boom height whereas the boom height has to be raised to 60 cm with 80° spray angle. The use of nozzles with a symmetrical spray angle and intended double overlap means that a small area outside the field will be sprayed directly by the outermost nozzle. In order to avoid this, different types of border nozzles with an asymmetric spray pattern are produced. A change to this nozzle type at the outermost position can reduce spray drift especially in the first couple of meters from the treated field edge, whereas the influence is small at larger distances from the field edge (van de Zande et al., 1995). Use of this type of nozzles is therefore especially interesting in order to avoid damage to nearby crops, watercourses and other susceptible areas. During field spraying the boom height will vary due to roughness of the spray tracks. When the boom height deviates from the height where double overlap of the spray pattern is achieved, an uneven distribution of the spray will occur. The variation in distribution of spray liquid will be greater when the boom height is below the optimal height compared to a boom height that is above the optimal. Until technical developments has eliminated boom movements during field applications and the associated variation in spray distribution, this will be a limiting factor towards how low a boom height that can be used under practical field spraying.

3.1.6 Air-assistance, shielding etc.

Different drift-reducing solutions to traditional field spraying equipment have been developed. One technology is to shield the spray in order to avoid the influence of the natural wind on the small droplets. Shielding of the individual nozzles (Maybank et al, 1990) as well as a shield covering the entire boom (Wolf et al, 1993) has been constructed. Shielding devices where part of the headwind is used to compensate the depression behind the nozzle has also been investigated (Ozkan et al, 1997). Effective drift reducing commercial shielding devices have been available for row application kits a number of years (Jensen and Spliid, 1998). For boom sprayers the technology seems not fully developed yet although commercial possibilities are available. Another technology is the use of air-assistance to conventional hydraulic nozzles. The purpose of the air-assistance is to counteract the effects the driving speed and the vacuum behind the nozzles exert on the droplets. The concept is to create an air-curtain behind the nozzles that will force small droplets back to the spray cloud if they have been sucked out (ICI, 1990). Furthermore the air-assistance will increase the droplet speed reducing the time to reach the target.

3.1.7 Factors influencing drop generation

In hydraulic nozzles the main factor determining the droplet size distribution is the nozzle size. Changes in the liquid pressure exert a minor effect as shown in the Fig. 20.

Pesticides are normally formulated with additives such as surface-active ingredients, oil additives and emulsifiers. The function is to increase the deposition and retention of the droplets on the target, and to improve the uptake of the pesticide. The changes in physico-chemical properties of the spray liquid also change the droplet formation from the nozzle. The way the droplet formation is changed varies from additive to additive and interactions between nozzle types and additives are seen (Ellis et al., 1999). In the same investigation it was demonstrated that additives can influence both droplet size distribution and droplet velocity. Compared to the droplet formation with pure water some additives reduce the MVD whereas others increase the VMD but no clear correlation to physico-chemical properties such as surface tension are seen (Chapple et al., 1993). Some additives are marketed as drift retardant chemicals. These additives can reduce drift (Ozkan et al., 1993) (Western et al., 1999) because they increase the VMD value.

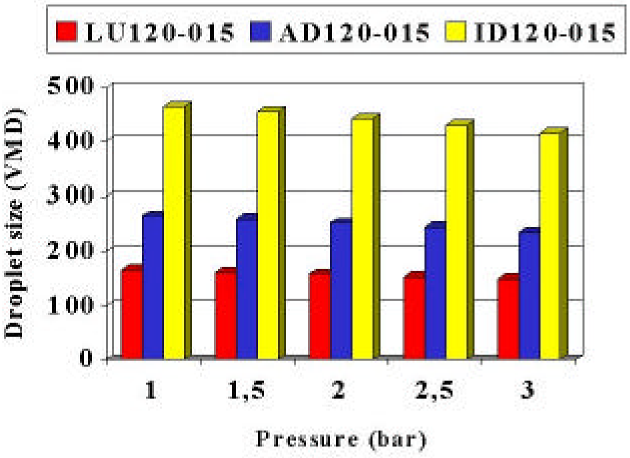

Figure 20. Influence of nozzle pressure on droplet size (VMD) of Lechler flat fan nozzles (LU= traditional flat fan, AD=low-drift, ID=air-inclusion nozzle).
Figur 20. Indflydelse af dysetryk på dråbestørrelsen (VMD ved Lechler fladspredеdyser. (LU = Traditionel fladspredеdyse AD = lavdrift dyse ID = Injektionsdyse).

3.1.8 Atomiser systems currently used in Denmark

Boom sprayers are used for applications in annual crops and in perennial crops in the establishment stages. This includes all agricultural crops, field grown vegetables, plantations of bush fruit and Christmas trees. Alternative sprayers are used in orchards but will not be discussed here. Boom sprayers consist of a vertical boom placed perpendicular to the driving direction. The boom is equipped with atomisers along it. The typical atomisers used on field sprayers in Denmark are different types of flat fan nozzles, typically with a spray angle close to 110^0 and used at a recommended boom height of 40-45 cm. When classified according to the BCPC classification system almost all traditional hydraulic nozzles recommended and used are in the “Fine” or “Medium” classes. This technique probably accounts for more than 90% of the applications with boom sprayers in Denmark. Systems which include air-assistance to hydraulic nozzles (Hardi Twin and others) the air-spraying system from Danfoil, and other systems occupies a small percentage of the market.

3.1.9 Recommendations for research/development

The atomisation process in hydraulic nozzles produces a broad spectrum of droplet sizes around the VMD value. Research has not documented one single droplet size to be the optimal. The different droplet sizes produced from hydraulic nozzles have different advantages and disadvantages due to their properties and generally supplement each other. As a consequence hydraulic nozzles can be used for all applications with a generally robust result. Small droplets have the advantage of better deposition characteristic whereas larger droplets have a better ability to penetrate into the crop. The smallest droplets, however, with sizes below 100 µm are very difficult to control under field conditions with conventional sprayers. They constitute a minor proportion of the total volume atomised, whereas they are responsible for most of the spray drift problems encountered according to studies discussed elsewhere. From the point of view of biological efficacy droplets below 100 µm are probably dispensable if they could be avoided without changing the total droplet spectrum towards a coarser atomisation. This seems, however, to require another atomisation technology than used in hydraulic nozzles.

Hydraulic nozzles with a very coarse atomisation such as air-inclusion nozzles have been marketed in the last few years. Their drift reducing properties are obvious due to the coarse atomisation and have been demonstrated in a number of studies. In general, however, smaller droplets are considered biologically more effective than larger ones. From an agronomic as well as from an environmental point of view, it is important that the biological efficacy of pesticides applied with alternative nozzle types is maintained. It is, therefore, necessary to find and define the areas where drift-reducing nozzles can replace traditional flat fan nozzles and maintain biological efficacy, since an effective application method allows the pesticide dose to be reduced to a minimum. Such investigations are in their early stages at the moment (Jensen, 1999).

3.1.10 Review of spray drift experiments

During the last 20 years a large number of spray drift investigations have been published. The field experiments include all aspects of application techniques, such as nozzle types and pressure, boom height, travelling speed and drift reducing equipment such as shielding devices and air-assistance. They also include investigations on the influence of climatic factors, and especially wind speed. Different techniques have been used as an international standard is not yet agreed on nor implemented but a proposal is at the time being discussed (Miller et al. unpublished). The general way to carry out field experiments investigating spray drift is to drive with a tractor-mounted sprayer in a spray track with the wind direction perpendicular to the driving direction. The spray drift is then measured downwind in different distances from the sprayed area. Measurements of sedimentation drift are carried out on horizontal objects placed on or near the ground level. Sometimes measurements of airborne drift in different heights on masts placed a few metres from the sprayed area are included. This is done with passive or active samplers. Generally, however, calculation of total drift or total spray account (deposition+evaporation+drift) is seldom done. This is also because the total drift is very dependent on the size of the field sprayed as spray drift often is defined as spray caught outside the sprayed field. As most of the drift sediments very close to the sprayed track, the outermost track/tracks of a field contributes by far the largest proportion of the total drift whereas drifting droplets from spray tracks inside the field causes a displacement and uneven distribution within the field, but contributes very little to drift out of the field. Arvidsson (1997), however, reviewing drift experiments reported a total drift of 5% as a mean from a number of studies where drift was measured outside a 12 meters wide area and the total calculated drift in his own investigations varied from a few percent up to 11%.

Results from drift investigations are, considering the sedimenting part of drift, normally presented as a percent of the applied dose rate. The amount of drift as a function of distance from the sprayed area fits an exponentially decreasing function as can be seen from Fig. 21.

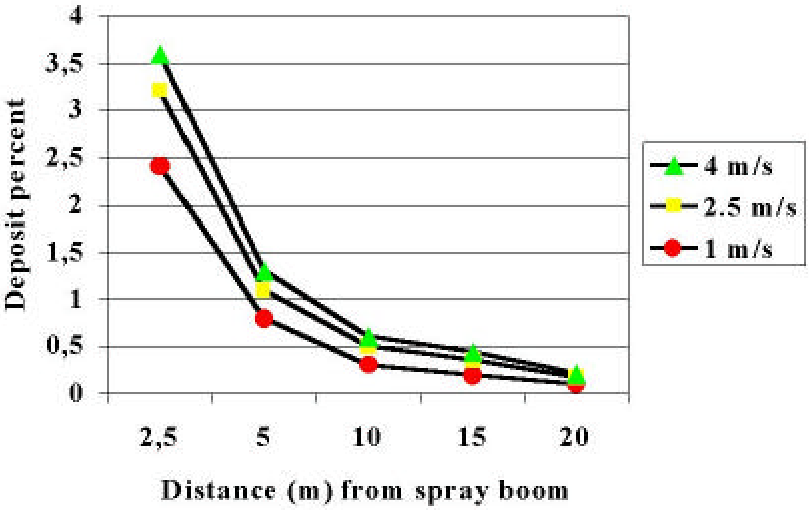

Figure 21. Deposited spray liquid (%) as a function of the distance from the spray boom for three wind speeds. Spray nozzle TeeJet 11001, spray pressure 2.5 bar (after Lagerfelt, 1988).

Figur 21. Afsat sprøjtevæske (%) som funktion af afstanden fra sprøjtebommen ved tre forskellige vindhastigheder. Sprøjtedyse TeeJet 11001, tryk 2.5 bar (efter Lagerfelt, 1988).

Probably the most intensive study comes from Germany (Ganzelmeier et al., 1995) where a large number of drift experiments has been carried out in field crops and in orchard crops such as blackcurrants, apples etc. The results from these studies, the so-called Basic Drift Values, constitute the basis for the approval of sprayers in Germany. They also constitute the basis for the determination of buffer zones to surface water in the pesticide approval procedure in many countries including Denmark. The determined mean values and the calculated 95% percentiles calculated for field crop spraying are shown in Table 6. It can be seen that the drift values are approximately halved every time the distance is doubled. These values has recently been updated with a larger number of drift studies but the 95% percentile values are not yet available (Rautmann, pers comm), and only minor changes in the level of the mean drift values have occurred. The values from the German work in field crops comes from trials carried out under continental conditions with wind speeds ranging from 1 – 3 m s^{-1} and with the use of medium atomising spray technique. Although finer atomising nozzles are used under Danish conditions drift values found are in the same order of magnitude at similar wind conditions (Jensen and Kirknel, 1997). However, a coastal climate as in Denmark is characterised with more windy conditions especially in the middle of the day. Weather conditions with wind speeds in the range 3 -

4 m s^{-1} during application seems to be reasonable assumption under Danish conditions. Taking into consideration the influence of wind speed on spray drift described in 4.3.1, the 95% percentile values in Table 6 seems to be a reasonable estimate for the average spray drift under Danish conditions. These values are used as mean spray drift values in the decision support system developed in the project "Pesticides in surface water". The use of larger spray drift values for Danish conditions is supported by data from a larger Dutch investigation (van de Zande, pers comm). The wind conditions in the Netherlands and in Denmark are more comparable and the general impression for Dutch conditions is that the spray drift values are significantly higher than the BBA values.

In the following, results from studies investigating the influence of different factors on spray drift are reviewed.

Table 6. Statistical evaluation of spray drift in field crops (early and late growth stages) in the study by Ganzelmeier et al. (1995). The figures are mean values and 95% percentiles shown as a percentage of the applied dose in increasing distance from the sprayed area. The 95% percentile is used as a mean value for Danish wind conditions in PestSurf.
Tabel 6. Statistisk vurdering af drift i markafgrøder (tidlige og sene vækststadier) i Ganzelmeiers et al. (1995) studie. Tabellen viser gennemsnitsværdier samt 95% percentiler af afdrift som procentdel af den udsprøjtede dosering i stigende afstand fra det sprøjtede område. 95% percentilen er anvendt som en gennemsnitlig afdriftsværdi for danske vindforhold i PestSurf.

Distance (m)	Mean (% of applied dose)	95% percentile (% of applied dose)
1	1.39	3.51
2	0.58	1.24
3	0.41	0.98
4	0.30	0.94
5	0.24	0.75
7.5	0.14	0.42
10	0.11	0.33
15	0.06	0.20
20	0.04	0.12
30	0.02	0.11

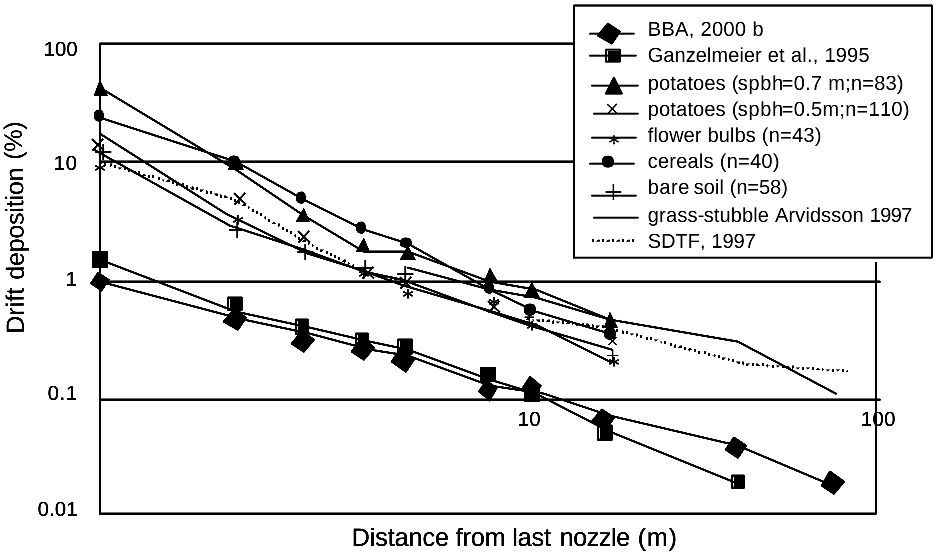

Figure 22.Effect of crop type and environmental circumstances on spray drift (50% percentiles based on measured data), originating from different sources (from van de Zande et al., 2002).
Figur 22. Effekt af afgrødetype og klimaforhold på afdrift (50% percentiler baseret på målinger) i forskellige undersøgelser (van de Zande et al., 2002).

3.2 Application technique

3.2.1 Droplet size

Droplet size distribution of the nozzles used has a major influence on spray drift as can be seen in Fig. 23, which is based on simulations by Kaul et al (1996).

These figures are in agreement with field experiments comparing drift from coarse/very coarse air-inclusion nozzles and traditional fine/medium flat fan nozzles. In a study by Taylor et al (1999) a reduction in sedimentation drift of around 90% were found using air-inclusion nozzles compared to standard flat fan nozzles.

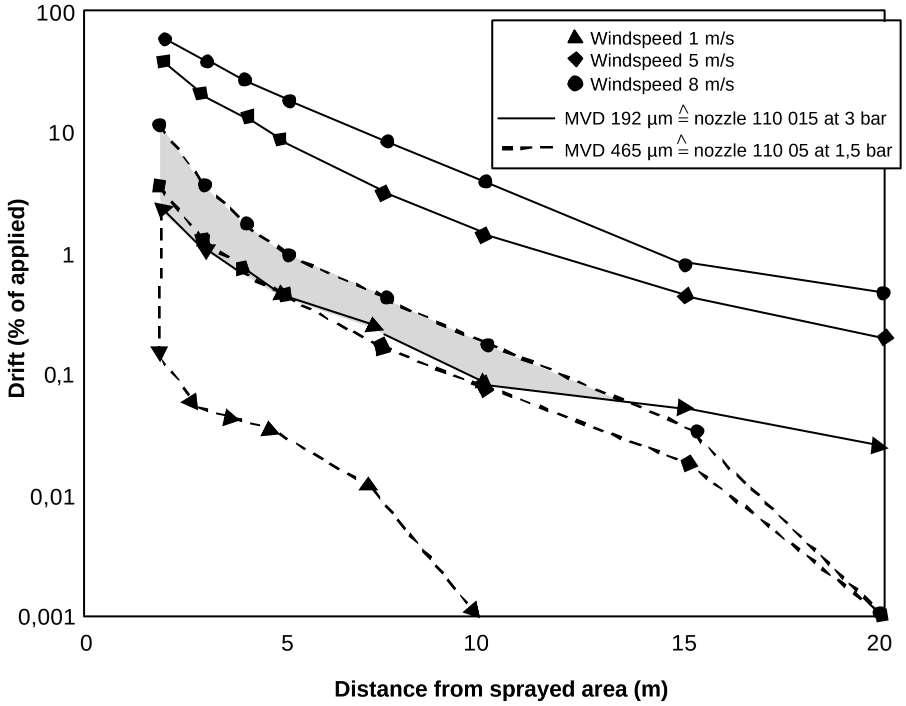

Figure 23. Influence of droplet size on simulated drift under different wind conditions (after Kaul et al., 1996).
Figur 23. Indflydelse af dråbestørrelse på simuleret drift for forskellige vindforhold (efter Kaul et al., 1996).

3.2.2 Boom height

The effect of changes in boom height on potential drift and the reason to the large influence is described above. From actual experiments a steep increase in drift is seen when the boom height is increased above the normal recommended 50 cm (Arvidsson, 1997; Miller, 1999).

3.2.3 Drift reducing equipment

Shielding devices has successfully been developed for band spraying equiment in row crops. In field experiments a reduction in spray drift above 90% has been achieved when band application kits are shielded (Jensen and Spliid, 1998; Porskamp et al., 1997). Different types of shielding devices are also developed for boom sprayers, but the drift reduction obtained is not as high as with the solutions for row crops. The typical drift reduction found in experiments with shielding devices to boom sprayers is in the order of 50 percent (Huijsmans et al., 1997).
The function of air-assistance in reducing the drift is described above. Commercially solutions have been available for more than ten years in different versions. It is not all types of air-assistance that reduce spray drift (Jensen and Kirknel, 1997; Arvidsson, 1997) but the air-assistance according to the Hardi Twin systems has in general reduced the drift. In this system, nozzles and air can be angled +/- 30^0 from the vertical but the angling of the air-current is fixed to the angling of the nozzles and the air therefore always follows the droplets the last part of the travel to the target. The effect of air-assistance according to the Hardi Twin systems also varies between studies. Porskamp et al (1997) found drift reductions varying from 45-79% when air-

assistance was used compared to the same application without the use of air-assistance. The danish experiences with spray drift when using the Hardi Twin system is in accordance with the Dutch results (Jensen and Kirknel, 1997).
Specially designed nozzles (off center nozzles, border nozzles with an asymmetric spray pattern) placed as the outermost nozzle on the boom during application near the edge of the field can decrease the spray drift to the adjacent zone with 20-40% (van de Zande et al., 1995).

3.2.4 Driving speed

When the driving speed is increased, the droplets experience a stronger force and the airflow due to this increased forward motion is responsible for the detrainment of droplets from the spray structure. In the same time, boom variations is more likely to increase with increasing speed. Together this increases the drift potential. A small increase in driving speed can cause a high increase in spray drift. Miller and Smith (1997) measured a 51% increase when travel speed was raised from 5 to 8 km h^{-1} and Taylor et al (1989) found a 90% increase in spray drift when speed was increased from 7 to 10 km h^{-1}.

3.3 Climatic factors

3.3.1 Wind speed

When the wind speed is below 0.5 to 1 m s^{-1}, the direction is often diffuse. At wind speeds above 1 m s^{-1} spray drift increases more or less linearly with wind speed which has been shown both under field conditions (Hobson et al., 1993; Gilbert and Bell, 1988) and in wind tunnel experiments (Sarker and Parkin, 1995). According to Jørgensen and Witt (1997) spray drift investigations carried out at different wind speeds can be normalized by dividing the measured drift with the factor (wind speed in m s^{-1}- 1m s^{-1}). This is equal to a 100% increase in drift when wind speed increases from 2 to 3 m s^{-1}.

3.3.2 Humidity and temperature

The effect of these factors is difficult to quantify in field experiments. Some analysis of the influence of these climatic factors on spray drift under field conditions was done by Arvidsson (1997) but otherwise the influence have been simulated as shown earlier in the report. The volatilisation conditions during the application constitutes according to Kaul et al (1996) one of the most important drift influencing factors when considering airborne drift, whereas the same authors rank volatilisation conditions as less important concerning sedimentation drift. This is in accordance with what would be expected from the calculations shown in Table 5.

3.3.3 Spray-free zone

The sharply decreasing spray drift measured in increasing distance from the edge of the sprayed field means that spray drift can be reduced by leaving a buffer zone or a spray-free zone in the field. A non-cropped spray-free zone of 2.25 m reduced the deposition by 70% on the strip of 1.5-6 m from the border of the field (Porskamp et al., 1995).The highest effect of a spray-free zone is obtained if either crop or another type of vegetation is present in the spray-free zone (van de Zande et al., 1995).

3.3.4 Potential drift reduction exploiting technical possibilities

In the previous section the influence of different factors evaluated separately was described. The combined influence of different factors on spray drift will be additive and can be calculated from the influence of the individual factors. If different combinations of drift reducing techniques/factors are combined large reductions in spray drift can be achieved compared to a standard application with a technique that doesn't take the drift aspect into consideration. This has also been demonstrated experimentally by Holterman and van de Zande (1996), who obtained a drift reduction varying from 90-98% depending on wind speed during the experiment. The result was obtained combining low-drift nozzles and the use of border nozzle with a reduced boom height and a spray-free zone of 1 meter. Taylor et al. (1999) demonstrated that drift could be reduced with 95-97% when the standard equipment was exchanged with coarse air-inclusion nozzles used in combination with air-assistance according to the Twin principle and eventually with the use of border nozzles.

4 Modelling spray drift

4.1 Introduction

In the previous chapter the processes have been discussed that influence spray drift. In this chapter mathematical formations are given for the most important spray drift processes. It should be noted, that was is not foreseen to develop such a model within this project.

4.2 Size distribution and speed

The initial size distribution and the speed of the drops have to be measured e.g. by a phase-Doppler particle analyser (Holterman et al., 1997).

4.3 Entrainment flow

Momentum of a spray droplet after launching is reduced to air resistance ("drag force"). As there is conservation of momentum, this lost momentum is transferred to the surrounding air thereby setting up a flow of entrained air downward in the same direction as the spray droplet motion.

The entrained air stream itself influences the vertical movement of the spray droplets and its velocity should therefore been taken into account when calculating the movement of the droplets.

Fig. 24 shows the co-ordinate system that is used in models.

The first spray drift models described the movement of droplets in a two-dimensional way: only in the spray fan direction (x) and the vertical direction (z). The sheet thickness of the spray is, however, not indefinitely small, but has a certain thickness in the y-direction due drop trajectories caused by instabilities at the base of the spray sheet (Briffa and Dombrowski, 1966). The vertical air velocity decreases with the distance to the centre of the spray. It decreases also with downward distance. The vertical air velocity decays at a faster rate across the fan thickness (y-direction) than along the spray fan field (x-direction). This will enhance spray drift (Smith and Miller, 1994). For this reason it is better to use three-dimensional models that can take these differences into account.

The spray volume patterns along the spray fan axis (x-direction) have been described with Gaussian functions. Such functions have been assumed to be representative of the entrained air field, as momentum is a function of the spray liquid volume flow. The same description can be given for the distribution in the y direction.

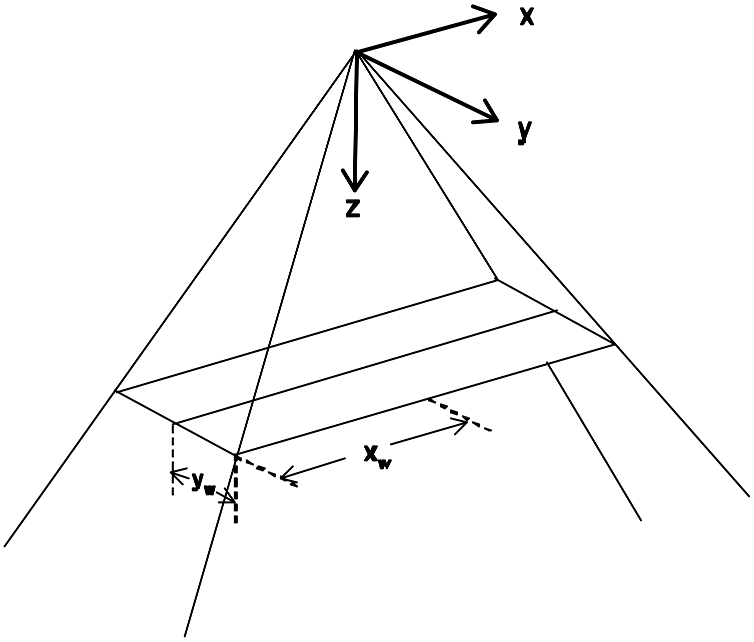

Figure 24.Co-ordinate system used in models. The nozzle opening is at the origin.
Figur 24. Koordinatsystem anvendt i modeller. Dyseåbningen er ved origo.

Briffa and Dombrowski (1966) present the following expression for the maximum vertical air velocity located at the centre the spray along the z-axis:

$$V_z(0,0) = V_s\left(\frac{l_c}{z}\right)^{\delta^2/2k} \tag{30}$$

where:

V_z = the centre-line vertical air velocity due to entrainment (m s^{-1}).
l_c = coherent length of liquid spray sheet (m).
z = (downward) distance in the z-direction (m)
δ = constant (dimensionless). For sprays into air δ takes the value 0.4.
k = entrained air parameter, that is defined by the width of the spray fan at right angles to the spray sheet at a given distance from the nozzle (dimensionless). Miller and Hadfield (1989) determined the value of k from photographic measurements of a number of 80° and 110° flat fan nozzles and found a mean value of 0.14.

The local velocity at position x, y, z can now be determined from (30) and two Gaussian functions that describe the entrained air along the x- and y-axis:

$$V_z(x,y,z) = V_z(0,0)\exp\left[\frac{-x^2}{2\sigma_x^2}\right]\exp\left[\frac{-y^2}{2\sigma_y^2}\right] \tag{31}$$

where:
σ_x = standard deviation in the x-direction (dimensionless)
σ_y = standard deviation in the y-direction (dimenisionless)

Mawer and Miller (1989) measured the spray liquid volume patterns for 110° and 80° nozzles and found the following relationship between height and standard deviation across the fan in the x-direction:

$$s_x = 0.274x_w + 0.048 \tag{32}$$

where:

$$x_w = z\tan b \tag{33}$$

In these equations x_w is the spray half width in the x-direction β is the spray fan half angle in the x-direction.

Smith and Miller (1994) found for a flat nozzle with a flow rate of 0.6 l min^{-1} and a pressure of 3.0 bar:

$$s_y = 0.260y_w + 0.001 \tag{34}$$

where:

$$y_w = z\tan g \tag{35}$$

In this equation y_w is the spray half width in the y-direction and γ is the spray fan half angle in y-direction.

4.4 Terminal velocity of water drops

Most pesticides are applied as emulsions or suspensions in water at concentrations of 1% and less (Thompson and Ley, 1983). Spray drops that consist of such a diluted solution fall with approximately the same terminal velocity as water drops. It should be noted, however, that the pesticide and any other additives might change the surface tension, which will affect the shape of the falling drops.

Water drops brought into the atmosphere by a nozzle will decelerate and they will after a certain distance approach their terminal velocity, i.e. the velocity that they would have if they were falling freely through the atmosphere. The larger the drops, the larger the distance is which they have to travel before they reach their terminal velocity. Beard (1976) modelled the terminal velocity of drops as a function of temperature and pressure for drops with a radius between 2.5×10^{-7} and 3.5×10^{-3} m. Drops larger than 3.5×10^{-3} m are not stable and will split up into smaller drops. The maximum difference between the terminal velocity at 30°C and 0°C is 7%. As this difference is relatively small the terminal velocity of e.g. 15°C can be taken for all calculations. The method of Beard (1976) is very general, but is rather complicated. It takes e.g. into account that the shape of larger falling drops is not spherical and that a Cunningham slip correction factor should be applied for drops that are so small that continuum flow cannot any longer be assumed. Moreover, it can calculate the terminal velocity for other pressures than 1 atm.

Fig. 25 shows the terminal velocity of water drops as a function of their radius calculated with the model of Beard (1976) for 15°C and 1 atmosphere. The following function was derived for the terminal velocity at at 15°C and 1 atmosphere for the radius range between 1×10^{-6} to 3.5×10^{-3} m (maximum error ±4%):

$$\begin{aligned}{}^{10}\log(v_{term}) = -3.422361 - 4.952938x - 2.161628x^2 \\ - 0.519742x^3 - 0.078728x^4 - 0.004812x^5\end{aligned} \qquad (36)$$

where:
v_{term} = terminal velocity water drop (m s^{-1})
x = $^{10}\log(r)$, where r is the radius of the water drop (m)

Thompson and Ley (1983) use the following functions to describe the terminal velocity of water drops in their spray drift model:

$$v_{term} = 4.47\times10^{3}\,r - 0.191 \qquad (\text{for } r \geq 1\times10^{-4}\text{ m})$$

and (37)

$$v_{term} = 3.2\times10^{7}\,r^{2} - 6.4\times10^{10}\,r^{3} \qquad (\text{for } r < 1\times10^{-4}\text{ m})$$

The function of Tompson and Ley (1983) is also shown in Fig. 25. It is a reasonable approximation for drops with a radius between 4×10^{-5} to 6×10^{-5} m (for radii less than about 3×10^{-5} m this function gives negative terminal velocities).

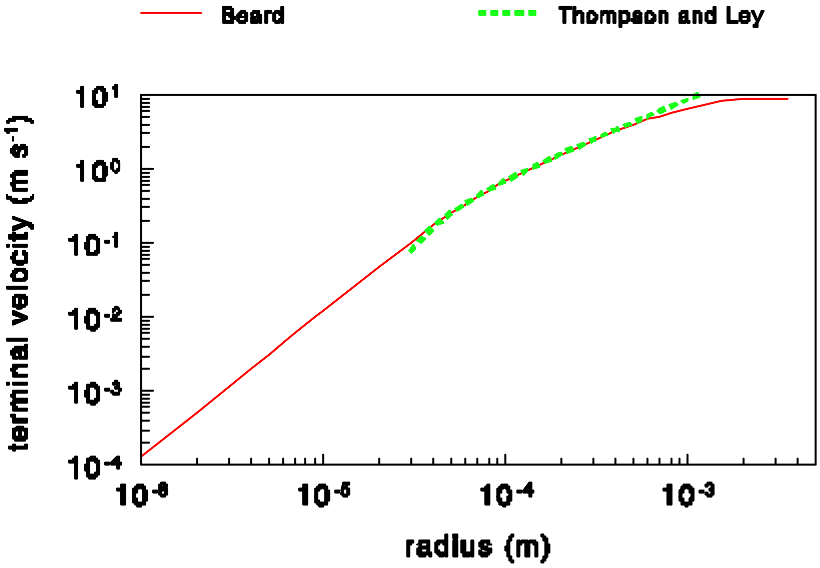

Figure 25. Terminal velocity of water drops at 15°C and 1 atmosphere according to Beard (1976) and Thompson and Ley (1983).
Figur 25. Faldhastighed for vanddråber ved 15°C og 1 atmosfæres tryk ifølge Beard (1976) og Thompson og Ley (1983).

During the fall of the drops evaporation of water and of pesticide may occur. If all water has been evaporated and no pesticide has been evaporated the radius of the drop is about one-fifth of the original one. In the case that water has been completely evaporated from the drop it gets the same density as the pesticide. Drops with an initial radius greater than about 2×10^{-4} m rarely contribute to drift, because they have such large terminal velocities that they are not deposited outside the field onto which pesticide has been applied (Thompson and Ley, 1983). A drop with a radius of 2×10^{-4} m gets a radius of about 4×10^{-5} m after water has been evaporated. The terminal velocity of such particles can be described by Stokes law, which is valid for spherical particles with a radius between 5×10^{-7} and 5×10^{-5} m (Hinds, 1999):

$$v_{\mathrm{term}} = \frac{2 g r^2 \left(\rho_{\mathrm{p}} - \rho_{\mathrm{a}}\right)}{9 \eta_{\mathrm{a}}} \tag{38}$$

where:
g = gravitation ($\mathrm{m\ s^{-2}}$)
ρ_p = density pesticide ($\mathrm{kg\ m^{-3}}$)
ρ_a = density air ($\mathrm{kg\ m^{-3}}$)
η_a = dynamic viscosity air ($\mathrm{kg\ m^{-1}\ s^{-1}}$)

For very small drops (of the order of 1×10^{-6} m) the description with Stokes law is not any longer adequate, because Stokes law assumes continuum flow, which is not the case for these small drops. In this case a "Cunningham" type slip correction factor can be applied to the result of Stokes law.

It is important to take the evaporation of water from drops into account because the terminal velocity of the drops depends on the radius.

4.5 Drop evaporation

Two processes play a role in the evaporation of water drops. The first process is the evaporation of water from the drop itself and diffusion of water vapour to the surrounding air. Evaporation depends on the temperature of the drop. For that reason it is necessary to have a description of the second process: the exchange of heat between the drop and the surrounding air. This process in turn depends on the first process, as heat is lost due to the evaporation of water. The following equations assume a steady state situation where water drops fall with their terminal velocity, i.e. they are not accelerated. This assumption is not valid close to the nozzle.

The change of the mass of the drop due to evaporation of water can be described by (Pruppacher and Klett, 1997):

$$\frac{\mathrm{dm}}{\mathrm{dt}} = -\frac{4\pi r M_{\mathrm{w}} D_{\mathrm{wa}} f_{\mathrm{w}}}{R}\left(\frac{p_{\mathrm{sat}}\left(T_{\mathrm{w}}\right)}{T_{\mathrm{w}}} - \frac{f\, p_{\mathrm{sat}}\left(T_{\mathrm{a}}\right)}{T_{\mathrm{a}}}\right) \tag{39}$$

where:
m = mass of the drop (m)
t = time (s)
r = radius (m)
M_w = molecular mass water ($\mathrm{kg\ mol^{-1}}$); value: 18.015×10^{-3} kg
D_{wa} = diffusivity of water vapour in air ($\mathrm{m^2\ s^{-1}}$)
f_w = mean ventilation coefficient for water vapour (dimensionless). This coefficient gives the ratio between the water vapour mass flux for a moving drop and the water vapour mass flux for a non-moving drop.

R = gas constant (8.314510 J mol^{-1} K^{-1})
p_{sat} = saturation pressure water (N m^{-2})
T_w = temperature water drop (K)
f = relative humidity divided by 100
T_a = temperature air (K)

The change in the temperature of the drop due to evaporation of water vapour from the drop and diffusion of heat to the drop is described by (Pruppacher and Klett, 1997):

$$\frac{dq}{dt} = 4\pi r k_a f_h \left(T_a - T_w\right) + L\frac{dm}{dt} \tag{40}$$

where:
q = heat (J). $q = mc_w T_w$, where c_w is the specific heat of water (J kg^{-1} K^{-1}) and m is the mass of the drop (kg); $m = (4/3)\pi r^3 \rho_w$.
f_h = mean ventilation coefficient for heat (dimensionless). This coefficient gives the ratio between the heat flux for a moving drop and the heat flux for a non-moving drop.
k_a = thermal conductivity of air (J m^{-1} s^{-1} K^{-1}). The influence of the humidity on the thermal conductivity is negligible and for that reason the value for dry air can be taken.
L = latent heat of evaporation of water (J kg^{-1})

The first term in (40) reflects the diffusion of heat and the second term reflects the heat used to evaporate water. It should be noted here that many variables in (39) and (40) are a function of temperature and some are a function of pressure as well.

Fortunately the problem can be simplified to describe the situation for spray drift. The temperature of the air as well as the relative humidity can be assumed to be constant in this case. Model results show that in this case the temperature of the drops of all sizes approaches after a short time the wet-bulb temperature. In that situation the heat lost by evaporation of water equals the heat gained by diffusion of heat to the drop:

$$4\pi r k_a f_h \left(T_a - T_w\right) + L\frac{dm}{dt} = 0 \tag{41}$$

Substituting (39) in this equation gives:

$$T_w - T_a + \frac{L\, M_w D_{wa}}{R k_a}\left(\frac{f_w}{f_h}\right)\left(\frac{p_{sat}\left(T_w\right)}{T_w} - \frac{f\, p_{sat}\left(T_a\right)}{T_a}\right) = 0 \tag{42}$$

If we examine this equation we can conclude the following (see Appendix F for a parameterisation of the variables):

- L is a function of temperature. Its value at value at 30°C is 3% less than at 0°C. This means that in principle L could be given the value for L at 15°C.
- M_w is a constant.
- D_{wa} is a function of both pressure and temperature. But as the pressure is 1 atm and constant here, it is only a function of temperature. Its value at 30°C is 18% larger than at 0°C.

- R is a constant.
- k_a is a function of temperature. It value at 30°C is 9% higher than at 0°C.
- f_w and f_h are both functions of the drop radius, the temperature and the pressure. The pressure is, however, 1 atm in this case. Examination of the ratio f_w/f_h shows that this ratio is almost independent of the temperature and varies to a very limited extent with the drop radius (Fig. 26). This means that larger drops have a somewhat higher temperature than smaller ones. I would be a reasonable approach to use a constant value of 0.98 for f_w/f_h.
- p_{sat} is a function of the temperature. Its value at 30°C is 6.95 times larger than at 0°C (see also Fig. F-1 in Appendix F).

Equation (42) can e.g. be solved with the bisection method (Press et al., 1989). All information on the variables in the equation can be found in Appendix F. It should be mentioned here that the drop temperature is slightly lower than the wet bulb temperature (max. ±0.5°C difference; Pruppacher and Klett, 1997).

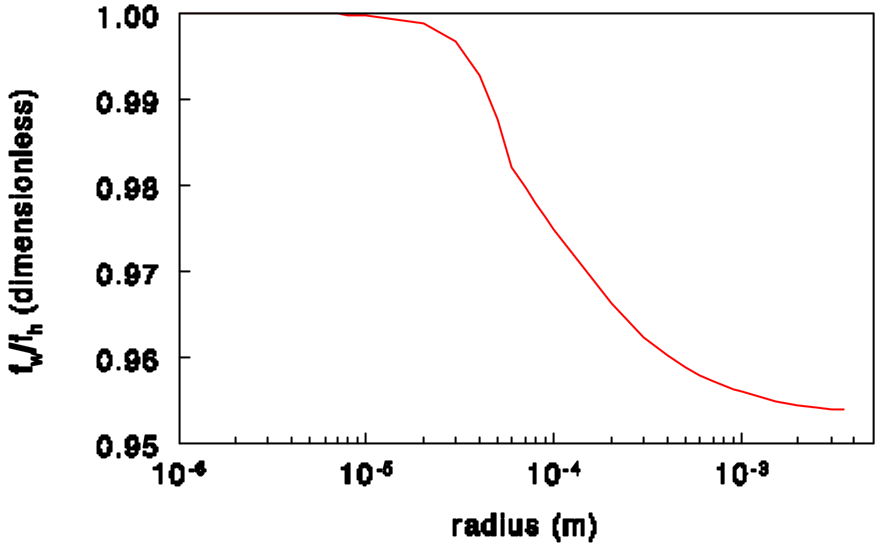

Figure 26. The ratio f_w/f_h as a function of the drop radius at 15°C and 1 atmosphere.
Figur 26. Forholdet f_w/f_h som funktion af dråberadius ved 15°C og 1 atmosfæres tryk.

The change in the drop radius can be found from (39), taking into account that the mass is $(4/3)\pi r^3\rho_w$, where ρ_w is about constant (1000 kg m^{-3}):

$$\frac{dr}{dt} = -\frac{M_w D_{wa} f_w}{r_w R r}\left(\frac{p_{sat}(T_w)}{T_w} - \frac{f\, p_{sat}(T_a)}{T_a}\right) \qquad (43)$$

For modelling purposes it can be useful to have an equation that describes the change in drop radius as a function of fall distance z_{fall}. Such an equation can be found from (43) using the relation:

$$\frac{dr}{dz_{fall}} = \frac{1}{v_{term}} \frac{dr}{dt} \qquad (44)$$

$$\frac{dr}{dz_{fall}} = -\frac{M_w D_{wa} f_w}{r_w R r v_{term}} \left(\frac{p_{sat}(T_w)}{T_w} - \frac{f\, p_{sat}(T_a)}{T_a} \right) \qquad (45)$$

We need now a value for the ventilation coefficient for water vapour f_w. Pruppacher and Klett (1997) give the following empirical expressions for f_w:

$$f_w = 1.00 + 0.108 \left(Sc^{\frac{1}{3}} Re^{\frac{1}{2}} \right)^2 ; \text{for } Sc^{\frac{1}{3}} Re^{\frac{1}{2}} < 1.4 \qquad \text{(a)}$$

$$(46)$$

$$f_w = 0.78 + 0.308 \left(Sc^{\frac{1}{3}} Re^{\frac{1}{2}} \right) ; \text{for } 1.4 \le Sc^{\frac{1}{3}} Re^{\frac{1}{2}} < 51.4 \qquad \text{(b)}$$

where:

Sc = Schmidt number = ν_a/D_{wa} = 0.627 at 15° and 1 atm; ν_a is the kinematic viscosity of air ($m^2\ s^{-1}$) and D_{wa} is the diffusivity of water vapour in air ($m^2\ s^{-1}$)

Re = Reynolds number = ($v_{term} r/\nu_a$); v_{term} is the terminal velocity of the drop ($m\ s^{-1}$), r is the radius of the drop (m) and ν_a is the kinematic viscosity of air ($1.42\times10^{-5}\ m^2\ s^{-1}$)

Expression (a) is valid for drops with a radius up to 6×10^{-5} m and expression (b) is valid for drops with a radius from 6×10^{-5} to 1.5×10^{-3} m.

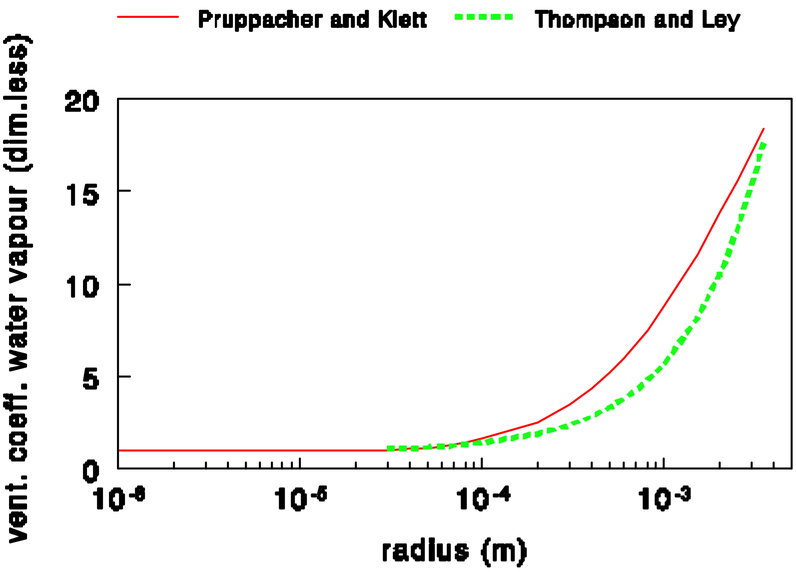

Figure 27. The ventilation coefficient for water vapour as a function to the drop radius according to Pruppacher and Klett (at 10°C) and Thompson and Ley (at 15°C) at 1 atmosphere.
Figur 27. Ventilationskoefficienten for vanddamp som funktion af dråberadius ifølge Pruppacher og Klett (ved 10°C) og Thompson og Ley (ved 15°C) ved 1 atmosfæres tryk.

The ventilation coefficient for water vapour according to Pruppacher and Klett (1997) was calculated for different temperatures. The values at 30°C appear at maximum to be 8% smaller than at 0°C and for the drops of the size of interest for spray drift ($< 2\times10^{-4}$ m) the difference is smaller. This means that one can use the ventilation coefficient for e.g. 10°C for the whole temperature range of interest. A reference temperature of 10°C in this case is chosen because the drop temperature will be somewhat lower than the air temperature (which was taken 15°C in the case of the terminal velocity). The following approximation was found for the ventilation coefficient using the same type of dependence on the Reynolds number as Pruppacher and Klett (1997) using the function for v_{term}, which was previously derived:

$$\begin{aligned} f_w &= 1.00 + 11289 v_{term}\, r && \text{for } r < 6\times10^{-5}\ \text{m} \\ f_w &= 0.785 + 98.54\sqrt{v_{term}\, r} && \text{for } r \geq 6\times10^{-5}\ \text{m} \end{aligned} \qquad (47)$$

This approximation is accurate within 1% for the radius range from 1×10^{-6} to 3.5×10^{-3} m.

Thompson and Ley (1983) use the ventilation coefficient derived by Ranz and Marshall (1952a and 1952b):

$$f_w = 1 + 0.225 Sc^{\frac{1}{3}} Re^{\frac{1}{2}} \tag{48}$$

In Fig. 27 this expression is compared with the expressions of Pruppacher and Klett (1997). It can be seen that the ventilation coefficient used by Thompson and Ley (1983) is smaller than that of Pruppacher and Klett (1997). Pruppacher and Klett use some newer information and for that reason their values should be used. The Tompson and Ley ventilation coefficient can only be used for a drop radius larger than about 3×10^{-4} m, because the terminal velocity of the drop can only be calculated for drops of this size (a negative terminal velocity is calculated for drops with a smaller radius).

In (43) the only parameters that depend on the radius are f_w and r. For that reason it can be useful to have a function for f_w/r if (dr/dt) has to be calculated. The following curve fit for was found to give good results:

$$\begin{aligned} \frac{f_w}{r} &= 1.569076139 r^{-0.963715} && \text{for } r < 6\times10^{-5}\text{ m} \\ \frac{f_w}{r} &= 1081.567214 r^{-0.29140065} && \text{for } r \geq 6\times10^{-5}\text{ m} \end{aligned} \tag{49}$$

Fig. 28 shows the modelled and approximated values of (f_w/r). The maximum error in the approximation is 9% and the error is usually less than 5%.

In (45) the only parameters that depend on the radius are f_w, v_{term} and r. For that reason it can be useful to have a function for $f_w/(rv_{term})$ if (dr/dz) has to be calculated. The following curve fit for was found to give good results:

$$\begin{aligned} {}^{10}\log\left(\frac{f_w}{rv_{term}}\right) = &-11.9388599 - 16.283676x - 6.771674x^2 \\ &-1.235304x^3 - 0.076352x^4 \end{aligned} \tag{50}$$

with x = ${}^{10}\log(r)$, where r is the radius of the water drop (m).
Fig. 29 shows the modelled and approximated values of $(f_w/(rv_{term})$. The maximum error in the approximation is 9% and the error is usually less than 5%.

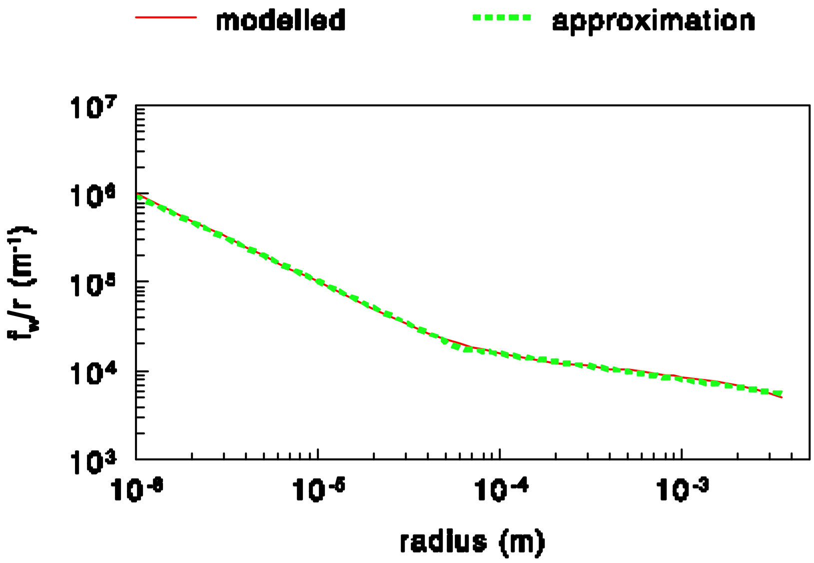

Figure 28. f_w/r as a function of the drop radius at 15°C and 1 atmosphere.

Figur 28. f_w/r som funktion af dråberadius ved 15°C og 1 atmosfæres tryk.

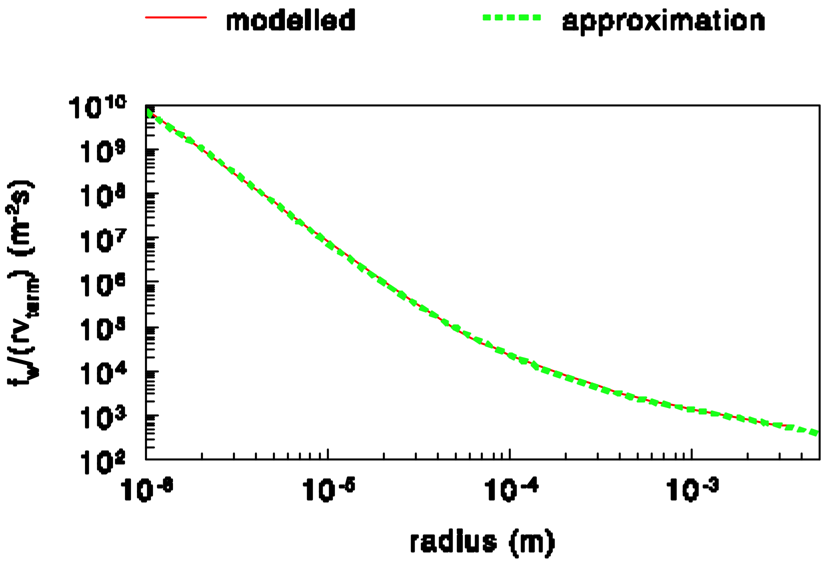

Figure 29. $f_w/(rv_{term})$ as a function of the drop radius at 15°C and 1 atmosphere.

Figur 29. $f_w/(rv_{term})$ som funktion af dråberadius ved 15°C og 1 atmosfæres tryk.

4.6 Wind speed above and in crops

Equation (3) gives the wind speed as a function of height. If the individual roughness elements on land (plants, trees and houses), however, are packed very closely together, then the top of those elements begins to act like a displaced surface. In that case the wind speed as a function of height under neutral atmospheric conditions has to be modified slightly and is given by:

$$u(z) = \frac{u_*}{k} \ln\left(\frac{z-d}{z_{0m}}\right) \tag{51}$$

where:

u(z) = wind speed at height z (m s^{-1})

u_* = friction velocity (m s^{-1}); this is a measure of turbulence.

κ = von Karman's constant (0.4; dimensionless)

z = height (m)

d = zero plane displacement (m); this is about 0.6 to 0.8 times the height of the obstacles (Thom, 1976)

z_{0m} = surface roughness length (m); this is a measure of the surface roughness, it is of the order of 1/10th of the height of obstacles

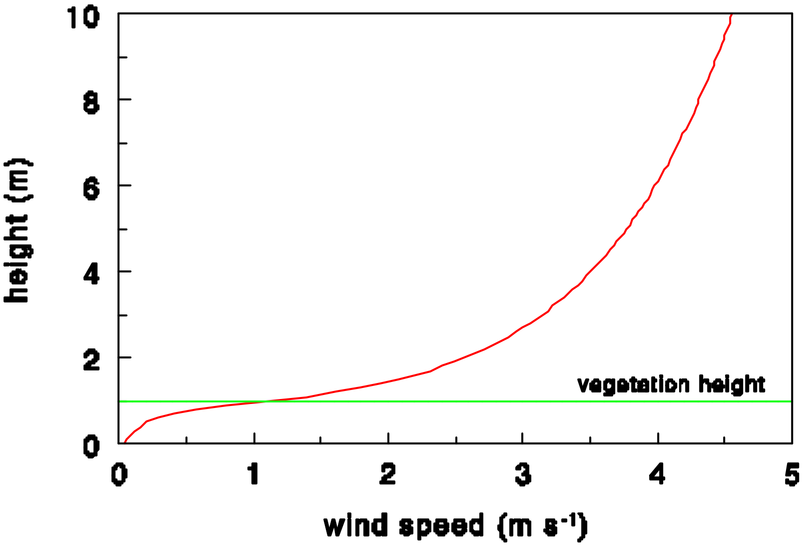

Figure 30. Wind speed above and in a 1 m high wheat field.
Figur 30. Vindhastighed oppe over samt nede i en 1 m høj hvedemark.

4.7 Position and velocity of the drops

The position and velocity of the drops relative to the air are found by subsequent integration of Newton's second law:

$$F = ma \tag{52}$$

where:

F = force (N)
m = mass (kg)
a = acceleration (m s^{-2})

The position and the speed at time step i+1 can be found from their values at timestep i (Holterman et al, 1997):

$$\vec{v}_{i+1} = \vec{v}_i \alpha_i + \vec{v}_{s,i}(1 - \alpha_i) \tag{53}$$

where:
$\vec{v}$ = velocity vector (m s^{-1})
α_i = $\exp(-\beta_i)$ (by definition)
β_i = $\Delta t/\tau_i$, where Δt is the time step (s) and τ_i is the relaxation time of the drop given by:

$$\tau_i = \frac{4\rho_s D}{3\rho_a v_r C_d} \tag{54}$$

where:
ρ_s = density of the spray drop (kg m^{-3})
ρ_a = density of air (kg m^{-3})
C_d = drag coefficient.

The drag coefficient is described by:

$$C_d = \left(\left(\frac{a}{Re}\right)^c + b^c\right)^{\frac{1}{c}} \tag{55}$$

where Re is the Reynolds number and a, b and c are constants with values of 24, 0.32 and 0.52 respectively.

The sedimentation velocity $\vec{v}_s$ depends on gravitation and wind velocity:

$$\vec{v}_s = \tau\vec{g} + \vec{u} \tag{56}$$

where:
g = gravitation (m s^{-2})

The first term in (56) describes the vertical settling velocity due to gravitation and the second term describes the wind speed (in both the horizontal and vertical direction).

4.8 Effect of turbulence

It would be logical to assume that the trajectories of drops can be described by their terminal velocity and the horizontal wind once they have been decelerated from their initial high speeds at the nozzle. This is, however, not completely true, at least not for the smallest droplets. The reason for this is that turbulence causes small up and downward movements. If a drop is subsequently “kicked” upward a few times it is somewhat higher in the atmosphere and can be transported over a somewhat larger distance. Some drops will be exposed to a few subsequent downward “kicks” and will for that reason travel over a shorter distance. The lesson learned from this is that some drops will travel over longer distances than calculated if only taking gravitational settling into account. This effect can be modelled with so-called “random-walk” turbulence models.

In random-walk models the displacements of drops are determined in part by a random selection from appropriate Gaussian distributions of turbulent air velocity (Thompson and Ley, 1983). The speed of the drop at time i+1 is related to the speed at time i, but with the addition of a random component due to turbulence and can be described with equations like (56). More elaborate information on this theory can be found in (Tompson, 1984; Tompson, 1987).

4.9 Empirical model for spray drift

Sarker and Parkin (1995) made an empirical model that predicts spray drift. In stead of describing the processes in detail, wind tunnel measurements of spray drift are used to find an empirical correlation between the most important parameters that influence spray drift. This is achieved by using dimensional analysis. They found the following equation to be valid:

$$\mathrm{Dp} = 1.612 \times 10^{-3} \left(\mathrm{C}_{\mathrm{dis}}\right)^{5.973} \left(\frac{\mathrm{h}}{\mathrm{D}}\right)^{-0.180} \left(\frac{\mathrm{h}}{\mathrm{x}}\right)^{1.0451} q^{-0.2664} \left(\mathrm{h}\sqrt{\frac{\mathrm{u}}{\mathrm{Q}}}\right)^{1.618} \qquad (57)$$

where:
Dp = drift potential
$\mathrm{C}_{\mathrm{dis}}$ = coefficient of discharge, which is a measure of the energy loss through an orifice. $\mathrm{C}_{\mathrm{dis}}$ is calculated from:

$$\mathrm{C}_{\mathrm{dis}} = \frac{\mathrm{Q}}{\mathrm{A}\sqrt{\dfrac{\Delta \mathrm{P}}{r}}} \qquad (58)$$

where Q is the discharge ($\mathrm{m}^3\ \mathrm{s}^{-1}$), A is the orifice area (m^2), ΔP is the pressure drop across the nozzle and ρ is the fluid density
h = nozzle height (m)
D = equivalent diameter of the orifice (m). D is calculated from

$$\mathrm{D} = 2\sqrt{\frac{\mathrm{A}}{p}} \qquad (59)$$

where A is the orifice area (m^2).
x = downwind distance (m)
θ = the angle in the vertical plane that the spray nozzle makes to the airstream. If θ = 0° the nozzle is fully aligned with the airstream. The singularity in the model caused when θ = 0° can be avoided by using θ = 2° for this setting.

u = wind speed (m s^{-1}); the wind speed was varied between 1 and 3 m s^{-1} in the experiments.
Q = discharge (m^3 s^{-1})

The experiments were made with water plus 0.1% Agral. The orifice area A as well as the pressure drop ΔP had to be determined experimentally as function of the discharge rate Q. Fig. 31 shows the relation between the predicted and measured drift potential.

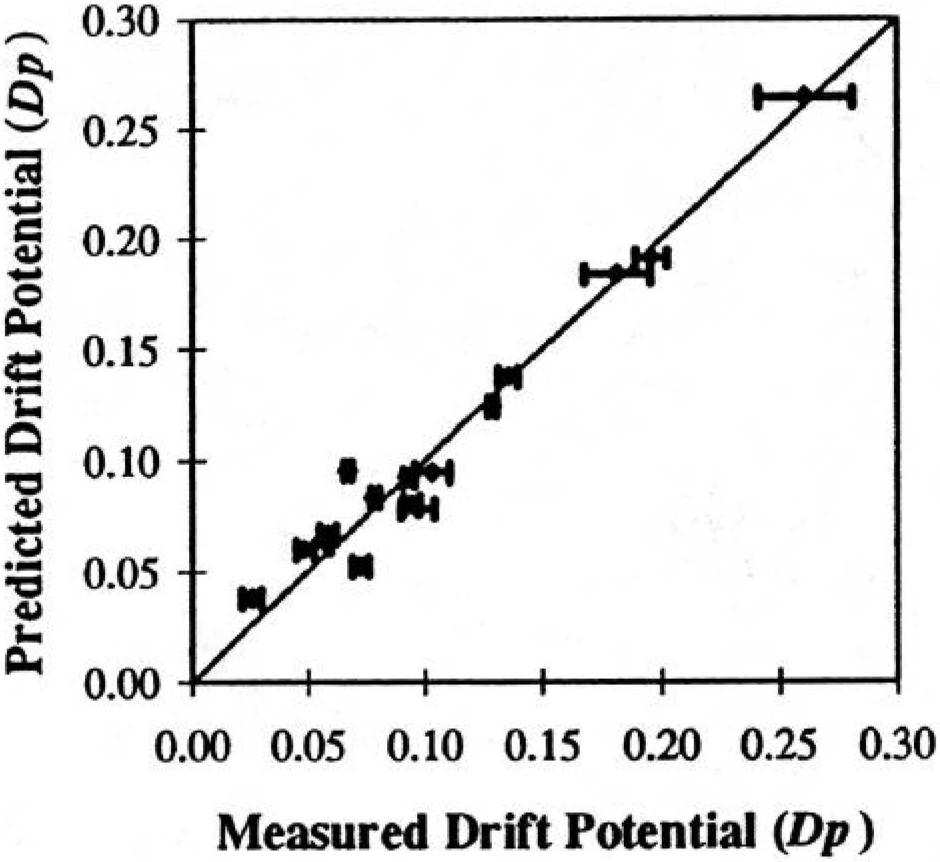

Figure 31. Predicted vs. measured drift potential with the model of Sarker and Parkin (1995). Reprinted with permission. From Sarker, K.U., Parkin, C.S. (1995) Prediction of spray drift from flat-fan hydraulic nozzles using dimensional analysis. Proceedings of the Brighton Crop Protection Conference – Weeds 1995, 529-534. British Crop Protection Council, Farnham, UK.
Figur 31. Modelleret vs. målt afdriftspotentiale med modellen udformet af Sarker og Parkin (1995). Trykt med tilladelse. Fra Sarker, K.U., Parkin, C.S. (1995) Prediction of spray drift from flat-fan hydraulic nozzles using dimensional analysis. Proceedings of the Brighton Crop Protection Conference – Weeds 1995, 529-534. British Crop Protection Council, Farnham, UK.

This model is suited for one type of nozzle. It would be worthwhile to extend the model for other nozzle types and also for higher wind speeds. The input parameter, which is most difficult to measure is A, the orifice area. It can be measured with a microscope fitted with a video camera connected to an image analysis computer. This model predicts an increase of the drift potential by 75% when the wind speed is increase by a factor two.

5 Discussion and conclusions

In this section the (potential) contribution from dry deposition to water bodies will be compared with the contribution from spray drift.

5.1 General comparison dry deposition and spray drift

Although spray drift to some extent depends on the properties of the additives the 95% percentile from Ganzelmeier et al. (1995) is here used for all pesticides in the comparison with the modelled dry deposition (see Table 6). The dry deposition of pesticides depends on many factors: the physico-chemical properties of the pesticides, the meteorological conditions and the properties of the water body. The following situation was chosen for all dry deposition calculations presented here:

- The wind blows over the field onto which pesticide is applied in the direction of the water body.
- The field with emission is 100 m long in the upwind direction. It should be noted here, that as spray drift is transported over short distances (30 m), only the application of pesticide in a small upwind zone contributes to the pesticide load of a water body. For transport of vapour leading to dry deposition the situation is different. It is transported over long distances and for that reason the contribution of dry deposition will to a great extent depend on the length of the field in the upwind direction. The relative contribution from the nearby part of the field to the dry deposition will, however, be larger than the contribution of an area of the same size that is further upwind. The upwind length of the field influences also how fast the dry deposition to the water body decreases as a function of distance to the field.
- In this case there is no non-spray zone.
- The surface roughness length z_{0m} is 0.1 m (crops).
- The friction velocity u_* is 0.386 m s^{-1} which is representative of Danish conditions.
- The calculations are made for neutral atmospheric conditions.
- The concentration of the pesticide in the water body is assumed to be 0 (i.e. or so low that the concentration will not have any influence on the flux.
- It is assumed that the mass accommodation coefficient of the pesticide is so large that it does not influence the uptake by water bodies (see Appendix C).
- It is assumed that the pesticide does not react in water.

The calculations have been made for 3 different types of water bodies:

- A stream, which has a typical minimum value of r_c for Danish conditions (K_{2d} 100 day^{-1} and a depth of 1.37 m).
- A stream, which has a maximum value of r_c for Danish conditions (K_{2d} 1 day^1 and a depth of 1.37 m).
- A lake (wind speed is 5 m s^{-1}).

For all these types of water bodies calculations have been made for 6 different values of Henry's law coefficients K_H and a molecular mass of 300 g mol^{-1}, which is representative for pesticides.
The calculations have been made for a situation where *100% of the amount of pesticide volatilises.* The results are presented in Figs. 32-34. The scales in all figures are the same so that a comparison is easily possible.

If, however, only a fraction f of the pesticide volatilises the values for the dry deposition in the figures have to be multiplied by this fraction. This means that the dry deposition in that case will be reduced. This is done to make a generalisation possible. It should be noted that the spray drift is not affected by the volatilisation.

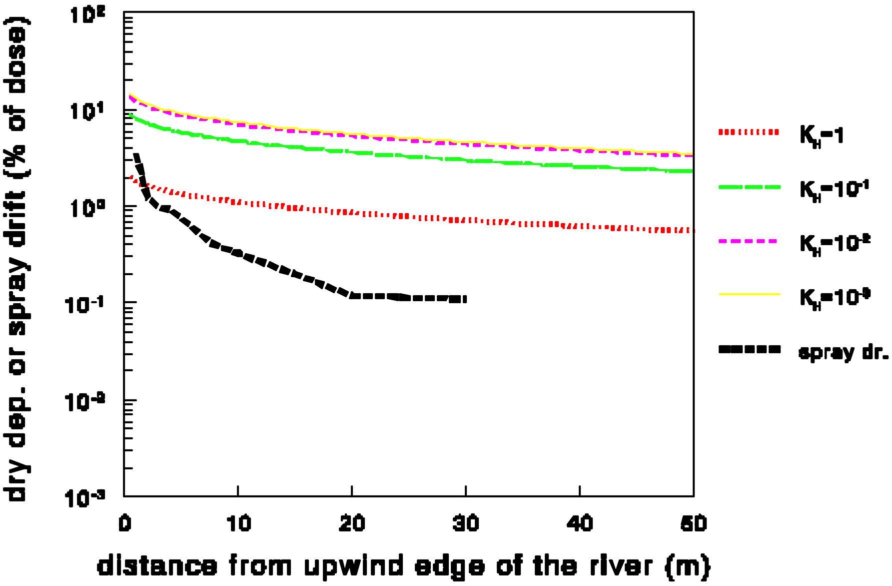

Figure 32. Dry deposition of pesticides to a stream with a low r_c for different Henry's law coefficients and spray drift as a function of the distance to the upwind edge of the stream. Only results for K_H values of 10^0 to 10^{-3} are shown. In the calculations it is assumed that 100% of the pesticide volatilises. If only a fraction f of the applied pesticide volatilises the dry deposition in the figure has to be multiplied by a factor f.
Figur 32. Tørdeposition af pesticider til et vandløb med en lav r_c-værdi for forskellige Henry's lov konstanter samt afdrift som funktion af afstanden til opstrøms kanten af vandløbet. Kun resultater for K_H værdier fra 10^0 til 10^{-3} er vist. I beregningerne er det antaget, at 100% af pesticidet fordamper. Hvis kun en fraktion f af pesticidet fordamper skal den i figuren viste tørdeposition multipliceres med en faktor f.

Figs. 32-34 show that dry deposition to water bodies potentially can be more important than spray drift, especially for streams. Whether it is more important depends e.g. on the fraction of the pesticides that volatilises and the Henry's law coefficient. It can be seen that the results are the same for compounds with a Henry's law coefficient of 10^{-4} and lower. In that case the deposition flux is limited by the laminar boundary layer resistance only and does not any longer depend on the properties of the water body. Figs. 32-34 show clearly that the relative decrease in the spray drift as a function of distance from the emission field is much larger than for dry deposition.

Although the dry deposition model has been based on the description of many processes that have been measured, most of these processes have only been studied for larger water bodies and not for small streams or ponds. For that reason there is a need for experimental studies to determine the dry deposition of pesticides to small water bodies.

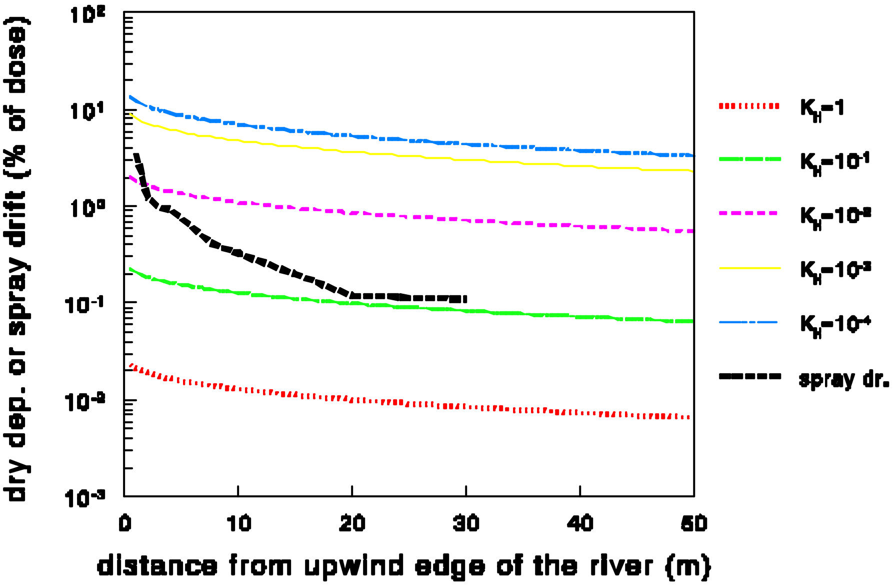

Figure 33. Dry deposition of pesticides to a stream with a high r_c for different Henry's law coefficients and spray drift as a function of the distance to the upwind edge of the stream. Only results for K_H values of 10^0 to 10^{-4} are shown. In the calculations it is assumed that 100% of the pesticide volatilises. If only a fraction f of the applied pesticide volatilises the dry deposition in the figure has to be multiplied by a factor f.

Figur 33. Tørdeposition af pesticider til et vandløb med en høj r_c-værdi for forskellige Henry's lov konstanter samt afdrift som funktion af afstanden til opstrøms kanten af vandløbet. Kun resultater for K_H værdier fra 10^0 til 10^{-4} er vist. I beregningerne er det antaget, at 100% af pesticidet fordamper. Hvis kun en fraktion f af pesticidet fordamper skal den i figuren viste tørdeposition multipliceres med en faktor f.

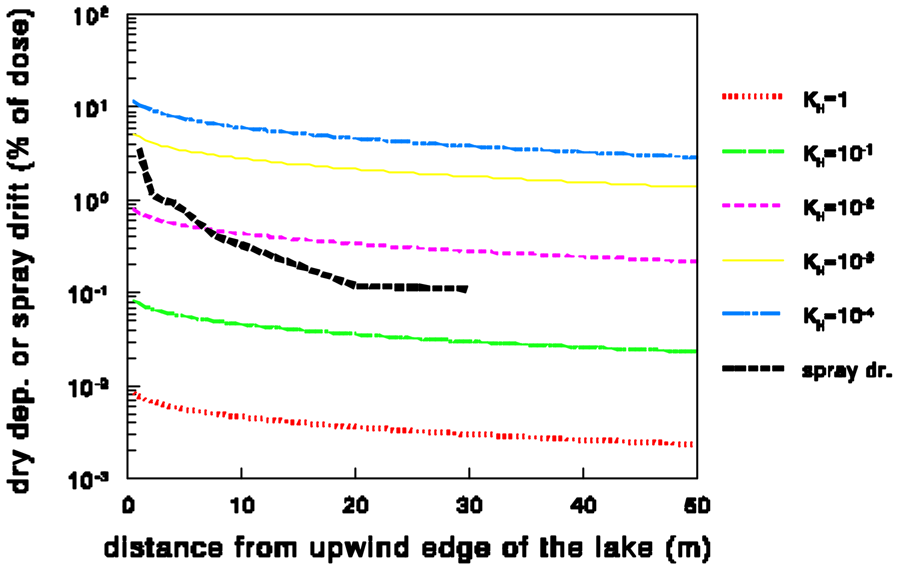

Figure 34. Dry deposition of pesticides to a lake for a wind speed of 5 m s^{-1} at 10 m height for different Henry's law coefficients and spray drift as a function of the distance to the upwind edge of the lake. Only results for K_H values of 10^0 to 10^{-4} are shown. In the calculations it is assumed that 100% of the pesticides volatilises. If only a fraction f volatilises the dry deposition in the figure has to be multiplied by a factor f

Figur 34. Tørdeposition af pesticider til en sø ved en vindhastighed på 5 m s^{-1} i 10 m højde for forskellige Henry's lov konstanter samt afdrift som funktion af afstanden til opstrøms kanten af søen. Kun resultater for K_H værdier fra 10^0 til 10^{-4} er vist. I beregningerne er det antaget, at 100% af pesticidet fordamper. Hvis kun en fraktion f af pesticidet fordamper skal den i figuren viste tørdeposition multipliceres med en faktor f.

.

5.2 Comparison for pesticides that are used in Denmark

For pesticides for which the dry deposition is limited by the laminar boundary resistance, the accumulated dry deposition flux is a direct function of the accumulated emission flux. As it is difficult to show the dry deposition flux for all compounds that were sold in large quantities in Denmark in the year 2000 a selection of compounds was made. Compounds were chosen for which the percentage of the dose that volatilises (Table 3) decreases with a factor of about two for each compound. The calculations were made for a stream, which has a typical minimum value of r_c for Danish conditions (K_{2d} 100 day^{-1} and a depth of 1.37 m).

Fig. 35 shows the results for these compounds. It should be noted that these curves look exactly the same for other water bodies for all compounds apart from fenpropimorph. For fenpropimorph the dry deposition flux would maybe be 40% lower for ditches or ponds. For pendimethalin for which no results are shown this difference would be larger: it could be up to a factor of 5 lower for ditches and ponds.

Fig. 35 shows that the accumulated dry deposition flux for many important compounds is larger or of the same order of magnitude as the spray drift flux. The dry deposition flux becomes relatively more important with the distance to the emission field.

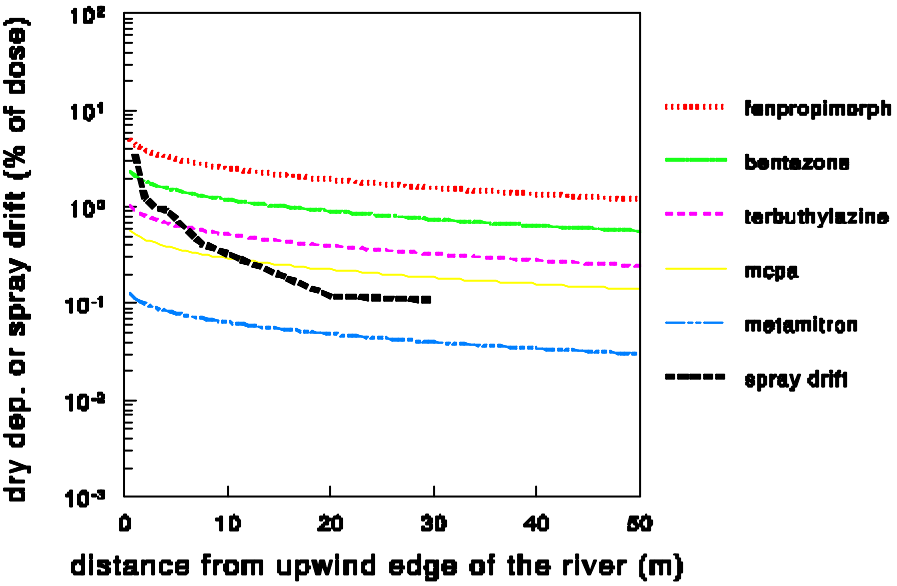

Figure 35. Dry deposition of pesticides to a stream with a low r_c for different Henry's law coefficients and spray drift as a function of the distance to the upwind edge of the stream.
Compounds: fenpropimorph (36%), bentazone (17%), terbuthylazine (8%), mcpa (4%), metamitron (1%). The numbers in brackets indicate the percentage of the dose that volatilises. In the calculations it is assumed that the pesticide does not dissociate in water.
Figur 35. Tørdeposition af pesticider til et vandløb med en lav r_c*-værdi for forskellige Henry's lov konstanter samt afdrift som funktion af afstanden til opstrømskanten af et vandløb. Stoffer: fenpropimorph (36%), bentazon (17%), terbuthylazine (8%), mcpa (4%), metamitron (1%).Tallene i parentes angiver procentdelen af dosen, som fordamper. Ved beregningerne er det antaget, at pesticiderne ikke dissocierer i vand.*

References

Asman, W.A.H. (2001) Modelling atmospheric transport and deposition of pesticides up to 2 km from a source. In: Asman, W.A.H., Felding, G., Kudsk, P., Larsen, J., Mathiassen, S., Spliid, N.H.: Pesticides in air and in precipitation and effects on plant communities. Report Pesticides Research 57, Danish Environmental Protection Agency, Copenhagen, Denmark.

Arvidsson, T. (1997) Spray drift as influenced by meteorological and technical factors, A methodological study. Acta Universitatis Agriculturae Sueciae, Agraria 71, 144pp.

Arya, S.P. (1988). Introduction to micrometeorology. Academic Press, San Diego, USA.

Atlas, E., Foster, R., Glam, C.S. (1982) Air-sea exchange of high molecular weight organic pollutants: laboratory studies. Environ. Sci. Technol. 16, 283-286.

Banks, R.B., Herrera, F.F. (1977) Effect of wind and rain on surface aeration. J. Environ. Eng. Div., Am. Soc. Civ. Eng. 103, 489-504.

Beard, K.V. (1976) Terminal velocity and shape of cloud and precipitation drops aloft. J. Atmos. Sci. 33, 851-864.

Briffa, F.E.J., Drombrowski, N. (1966) Entrainment of air into a liquid spray. I. A model of aerial dispersion. Agri. Meteorol. 15, 257-271.

Brown, M.J., Arya, S.P. Schnyder, W.H. (1993) Vertical dispersion from surface and elevated releases: An investigation of a non-Gaussian plume model. J. Appl. Met. 32, 490-505.

Brumley, B.H., Jirka, G.H. (1988) Air-water transfer of slightly soluble gases: turbulence, interfacial processes and conceptual models. PhysicoChemical Hydrodynamics 10, 295-319.

Brutsaert, W. (1975). The roughness length for water vapor, sensible heat, and other scalars. J. Atmos. Sci. 32, 2028-2031.

Cadwallader, T.E., McDonnell, A.J. (1969) A multivariate analysis of reaeration data. Water Res. 3, 731-742.

Chapple, A. C., Downer, R. A., Hall, F. R. (1993) Effects of spray adjuvants on swath patterns and droplet spectra for a flat-fan hydraulic nozzle. Crop Protection 12, 579-590.

Chapra, S.C., Wilcock, R.J. (2000) Transient storage and gas transfer in lowland stream. J. Envir. Engrg. ASCE 126, 708-712.

Churchill, M.A., Elmore, H.L., Buckingham, E.A. (1962). The prediction of stream reaeration rates. J. Sanitary Engrg. Div., Proc. ASCE 88, 1-46.

Cirpka, O. Reichert, P., Wanner, O. Müller, S.R. , Schwarzenbach, R.P. (1993) Gas exchange at river cascades: field experiments and model calculations. Environ. Sci. Technol. 27, 2086-2097.

Csanady, G.T. (1990) The role of breaking wavelets in air-sea gas transfer. J. Geophys. Res. 95, 749-759.

Danckwerts, P.V. (1951). Significance of liquid-film coefficients in gas absorption. Ind. Eng. Chem. 43, 1460-1467.
Deinum, G., Baart, A.C., Bakker, D.J. Duyzer, J.H., van den Hout, K. (1995) The influence of uptake by leaves on atmospheric deposition of vapor-phase organics. Atmospheric Environment 29, 997-1005.

Deacon, E.K. (1977) Gas transfer to and across an air-water interface. Tellus 29, 363-374.

Denmead, O.T. (1976) Temperate cereals. In: Monteith, J.L. (ed.) Vegetation and the atmosphere, Volume 2. Academic Press, London, 1-31.

Denmead, O.T. (1992) Transfer coefficients for water-air exchange of ammonia, carbon dioxide and methane. Ecological Bulletins 42, 31-41.

Dilling, W.L. (1977) Interphase transfer processes. II. Evaporation rates of chloromethanes, ethanes, ethylenes, propanes, and propylenes from dilute aqueous solutions. Comparisons with theoretical predictions. Environ. Sci. Technol. 11, 405-409.

Doble, S. J., Matthews, G. A., Rutherford, I. S., Southcombe, E. S. E. (1985) A system for classifying hydraulic nozzles and other atomisers in to categories of spray quality. Proc. 1985 British Crop Protection Conference – Weeds, 1125-1133.

Duyzer, J.H., van Oss, R.F. (1997) Determination of deposition parameters of a number of persistent organic pollutants by laboratory experiments. Report R97/150, TNO-MEP, Apeldoorn, The Netherlands.

Elliott, J. G., Wilson, B. J. (1983) The influence of weather on the efficiency and safety of pesticide application. The drift of herbicides. Occasional Publication No 3. BCPC Publications, London, 135pp.

Ellis, M. C. B., Tuck., C. R. (1999) How adjuvants influence spray formation with different hydraulic nozzles. Crop Protection 18, 101-109.

Ferrell, R.T., Himmelblau, D.M. (1967) Diffusion coefficients of nitrogen and oxygen in water. J. Chem. Eng. Data 12, 111-115.

Garratt, J.R. (1992) The atmospheric boundary layer. Cambridge Atmospheric and Space Science Series.

Ganzelmeier, H., Rautmann, D., Spangenberg, R., Streloke, M., Herrmann, M., Wenzelburger, H.-J., Walter, H.-F., (1995) Studies on the spray drift of plant protection products. Mitt. Aus der BBA für Land- und Forstwirtschaft, Berlin-Dahlem, Heft 305.

Genereux, D.P., Hemond, H.F. (1992) Determination of gas exchange rate constants for a small stream on Walker Branch Watershed, Tennessee. Water Resour. Res. 28, 2365-2374.

Gilbert, A. J., Bell, G. J. (1988) Evaluation of drift hazards from pesticide spray application. Aspects of Applied Biology 17, 363-375.

Gryning, S.E., van Ulden, A.P., Larsen, S.E. (1983) Dispersion from a continuous ground-level source investigated by a K-model. Quart. J. R. Met. Soc. 109, 355-364.

Heikinheimo, M., Kangas, M., Tourula, T., Venäläinen, A. Tattari, S. (1999) Momentum and heat fluxes oveer lakes Tämnaren and Råksjö. Agric. For. Meteor. 98-99, 521-534.

Hibbs, D.E., Parkhill, K.L., Gulliver, J.S. (1998) Sulfur hexafluoride gas tracer studies in streams. J. Envir. Engrg. ASCE 124, 752-760.

Hicks, B.B., Baldocchi, D.D., Meyers, T.P., Hosker, R.P., Matt, D.R. (1987) A preliminary multiple resistance routine for deriving dry deposition velocities from measured quantities. Wat. Air Soil. Pollut. 36, 311-330.

Hinds, W.C. (1999) Aerosol technology. John Wiley, New York, USA.

Hobson, P. A., Miller, P. C. H., Walklate, P. J., Tuck, C. R., Western, N. M. (1993). Spray drift from hydraulic spray nozzles: the use of a computer simulation model to examine factors influencing drift. Journal of Agricultural Engineering Research, 54, 293-305.

Holterman, H. J., van de Zande, J. C. (1996) Drift reduction in crop protection: Evaluation of technical measures using a drift model. Proc. Brighton Crop Protection Conference – Pests and Diseases. 111-116.

Holterman, H.J., van de Zande, J.C., Porskamp, H.A.J., Huijsmans, J.F.M. (1997) Modelling spray drift from boom sprayers. Computers and Electronics in Agriculture 19, 1-22.

Huijsmans, J. F. M., Porskamp, H. A. J., van de Zande, J. C. (1997) Drift(beperking) bij de toediening van gewasbeschermingsmiddelen. Evaluatie van de drift van spuitvloestof bij bespuitingen in de fruitteelt, de volveldsteelten en de boomteelt (stand van zaken december 1996). IMAG-DLO. Rapport dienst landbouwkundig onderzoek, Institut voor milieu- en agritechniek, 97-04, 40 pp.

ICI (1990) Unpublished results.

Jensen, P. K., Kirknel, E. 1997. Sammenligning af afdrift fra konventionel sprøjte, Hardi Twin, Kyndestoft Airsprayer og Danfoil. 14. Danske Planteværnskonference - Ukrudt. SP Rapport nr 7, 159-167.

Jensen, P. K., Spliid, N. H. 1998. Afdrift fra sprøjteudstyr til svampebekæmpelse i jordbær. Effekt af afskærmet jordbærbom og ledsageluft til almindelig marksprøjte. 15. Danske Planteværnskonference - Ukrudt. DJF Rapport nr 3, 229-238.

Jensen, P. K. (1999) Herbicide performance with low volume low-drift nozzles and air-inclusion nozzles. Proc. The 1999 Brighton Conference – Weeds, 453-460.

Jähne, B., Münnich, K.O., Bösinger, R., Dutzi, A., Huber, W., Libner, P. (1987) On the parameters influencing air-water gas exchange. J. Geophys. Res. 92, 1937-1949.

Joffre, S.M. (1988). Modelling the dry deposition velocity of highly soluble gases to the sea surface. Atmospheric Environment 22, 1137-1146.

Jury, W.A., Spencer, W.F., Farmer, W.J. (1983) Behavior assessment models for trace organics in soil: I. Model description. J. Environ. Qual. 12, 558-564. (Errata: see J. Environ. Qual. 16, 448).

Jørgensen, M. K., Witt, K. L. 1997. Sprøjteteknik i relation til godkendelse og brugen af pesticider i Nordeuropa. 14. Danske Planteværnskonference - Ukrudt. SP Rapport nr 7, 169-178.

Kaul, P., Gebauer, S., Neukampf, R., Ganzelmeier, H. 1996. Modellierung der direkten abtrift von pflanzenschutzmitteln - pflanzenschutzgeräte für flächenkulturen. Nachrichtenblatt Deutschen Pflanzenschutzdienst, 48, 21-31.

Lagerfelt, P. 1988. Spray drift deposits during application with field crop sprayer. Int symposium on pesticide application. ANPP Annales 18-19 januar 1988, Paris, 30-39.

Lindfors, V., Joffre, S.M., Damski, J. (1991) Determination of the wet and dry deposition of sulphur and nitrogen compounds over the Baltic Sea using actual meteorological data. Finnish Meteorological Institute contributions No. 4, Finnish Meteorological Institute, Helsinki, Finland.

Liss, P.S., Merlivat, L. (1986) Air-sea gas exchange rates: Introduction and synthesis. In: Buat-Ménard, P. (Ed.) The role of air-sea exchange in geochemical cycling. Reidel, Dordrecht, The Netherlands, 113-129.

Lund, I. 1997. Analysering af afdriftspotentialet fra marksprøjter. 14. Danske Planteværnskonference - Ukrudt. SP Rapport nr 7, 149-157.

MacIntyre, S., Wanninkhof, R., Chanton, J.P. (1995) Trace gas exchange across the air-water interface in freshwater and coastal marine environments. In: Matson, P.A., Harriss, R.C. Biogenic trace gases: measuring emissions from soil and water, Blackwell Science, Oxford, UK, 52-97.

Mackay, D., Yeun, A.T.K. (1983) Mass transfer coefficient correlations for volatilization of organic solutes from water. Environ. Sci. Technol. 17, 211-217.

Maybank, J., Shewchuk, S. R., Wallace, K. (1990) The use of shielded nozzles to reduce off-target herbicide spray drift. Canadian Agricultural Engineering 32, 235-241.

Miller, P. C. H. (unpublished) Draft international standard methods for the field measurement of spray drift.

Miller, P. C. H. 1988. Engineering aspects of spray drift control. Aspects of Applied Biology 17, Environmental aspects of applied biology, 377-384.

Miller, P. C. H., Smith, R. W. (1997) The effects of forward speed on the drift from boom sprayers. Proc The 1997 Brighton Crop Protection Conference – Weeds. 399-406.

Miller, P. C. H. (1999) Factors influencing the risk of drift into field boundaries. Proc. The 1999 Brighton Conference – Weeds, 439-446.

Miller, P.C.H., Hadfield, D.J. (1989) A simulation model of the spray drift from hydraulic nozzles. J. Agri. Eng. Res. 42, 135-147.

Moog, D.B., Jirka, G.H. (1998) Analysis of reaeration equations using mean multiplicative error. J. Envir. Engrg. ASCE 124, 104-110.

O'Connor, D.J., Dobbins, W.E. (1958). Mechanisms of reaeration in natural streams. Trans. Am. Soc. Civ. Eng. 123, 641-684.

Ozkan, H. E., Reichard, D. L., Zhu, H., Ackerman, K. D. (1993) Effect of drift retardant chemicals on spray drift, droplet size and spray pattern. Pesticide Formulations and Application Systems 13. 173-190.

Ozkan, H. E., Miralles, A., Sinfort, C., Zhu, H., Fox, R. D. (1997) Shields to reduce drift. Journal of Agricultural Engineering Research 67, 311-322.

Porskamp, H. A. J., Michielsen, J. M. G. P., van de Zande, J. C. (1997) Driftbeperkende spuittechnieken voor de bloembollen. Drift bij een luchtondersteunde veldspuit, een spuit met afgeschermde spuitbom en een tunnelspuit voor bedden. IMAG-DLO. Rapport dienst landbouwkundig onderzoek, Institut voor milieu- en agritechniek, 97-08, 36 pp.

Press, W.H., Flannery, B.P., Teukolsky, S.A., Vetterling, W.T. (1989) Numerical recipes. Cambridge University Press, Cambridge, UK.

Pruppacher, H.R., Klett, J.D. (1997) Microphysics of clouds and precipitation. Kluwer, Dordrecht, The Netherlands.

Ranz, W.E., Marshall, W.R. (1952a) Evaporation from drops, Part I. Chem. Engng. Prog. 48, 141-146.

Ranz, W.E., Marshall, W.R. (1952b) Evaporation from drops, Part II. Chem. Engng. Prog. 48, 173-180.

Rathburn , R.E., Tai, D.Y. (1982) Volatilization of organic compounds from streams. J. Envir. Engrg. ASCE 108, 973-989.

Raupach, M.R., Briggs, P.R., Ahmad, N., Edge, V.E. (2001a) Endosulfan transport: II. Modeling airborne dispersal and deposition by spray and vapor. J. Environ. Qual. 30, 729-740.

Raupach, M.R., Brigss, P.R., Ford, P.W., Leys, J.F., Muschal, M., Cooper, B., Edge, V.E. (2001b) Endosulfan transport: I. Integrative assessment of airborne and waterborne pathways. J. Environ. Qual. 30, 714-728.

Raupach, M.R. (1994) Simplified expressions for vegetation roughness length and zero-plane displacement as functions of canopy height and area index. Boundary-Layer Meteorol. 71, 211-216.

Raupach, M.R. (1995) Corrigenda. Boundary-Layer Meteorol. 76, 303-304.

Reichard, D. L., Zhu, H., Fox, R. D., Brazee, R. D. (1992) Computer simulation of variables that influence spray drift. Transactions of the ASAE, 35, 1401-1407.

Sarker, K.U., Parkin, C.S. (1995) Prediction of spray drift from flat-fan hydraulic nozzles using dimensional analysis. Proceedings Brighton Crop Protection Conference – Weeds, 529-534. British Crop Protection Council, Farnham, UK.

Schwarzenbach, R.P., Gschwend, P.M., Imboden, D.M. (1993). Environmental organic chemistry. John Wiley, New York, USA.

Seinfeld, J.H., Pandis, S.N. (1998) Atmospheric chemistry and physics. John Wiley, New York, USA.

Smit, A.A.M.F.R., van den Berg, F., Leistra, M. (1997) Estimation method for the volatilization of pesticides from fallow soil. Report Environmental Planning Bureau Series 2, DLO Winand Staring Centre, Wageningen, the Netherlands.

Smit, A.A.M.F.R., Leistra, M., van den Berg, F. (1998) Estimation method for the volatilization of pesticides from plants. Report Environmental Planning Bureau Series 4, DLO Winand Staring Centre, Wageningen, the Netherlands.

Smith, J.H. Bomberger, D.C. Haynes, D.L. (1980) Prediction of the volatilization rates of high-volatility chemicals from natural water bodies. Environ. Sci. Technol. 14, 1332-1337.

Smith, R.W., Miller, P.C.H. (1994) Drift prediction in the near nozzle region of a flat fan spray. J. Agric. Eng. Res. 111-120.

Southcombe, E. S. E., Miller, P. C. H., Ganzelmeier, H., van de Zande, J. C., Miralles,,A., Hewitt, A. J. (1997) The international (BCPC) spray classification system including a drift potential factor. Proc 1997 Brighton Crop Protection Conference – Weeds. 371-380.

Southworth, G.R. (1979). The role of volatilization in removing polycyclic aromatic hydrocarbons from aquatic environments. Bull. Environm. Contam. Toxicol. 21, 507-514

Taylor, W. A., Andersen, P. G., Cooper, S. (1989) The use of air-assistance in a field crop sprayer to reduce drift and modify trajectories. Proceedings Brighton Crop Protection Conference - Weeds, 631-639.

Taylor, W. A., Cooper, S. E., Miller, P. C. H. (1999) An appraisal of nozzles and sprayers abilities to meet regulatory demands for reduced airborne drift and downwind fallout from arable crop spraying. Proc. The 1999 Brighton Conference – Weeds, 447-452.

Thom, A.S. (1976) Momentum, mass and heat exchange of plant communities. In: Monteith, J.L. (ed.) Vegetation and the atmosphere, Volume 1. Academic Press, London, 57-109.

Thyssen, N., Erlandsen, M. (1987) Reaeration of oxygen in shallow, macrophyte rich streams: II. Relationship between the reaeration rate coefficient and hydraulic properties. Int. Revue. ges. Hydrobiol. 72, 575-597.

Thomson, D.J. (1984) Random walk modelling of diffusion in inhomgeneous turbulence. Quart. J. R. Met. Soc. 110, 1107-1120.

D.J. Tomson (1987) Criteria for the selection of stochastic models of particle trajectories in turbulent flows. J. Fluid. Mech. 180, 529-556.

Thompson, N. Ley, A.J. (1983) Estimating spray drift using a random-walk model of evaporating drops. J. Agric. Engng. Res. 28, 419-435.

Tsivouglou, E.C., Wallace, J.R. (1972) Characterization of stream reaeration capacity. U.S. Environmental Protection Agency report EPA-R3-72-012, Washington D.C., USA. Cited in Thyssen and Jeppesen (1980).

Van de Zande, J. C., Holterman, H. J., Huijsmans, J. F. M. (1995) Driftbeperking bij de toediening van gewasbeschermingsmiddelen. Evaluatie van de technische mogelijkheden met een driftmodel. IMAG-DLO. Rapport dienst landbouwkundig onderzoek, Instituut voor Milieu- en Agritechniek, 95-15, 44 pp.

Van de Zande, J.C., Michielsen, J.M.G.P., Stallinga, H., Porskamp, H.A.J., Holterman, H.J., Huijsmans, J.F.M. (2002) Environmental risk control. Aspects of Applied Biology 66, International Advances in Pesticide Application, 165-176.

Van Ulden, A.P. (1978) Simple estimates for vertical diffusion from sources near the ground. Atmospheric Environment 12, 2125-2129.

Wanninkhof, R., Mulholland, P.J., Elwood, J.W. (1990) Gas exchange rates for a first-order stream determined with deliberate and natural tracers. Water Resour. Res. 26, 1621-1630.

Western, N. M., Hislop, E. C., Bieswal, M., Holloway, P. J., Coupland, D. (1999) Drift reduction and droplet-size in sprays containing adjuvant oil emulsions. Pesticide Science 55, 640-642.

Wolf, T. M., Grover, R., Wallace, K., Shewchuk, S. R., Maybank, J. (1993) Effect of protective shields on drift and deposition characteristics of field sprayers. Canadian Journal of Plant Science 73, 1261-1273.

Zhu, H., Reichard, D. L., Fox, R. D., Brazee, R. D., Ozkan, H. E. (1994) Simulation of drift of discrete sizes of water droplets from field sprayers. Transactions of the ASAE, 37, 1401-1407.

1 Calculation of the fraction of the pesticide in the gas phase in the soil

1.1 Deriviation of the equation for the fraction in the gas phase

The following set of equations is necessary to find the fraction of the pesticide in the gas phase (Smit et al., 1997).

The Henry's law coefficient gives the relation between the concentration of the pesticide in the gas and water phase:

$$K_H = \frac{c_{gas}}{c_{liquid}} \qquad \text{(A-1)}$$

where:
K_H = Henry's law coefficient (dimensionless),
c_{gas} = concentration of the pesticide in the gas phase in the soil (kg pesticide m^{-3} air),
c_{liquid} = concentration of the pesticide in the water phase in the soil (kg pesticide m^{-3} water).

Henry's law coefficient can be determined directly or can be determined from the molecular weight, vapour pressure and the solubility in water of the pesticide (see section 1.3). Both the measured or calculated values can be uncertain. It is not unusual that for one compound Henry's law coefficients are reported in the literature, which differ an order of magnitude.

Henry's law coefficient is rather temperature dependent (see section 1.4).

The solid-liquid partitioning coefficient K_d gives the relation between the mass of pesticide adsorbed to the soil particles and the concentration in the water phase in the soil. If a linear sorption isotherm is assumed K_d the following equation is found:

$$K_d = \frac{X}{c_{liquid}} \qquad \text{(A-2)}$$

where:
K_d = solid-liquid partitioning coefficient of the pesticide (kg pesticide kg^{-1} solid)/(kg pesticide m^{-3} water).
X = mass of pesticide adsorbed to the soil particles (kg pesticide kg^{-1} solid).

Often the sorption is not linear and K_d is decreasing with increasing concentration in the water phase increases (Green and Karickhoff, 1990). K_d

is not very temperature dependent (F. van den Berg, Alterra, Wageningen, personal communication, 2001).

The total concentration of pesticide in the soil (in all phases) can now be described by:

$$c_{soil} = \theta_{air} c_{gas} + \theta_{water} c_{liquid} + \rho_{soil,dry} X \qquad \text{(A-3)}$$

where:
c_{soil} = concentration of pesticide in the whole soil matrix (kg pesticide m^{-3} soil)
(Note: soil includes both the solid, water and gas phase of the soil),
θ_{air} = volume fraction of air in the soil (m^3 air m^{-3} soil),
θ_{lwater}= volume fraction of water in the soil (m^3 water m^{-3} soil),
$\rho_{soil,dry}$= dry bulk density of the soil, i.e. soil without water, but including air (kg solid m^{-3} soil).

Equation (3) can also be written as:

$$c_{soil} = Q\, c_{gas} \qquad \text{(A-4)}$$

with the (dimensionless) capacity factor Q:

$$Q = \theta_{air} + \theta_{water} K_d + \rho_{soil,dry} K_H K_d \qquad \text{(A-5)}$$

The dimensionless fraction of the pesticide in the gas phase is then:

$$FP_{gas} = \frac{\theta_{air}}{Q} \qquad \text{(A-6)}$$

K_H and K_d should be known, or can be derived from other properties of the pesticide and/or the soil.

θ_{air} and θ_{water} are usually not given, but have to be derived from the following parameters:

- c_{org} = organic matter content of the solid part of the soil (% of the volume).
- $\rho_{soil, mineral}$ = density of the mineral part of the solid phase of the soil (kg m^{-3}). A constant value of 2660 kg m^{-3} is chosen (F. van den Berg, Alterra, Wageningen, personal communication, 2001).
- $\rho_{soil,org}$ = density of the organic matter part of the solid phase of the soil (kg m^{-3}). A constant value of 1470 kg m^{-3} is chosen (F. van den Berg, Alterra, Wageningen, personal communication, 2001).
- $\rho_{soil,dry}$ = dry bulk density of the soil (without water, but including air) (kg m^{-3}),
- ρ_{air} = density of air (kg m^{-3}). A value of 1.25 kg m^{-3} is taken, which is representative of a pressure of 1 atmosphere and a temperature of 10°C,
- c_{moist} = volumetric moisture content of the soil (% of the volume).

The volume fraction of moisture can be found from:

$$\theta_{\mathrm{water}} = \frac{c_{\mathrm{moist}}}{100} \tag{A-7}$$

Dry soil consists of organic matter and mineral parts. The density of the solid part of the soil $\rho_{\mathrm{soil,solid}}$ (kg m^{-3}) is calculated from the information on the organic matter content and the densities of the organic and mineral parts of the soil:

$$\rho_{\mathrm{soil,solid}} = \left(\frac{c_{\mathrm{org}}}{100}\right)\rho_{\mathrm{soil,org}} + \left(1 - \left(\frac{c_{\mathrm{org}}}{100}\right)\right)\rho_{\mathrm{soil,mineral}} \tag{A-8}$$

As an intermediate step $\theta_{\mathrm{air+water}}$, the volume fraction of air and water together in the moist soil, can be found from:

$$\theta_{\mathrm{air+water}} = \left(\frac{\rho_{\mathrm{soil,dry}} - \rho_{\mathrm{soil,solid}}}{\rho_{\mathrm{air}} - \rho_{\mathrm{soil,solid}}}\right) \tag{A-9}$$

When deriving this equation one should note that the difference between dry soil and moist soil is that part of the volume fraction of air of the dry soil is replaced by water in the moist soil. This means that the volume fraction of air in the dry soil is equal to the volume fraction of air and water together in the moist soil.

The volume fraction of air θ_{air} can then be found from:

$$\theta_{\mathrm{air}} = \theta_{\mathrm{air+water}} - \theta_{\mathrm{water}} \tag{A-10}$$

1.2 Derivation of K_d from K_{om}, K_{oc} or K_{ow}

Many pesticides adsorb to organic matter in the soil, but not all. If the soil contains organic matter and the pesticide adsorbs mainly to organic matter, K_d can be calculated from K_{om} and the organic matter content (in %):

$$K_d = \frac{K_{om} c_{org}}{100} \tag{A-11}$$

where:
K_{om} = coefficient for sorption to soil organic matter (m^3 kg^{-1}). It should be noted that K_{om} is often given in (l kg^{-1}) in the literature.

If K_{om} is not known it can be estimated from K_{oc} (Chiou, 1989):

$$K_{om} = 0.58\ K_{oc} \tag{A-12}$$

where:

K_{oc} = organic carbon distribution coefficient (kg kg^{-1} organic carbon)/(kg m^{-3} water).

If K_{oc} is not known it can be found from K_{ow} using the following equation (Rao and Davidson, 1980):

$$^{10}\log(K_{oc}) = 1.029\ ^{10}\log(K_{ow}) - 0.18 \qquad \text{(A-13)}$$

If no value of K_d is not availabe, it may be estimated with the methods presented here, but in that case the uncertainty in K_d becomes larger.

1.3 Derivation of K_H from molecular weight, vapour pressure and solubility

The Henry's law coefficient as defined by (A-1) can be found from the molecular weight, vapour pressure and solubility given in units that are often used:

$$K_H = \frac{\text{molw}\ VP}{R_{gas}\, T\, S} \qquad \text{(A-14)}$$

where:

molw = molecular weight (g mol^{-1})
VP = vapour pressure (mPa)
R_{gas} = gas constant (8314.5 Pa l K^{-1} mol^{-1})
T = temperature (K)
S = solubility (mg l^{-1})

1.4 Temperature dependence of the vapour pressure

The Clausius-Clapeyron equation describes the temperature dependence of the vapour pressure:

$$\frac{d(\ln(VP))}{dT} = -\frac{\Delta H_v}{R T^2} \qquad \text{(A-15)}$$

where:

VP = vapour pressure at temperature T (Pa)
ΔH_v = heat of vaporisation (J mol^{-1})
R = universal gas constant (8.314 J mol^{-1} K^{-1})
T = temperature (K)

If it is assumed that ΔH_v is constant with changes in temperature the following equation can be obtained (Lyman et al., 1990):

$$VP(T) = VP_{ref} \exp\left(\frac{\Delta H_v}{R}\left(\frac{1}{T_{ref}} - \frac{1}{T}\right)\right) \qquad \text{(A-16)}$$

where:

VP(T) = vapour pressure at temperature T (Pa)
VP_{ref} = vapour pressure at reference temperature T_{ref}

T_{ref} = reference temperature (K)

There are methods to estimate ΔH_v if it is not known, but these methods are rather uncertain (Lyman et al., 1990). The heat of vaporisation has only been determined for a limited number of pesticides. Smit et al. (1997) found an average value for ΔH_v of 95000 J mol^{-1} for about 15 pesticides. The values range from 58000 to 146000 J mol^{-1}. In PESTDEP model a default value for ΔH_v of 95000 J mol^{-1} is used if no values are known.

1.5 Temperature dependence of the solubility

The solubility as a function of the temperature can be found from:

$$S(T) = S_{ref} \exp\left(\frac{\Delta H_s}{R}\left(\frac{1}{T_{ref}} - \frac{1}{T}\right)\right) \quad \text{(A-17)}$$

where:
$S(T)$ = solubility at temperature T
S_{ref} = solubility at reference temperature T_{ref}
T_{ref} = reference temperature (K)
ΔH_s = differential heat of solution (J mol^{-1})

Smit et al. (1997) found an average value for ΔH_s of 27000 J mol^{-1} for about 11 pesticides. The values range from -17380 to 54350 J mol^{-1}. In the PESTDEP model a default value for ΔH_v of 27000 J mol^{-1} is used if no values for ΔH_s are known.

1.6 Temperature dependence of the Henry's law coefficient

The relation for the temperature dependence of the Henry's law coefficient is given by (Seinfeld and Pandis, 1998):

$$H(T) = H(T_{ref}) \exp\left(\frac{\Delta H_A}{R_g}\left(\frac{1}{T_{ref}} - \frac{1}{T}\right)\right) \quad \text{(A-18)}$$

where:
H = Henry's law coefficient (mol l^{-1} atm^{-1})
T = actual temperature (K)
T_{ref} = reference temperature (K)
R_g = gas constant (8.314 Pa m^3 K^{-1} mol^{-1} = 8.314 J K^{-1} mol^{-1}); note that the gas constant used here is expressed in different units than the one used in (A-14).
ΔH_A = heat of dissolution at constant temperature and pressure (J mol^{-1}); ΔH_A can be calculated from ΔH_v and ΔH_s using relation (A-14). A default value of –(95000 – 27000) = -68000 J mol^{-1} is used in PESTDEP if no values are known.

The relation between Henry's law coefficients K_H and H that are defined in different ways is:

$$K_H = \frac{1}{H\, R_g\, T} \quad \text{(A-19)}$$

From (A-15) and (A-16) the following function for K_H as a function of temperature can be found:

$$K_H(T) = K_H(T_{ref})\left(\frac{T_{ref}}{T}\right)\exp\left(\left(-\frac{\Delta H_A}{R_g}\right)\left(\frac{1}{T_{ref}} - \frac{1}{T}\right)\right) \qquad \text{(A-20)}$$

K_H generally increases with temperature. ΔH_A will be different for different compounds.

References

Chiou, C.T. (1989) Theoretical considerations of the partition uptake of nonionic organic compounds by soil organic matter. In Sawhney, B.L., Brown, K.: Reactions and movement of organic chemicals in soils. SSSA special publication 22, Soil Science Society of America, Madison, Wisconsin, USA, 1-30.

Green, R.E., Karickhoff, S.W. (1990) Sorption estimates for modeling. In: Cheng, H.H. (ed.) Pesticides in the soil environment: processes, impacts, and modeling. Soil Science Society of America Inc., Madison, Wisconsin, USA, 79-101.

Lyman, W.J., Reehl, W.F., Rosenblatt, D.H. (eds.) (1990) Handbook of chemical property estimation methods, American Chemical Society, Washington DC, USA.

Rao, P.S.C., Davidson, J.M. (1980) Estimation of pesticide retention and transformation parameters required in nonpoint source pollution models. In: Overcash, M.R., Davidson, J.M. (eds.): Environmental impact of nonpoint source pollution. Ann Arbor Sci. Publ., Ann Arbor, USA, 23-67.

Seinfeld, J.H., Pandis, S.N. (1998) Atmospheric chemistry and physics. John Wiley, New York, USA, 342.

Smit, A.A.M.F.R., van den Berg, F., Leistra, M. (1997) Estimation method for the volatilization of pesticides from fallow soil. Report Environmental Planning Bureau Series 2, DLO Winand Staring Centre, Wageningen, the Netherlands.

1 Viscosity of air and water and estimation of diffusivity of pesticides in air and water

1.1 Diffusivity of gaseous pesticides in air

The diffusivity of a gas in air can be estimated by the method of Fuller, Schettler and Giddings (FSG method) (Lyman et al., 1982). It is most accurate for non-polar gases at low to moderate temperatures. Its accuracy is poorest for polar acids (12%) and glycols (12%) and minimal errors are found for aliphatics (4%) and aromatics (4%) (Lyman et al., 1982).
The FSG method is based on the following equation:

$$D_g = k_1 \frac{10^{-11}\ T^{1.75} \sqrt{\dfrac{M_A + M_B}{M_A M_B}}}{P\ \left[(V_A)^{1/3} + (V_B)^{1/3}\right]^2} \qquad \text{(B-1)}$$

where:
D_g = diffusivity in air($m^2\ s^{-1}$)
T = temperature (K)
P = pressure (atm)
V = molar volume based on the method developed by Fuller et al. (1966) ($m^3\ mol^{-1}$)
M = molecular weight ($g\ mol^{-1}$).
k_1 = constant necessary to obtain the right dimensions. Its value is 1.0 and its dimension is $\frac{atm\ m^4\ g^{0.5}}{s\ mol^{1.167}\ K^{1.75}}$.

The subscipts A and B in (B-1) refer to the air and the gaseous pesticide, respectively. M_A is 28.97 g mol^{-1} and V_A is $20.1 \times 10^{-6}\ m^3\ mol^{-1}$.

V_B can be estimated from the chemical structure of the molecule using the increments listed in Table 1:

$$V_B = \sum_i n_i\ \Delta V_{B,i} \qquad \text{(B-2)}$$

where n_i is the number of atoms of kind i and $\Delta V_{B,i}$ is the volume increment cause by atom i. A correction has to be made to the sum in case of aromatic and heterocyclic rings are present.

Table 1. Atomic and structural diffusion volume increments ΔV_B (m^3 mol^{-1}) (Fuller et al., 1966).

Tabel 1. Atom og andre strukturelle diffusions volume inkrementer DV_B *(*m^3 mol^{-1}*) (Fuller et al., 1966).*

Atom	ΔV_B
C	16.50×10^{-6}
H	1.98×10^{-6}
O	5.48×10^{-6}
N	(5.69×10^{-6})
Cl	(19.5×10^{-6})
S	(17.0×10^{-6})
Aromatic and hyterocyclic rings	-20.2×10^{-6}

Values in parentheses are based upon few data points (Fuller et al., 1966). (Reprinted with permission from Fuller et al. (1966). Copyright 1966 American Chemical Society)

For chemicals not listed in Table 1, V_B can be estimated as 85-90% of the LeBas volume V_B'. In the following calculations we have used $V_B = 0.875V_B'$. V_B' can be found from Table 2.

Table 2. Additive volume increments $\Delta V_B'$ for calculating the LeBas molar volume V_B' (m^3 mol^{-1}) (Reid et al., 1977).

Tabel 2. Additive volume inkrementer til beregning af LeBas molær volumen V_B¢ *(*m^3 mol^{-1}*) (Reid et al., 1977).*

Atom	$\Delta V_B'$	Atom	$\Delta V_B'$
C	14.8×10^{-6}	Br	27.0×10^{-6}
H	3.7×10^{-6}	Cl	24.6×10^{-6}
O (except as noted below)	7.4×10^{-6}	F	8.7×10^{-6}
- in methyl esters and ethers	9.1×10^{-6}	I	37.0×10^{-6}
- in ethyl esters and ethers	9.9×10^{-6}	S	25.6×10^{-6}
- in higher esters and ethers	11.0×10^{-6}	Ring	
- in acids	12.0×10^{-6}	- 3-membered	-6.0×10^{-6}
- joined to S, P, N	8.3×10^{-6}	- 4-membered	-8.5×10^{-6}
N		- 5-membered	-11.5×10^{-6}
- double bounded	15.6×10^{-6}	- 6-membered	-15.0×10^{-6}
- in primary amines	10.5×10^{-6}	- naphthalene	-30.0×10^{-6}
- in secondary amines	12.0×10^{-6}	- anthracene	-47.5×10^{-6}

Reid et al. (1977) (Reprinted with permission from McGraw-Hill).

V_B' is calculated from the increments in the same fashion as V_B. It should be noted that there are no values of ΔV_B or $\Delta V_B'$ for phosphorous. This means that it is not possible to estimate the diffusivity in air for organophosphorous pesticides with this method.

The method mentioned above is somewhat complicated. A more simple method was developed here where the diffusivity at one temperature and pressure is estimated from the molecular weight alone. The idea behind this is that the molar volume is proportional to the molecular weight. First the diffusivity was calculated with the FSG method for 11 pesticides with different molecular weights between about 100 and 500 g mol^{-1}. The following expression was found to give a good description for the relation between D_g and M_B at 298.15 °K and 1 atmosphere:

$$D_g(298.15,\, 1) = k_2 \frac{1.42\times10^{-4}}{M_B{}^{0.589}} \tag{B-3}$$

In this equation $D_{g,298.15,\,1}$ is in m^2 s^{-1} and M_B is in g mol^{-1}; k_2 is a constant necessary to obtain the right dimensions. Its value is 1.0 and its dimension is $\frac{m^2\, g^{0.589}}{s\, mol^{0.589}}$.

It would be possible to derive a slightly better fit with a more complicated relation than was used here. It was, however, decided that this was not necessary in view of the uncertainty in other factors in the model in which D_g is used.

D_g can be calculated for other temperatures (and pressures) using the relation of B-1:

$$D_g(T, P) = D_g(298.15,\, 1)\frac{T^{1.75}\;\; P_{ref}}{T_{ref}{}^{1.75}\; P} \tag{B-4}$$

where T_{ref} is 298.15°K and P_{ref} is 1 atmosphere.

Table 3 shows the results of both methods and their difference. The average absolute difference between the two methods is 5.0 %, which is very reasonable. The results are also shown in Figure 1.

Table 3. Diffusivity in air at 298.15 °K and 1 atmosphere calculated with the FSG method and the simple method.

Tabel 3. Diffusionskoefficient i luft ved 298.15 °K og 1 atmosfære beregnet med FSG-metoden og den simple metode.

	molecular weight (g mol^{-1})	Diffusivity FSG method (m^2 s^{-1})	Diffusivity simple method (m^2 s^{-1})	% difference
Ethylene dichloride	99.0	9.2×10^{-6}	9.5×10^{-6}	-3.6
Fenuron	164.2	6.3×10^{-6}	7.0×10^{-6}	-11.0
DNOC	198.1	6.7×10^{-6}	6.3×10^{-6}	5.6
Ethylchlorate	238.7	5.7×10^{-6}	5.6×10^{-6}	0.5
Bentazone	240.3	5.8×10^{-6}	5.6×10^{-6}	3.4
Formethanate hydrochlorid	222.3	5.5×10^{-6}	5.9×10^{-6}	-7.1
Desmedipham	300.3	4.8×10^{-6}	4.9×10^{-6}	-3.1
DDT	354.5	4.6×10^{-6}	4.5×10^{-6}	3.2
Dimethomorph	387.9	4.2×10^{-6}	4.2×10^{-6}	-1.7
Lactofen	461.8	4.1×10^{-6}	3.8×10^{-6}	6.5
Deltamethrin	505.2	4.0×10^{-6}	3.6×10^{-6}	9.1
Average absolute difference (%)				5.0

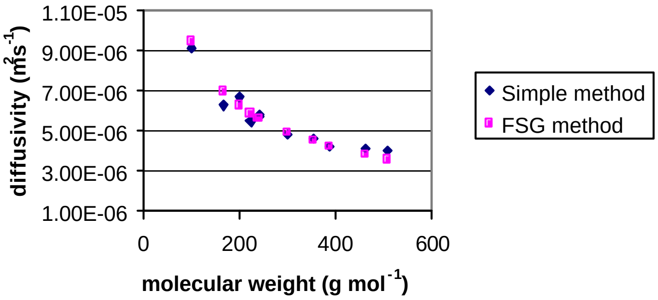

Figure 1. Comparison of the diffusivity in air calculated with the FSG method and the simple method.
Figur 1. Sammenligning af diffusionskoefficienten i luft beregnet med FSG-metoden og den simple metode.

1.2 Diffusivity of pesticides in water

The diffusivity of pesticides in water can be estimated with the method of Hayduk and Laudie (Lyman et al., 1990):

$$D_w = k_3 \frac{1.474 \times 10^{-15}}{h_W^{1.14} \cdot V'_B{}^{0.589}} \qquad \text{(B-5)}$$

where:
D_w = diffusivity in water ($m^2\ s^{-1}$)
η_w = viscosity of water (which is a function of temperature) ($kg\ m^{-1}\ s^{-1}$); for sea water the viscosity of sea water should be used.
$V_B{}'$ = LeBas molar volume ($m^3\ mol^{-1}$)
k_3 = constant necessary to obtain the right dimensions. Its value is 1.0 and its dimension is $\frac{m^{2.627}\ kg^{1.14}}{mol^{0.589}\ s^{2.14}}$.

Eq. B-5 does not include a temperature term, since temperature dependence is incorporated in the viscosity term. In section 1.3 of this appendix the viscosity of water is given as a function of temperature for freshwater and sea water (also as a function of salinity).

The method mentioned above is somewhat complicated. A more simple method was developed where the diffusivity in pure water (freshwater) at one temperature is estimated from the molecular weight alone. The idea behind this is that the molar volume is proportional to the molecular weight. First the diffusivity was calculated with the Hayduk and Laudie method for 11 pesticides with different molecular weights between about 100 and 500 g mol^{-1}. The following expression was then found for the relation between D_w and M_B 298.15 °K:

$$D_w(298.15) = k_4 \frac{1.44 \times 10^{-8}}{M_B^{0.589}} \qquad \text{(B-6)}$$

In this equation $D_{w,298.15}$ is in $m^2\ s^{-1}$ and M_B is in $g\ mol^{-1}$. k_4 = constant necessary to obtain the right dimensions. Its value is 1.0 and its dimension is $\frac{m^2\ g^{0.589}}{s\ mol^{0.589}}$.

The diffusivity of the gaseous pesticide $D_{sw}(S,T)$ for (sea) water at temperature T (°K) and salinity S (pro mille) can be calculated from the following relation, which is derived from (B-5):

$$D_{sw}(S,T) = \left(\frac{\eta_w(0,298.15)}{\eta_{sw}(S,T)} \right)^{1.14} D_w(0,298.15) \qquad \text{(B-7)}$$

where: $\eta_w(0,298.15)$ is the viscosity of pure water at 298.15 °K and $\eta_w(S,T)$ is the viscosity of (sea) water at salinity S and temperature T.

Table 4 shows the results of both methods and their difference. The average absolute difference between the two methods is 5.7%, which is quite reasonable. The results are also shown in Figure 2.

Table 4. Diffusivity in water at 298.15 °K calculated with the FSG method and the simple method.

Tabel 4. Diffusionskoefficient i vand ved 298.15 °K beregnet med FSG-metoden og den simple metode.

	molecular weight ($g\ mol^{-1}$)	Diffusivity Hayduk and Laudie method ($m^2\ s^{-1}$)	Diffusivity simple method ($m^2\ s^{-1}$)	% difference
Ethylene dichloride	99.0	1.04×10^{-9}	9.60×10^{-10}	7.9
Fenuron	164.2	6.80×10^{-10}	7.10×10^{-10}	-5.0
DNOC	198.1	7.00×10^{-10}	6.40×10^{-10}	9.3
Ethylchlorate	238.7	5.90×10^{-10}	5.70×10^{-10}	2.4
Bentazone	240.3	6.05×10^{-10}	5.70×10^{-10}	5.8
Formethanate hydrochlorid	222.3	5.60×10^{-10}	6.00×10^{-10}	-6.5
Desmedipham	300.3	5.00×10^{-10}	5.00×10^{-10}	-1.0
DDT	354.5	4.90×10^{-10}	4.50×10^{-10}	8.1
Dimethomorph	387.9	4.30×10^{-10}	4.30×10^{-10}	0.2
Lactofen	461.8	4.20×10^{-10}	3.90×10^{-10}	7.2
Deltamethrin	505.2	4.10×10^{-10}	3.70×10^{-10}	9.6
Average absolute difference (%)				5.7

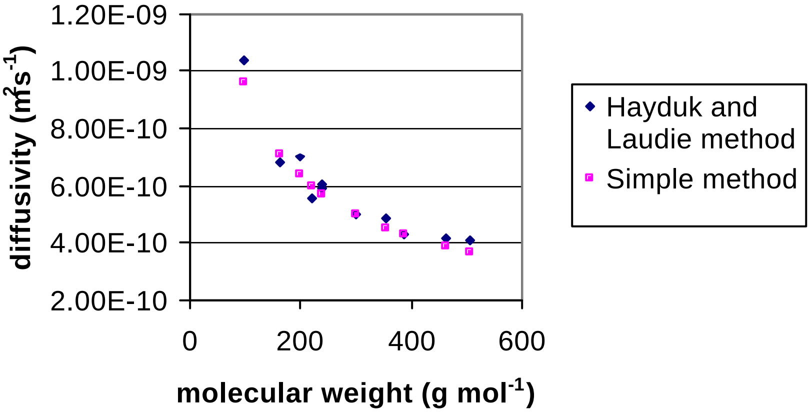

Figure 2. Comparison of the diffusivity in water calculated with the Hayduk and Laudie method and the simple method.

Figur 2 Sammenligning af diffusionskoefficienten i vand beregnet med Hayduk og Laudie metoden og den simple metode.

1.3 Dynamic viscosity and kinematic viscosity of air

The kinematic viscosity of air is a function of the dynamic viscosity of air and the density of air. For that reason the density of dry air has to be calculated (Pruppacher and Klett, 1997):

$$\rho_a = \frac{10^{-3} M_{da} P}{R T} \qquad \text{(B-8)}$$

where:

ρ_a = density of dry air (kg m^{-3})
M_{da} = molecular weight dry air (28.9644 g m^{-2})
P = pressure (atm)
R = gas constant (8.2057×10^{-5} atm m^3 mol^{-1} K^{-1})
T = temperature (K)

The dynamic viscosity of air between -50°C and +50°C is given by (Pruppacher and Klett, 1997):

$$\eta_a = 1.718 \times 10^{-5} + 0.0049 \times 10^{-5} t \qquad (\text{for } t \geq 0°C) \quad \text{(B-9a)}$$

$$\eta_a = 1.718 \times 10^{-5} + 0.0049 \times 10^{-5} t - 1.2 \times 10^{-10} t^2 \qquad (\text{for } t < 0°C) \quad \text{(B-9b)}$$

where:

η_a = dynamic viscosity of the air (kg m^{-1} s^{-1})
t = temperature (°C)

The kinematic viscosity of air ν_a (m^2 s^{-1}) is:

$$\nu_a = \frac{\eta_a}{\rho_a} \qquad \text{(B-10)}$$

1.4 Viscosity and kinematic viscosity of (sea)water

The kinematic viscosity of (sea) water at 1 atmosphere is a function of the viscosity of water, but also of the density of water and for seawater also of the salinity. For that reason the density of (sea) water has to be calculated. The density of pure (fresh) is (kg m^{-3}) (Sündermann, 1986):

$$\begin{aligned}\rho_{w}(t) = {} & 999.842594 + 6.793952\times10^{-2}t \\ & - 9.095290\times10^{-3}t^{2} + 1.001685\times10^{-4}t^{3} \\ & - 1.120083\times10^{-6}t^{4} + 6.536332\times10^{-9}t^{5}\end{aligned} \qquad \text{(B-11)}$$

where ρ_w is the density of pure (fresh) water (kg m^{-3}) and t is the temperature (°C).

The density of seawater at 1 atmosphere as a function of the temperature and the salinity is now given by (Sündermann, 1986):

$$\begin{aligned}\rho_{sw}(S,t) = \rho_{w}(t) + {} & (8.24493\times10^{-1} - 4.0899\times10^{-3}t \\ & + 7.6438\times10^{-5}t^{2} - 8.2467\times10^{-7}t^{3} \\ & + 5.3875\times10^{-9}t^{4})S \\ & + (-5.72466\times10^{-3} + 1.0227\times10^{-4}t \\ & - 1.6546\times10^{-6}t^{2})S^{3/2} \\ & + 4.8314\times10^{-4}S^{2}\end{aligned} \qquad \text{(B-12)}$$

The above equation is valid for salinities between 0 and 42 pro mille and a temperature between –2 and +40 °C.

The viscosity of pure water is given by (Sündermann, 1986):

$${}^{10}\log\left(\frac{\eta_{w}(t)}{\eta_{w}(20)}\right) = \frac{1.1709(20-t) - 1.827\times10^{-3}(t-20)^{2}}{t+89.93} \qquad \text{(B-13)}$$

where t is the temperature (°C) and $\eta_w(20) = 1.002\times10^{-3}$ (kg m^{-1} s^{-1}). This equation is valid for 1 atmosphere and a temperature range of 10 to 70 °C.

The viscosity of sea water at 1 atmosphere can be obtained from (Sündermann, 1986):

$$\eta_{sw}(S,t) = \eta_{w}(t)\left(1 + A\,Cl_{v}^{1/2} + B\,Cl_{v}\right) \qquad \text{(B-14)}$$

with:

$$A = 5.185\times10^{-5}t + 1.0675\times10^{-4} \qquad \text{and}$$

$$B = 3.300\times10^{-5}t + 2.591\times10^{-3}$$

In this equation $\eta_{sw}(S,t)$ is the dynamic viscosity of sea water at 1 atmosphere at salinity S (pro mille) and temperature t(°C). Cl_v is the volume chlorinity, which is related to salinity by (Sündermann, 1986):

$$\mathrm{Cl}_v = \frac{r_{sw}\,\mathrm{S}}{1806.55} \qquad \text{(B-15)}$$

This is valid for salinities between 0 and 40 pro mille and temperatures between 5 and 25 °C.

The kinematic viscosity of (sea) water at 1 atmosphere ν_{sw} ($\mathrm{m}^2\ \mathrm{s}^{-1}$) is defined by:

$$n_{sw}(\mathrm{S},\mathrm{t}) = \frac{h_{sw}(\mathrm{S},\mathrm{t})}{r_{sw}(\mathrm{S},\mathrm{t})} \qquad \text{(B-16)}$$

Note: the equations for sea water can also be used to calculate the kinematic viscosity of freshwater by putting a value of 0 for the salinity in the equations.

References

Fuller, E.N., Schettler, P.D., Giddings, J.C. (1966) A new method for prediction of binary gas-phase diffusion coefficients. Ind. Eng. Chem. 58, 19-27.

Lyman, W.J., Reehl, W.F., Rosenblatt, D.H. (eds.) (1990) Handbook of chemical property estimation methods, American Chemical Society, Washington DC, USA.

Pruppacher, H.R., Klett, J.D. (1997) Microphysics of clouds and precipitation. Kluwer, Dordrecht, The Netherlands.

Reid, R.C., Prausnitz, J.M., Sherwood, T.K. (1977) The properties of gases and liquids, 3rd. edition, McGraw-Hill, New York.

Sündermann, J. (ed.) (1986) Landolt-Börnstein, Numerical data and functional relationships in science and technology. New series. Group V: Geophysics and space research, Vol. 3: Oceanography, subvolume a. Springer, Berlin, Germany.

Appendix C

1 Derivation of the basic equation for the surface resistance of water

In this appendix the surface resistance r_c for water bodies will be derived. The exchange of gases between the atmosphere and streams, lakes and seas has traditionally been described in a way that is more familiar to engineers than to atmospheric scientists. In stead of describing the exchange with the resistances as atmospheric scientists do they describe the exchange with mass transfer coefficients. For that reason we will describe the engineering approach of exchange here first and then we will see how the derived mass transfer coefficients can be translated into resistances. The physics and chemistry of the processes involved are of course the same for both approaches, only the way they are described is different.

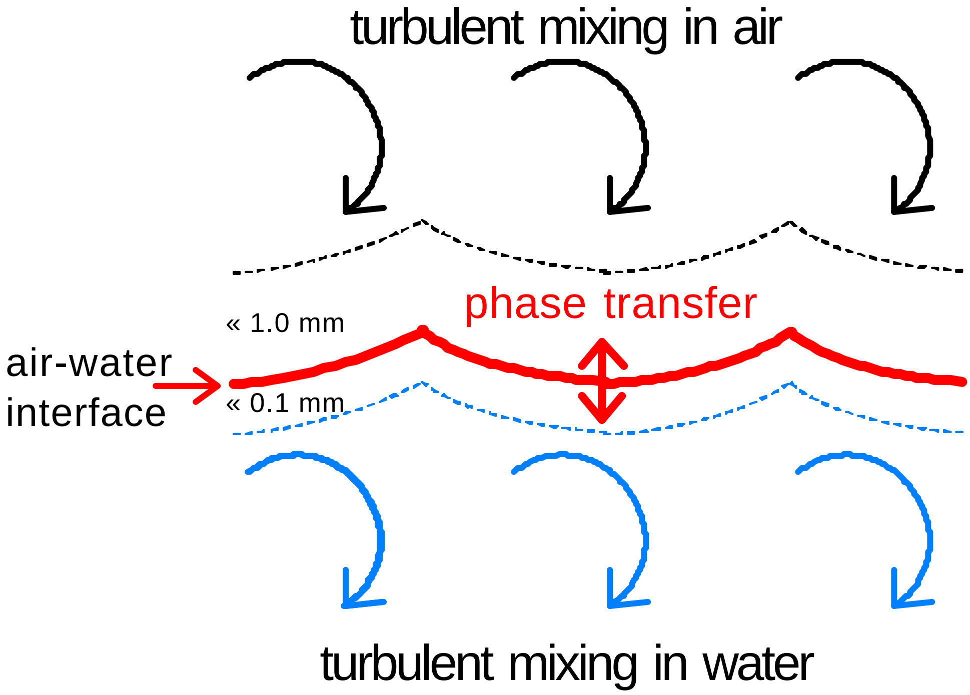

Figure C-1. Model for air-water exchange. On both sides of the air-water interface there is a stagnant or intermittently mixed boundary layer (about 1 mm thick in the air and about 0.1 mm thick in the water). The remaining parts of the air and the water are assumed to be well mixed by turbulence. Phase transfer takes place at the air-water interface.
Figur C-1. Model for udveksling mellem atmosfæren og vand. På begge sider af overfladen befinder sig et stagnerende eller periodisk

blandet grænselag (ca. 1 mm tyk i atmosfæren og ca. 0.1 mm tyk i vand). Det antages, at resten af atmosfæren og vandet er vel opblandet pga. af turbulens.

Fig.C-1. visualises the processes that play a role in the exchange of gases between the atmosphere and water (Schwarzenbach, 1993):

1) Turbulent transport in the atmosphere by turbulence to a stagnant or intermittently mixed boundary layer.
2) Transport through a stagnant or intermittently mixed boundary layer of air, which has a thickness of the order of 1 mm.
3) Transport across the air-water interface.
4) Transport through the stagnant or intermittently mixed boundary layer of water, which has a thickness of the order of 0.1 mm.
5) Turbulent transport by turbulence in the water.

The mass transfer from the atmosphere to the water and vice versa depends in principle on the speed for each subsequent step. There are different models available to describe this situation (Schwarzenbach et al., 1993).

a) The stagnant two-film model. In this model it is assumed, that the transport through the two stagnant boundary layers occurs by molecular diffusion. As a result, the transport velocity through these layers increases linearly with the diffusivity of the gas in air or water.
b) The surface-renewal model. In this model it is assumed that there is a continual turnover of air and water parcels with the (dissolved) gas within the intermittent boundary layers. As a result the transport through the layers increases with the square root of the diffusivity of the gas in air or water (Schwarzenbach et al., 1993).

The main difference between the results of these models is the fact that the transport velocity through the stagnant or intermittent layer increase with the diffusivity in model a) and with the square root of the diffusivity in model b).

It should be noted that many of the parameters that are important in such models like the thickness of the stagnant or intermittent layer cannot be measured, nor can the rate at which the surface is renewed in the surface renewal model. In practice this means that both models include fitting parameters that when appropriately adjusted yield exchange rate estimates that are in agreement with experimental values. It should also be noted that the basic equations for exchange are the same in the stagnant two-film model and the surface-renewal model (Schwartz, 1992; Schwarzenbach et al., 1993). It is only the parameterization of the exchange rate that is different. In the following the basic equations are derived.

In the basic equations concentrations are either expressed in the gas phase or in the aqueous phase. In case of equilibrium gas phase and aqueous phase concentrations are related through Henry's law:

$$K_H = \frac{equilibrium\ conc.\ in\ gas\ phase\ \left(kg\ m^{-3}\right)}{equilibrium\ conc.\ in\ aqueous\ phase\ \left(kg\ m^{-3}\right)} \qquad \text{(C-1)}$$

It should be noted here, that there are numerous definitions of Henry’s law coefficients, having different units and even different senses.

In the model it is assumed that that the bulk of the gaseous and aqueous phases is homogeneously mixed. In the following equations are given for the fluxes in each step.

The flux (F_g in kg m^{-2} s^{-1}) from the bulk gas phase through the stagnant or intermittent layer in the atmosphere to the interface is described by:

$$F_g = -k_g\left(c_g - c_{g,i}\right) \tag{C-2}$$

where:

k_g = gaseous phase mass transfer coefficient (m s^{-1})
c_g = concentration in the bulk gas phase (kg m^{-3})
$c_{g,i}$ = concentration in the gas phase at the air-water interface (kg m^{-3})

This equation states that the flux depends on a speed, also called mass transfer coefficient k_g and the difference in concentration between the bulk gas phase and the interface. Hence it will depend on the concentration differences in which way (to or from the water) the transport will go.

The flux (F_i in kg m^{-2} s^{-1}) across the interface is described by:

$$F_i = -\frac{\bar{v}a}{4}\left(c_{g,i} - c_{w,i}K_H\right) \tag{C-3}$$

where:

$\bar{v}$ = mean molecular speed of the gas molecule (m s^{-1}); $\bar{v}\,c_{g,i}/4$ is the gas kinetic collision rate
α = mass-accommodation coefficient (dimensionless). This is the probability that a collision at the interface will result in interfacial mass transfer.
$c_{w,i}$ = concentration in the aqueous phase at the air-water interface (kg m^{-3})

This flux depends on the concentration differences between both sides as well as on the molecular speed of the molecule and how big the change is that a collision will result in a transport across the interface. K_H is just used to “translate” an aqueous phase concentration in a gas phase concentration, because otherwise concentrations cannot be compared.

The flux (F_w in kg m^{-2} s^{-1}) from the interface through the stagnant or intermittent layer in the water to the bulk aqueous phase is described by:

$$F_w = -b\ k_w\left(c_{w,i} - c_w\right) \tag{C-4}$$

where:

β = factor by which the aqueous phase mass transfer enhances due to removal of the material by chemical reaction. If there is no enhancement β is 1. If there is enhancement β will be larger than 1.

k_w = aqueous phase mass transfer coefficient (m s^{-1})
c_w = concentration in the bulk aqueous phase (kg m^{-3})

This equation indicates that the flux depends on a speed, also called mass transfer coefficient k_w and the difference in concentration between the interface and the bulk water phase. Hence it will depend on the concentration differences in which way (to or from the air-water interface) the transport will go.

After a very short time a steady state situation will be reached, where the fluxes F_g, F_i and F_w are equal to each other. The concentrations $c_{g,i}$ and $c_{w,i}$ at the interface are generally not known. For that reason it is useful to express the fluxes in the bulk concentrations c_g and c_w. This can e.g. be done by finding $c_{w,i}$ that still is a function of $c_{g,i}$ from equations (C-3) and (C-4). Then substituting the expression for $c_{w,,i}$ in equation (C-4) and then finding $c_{g,i}$ from equations (C-4) and (C-2).

In this way the following equation is found for the flux:

$$F = -K_g \left(c_g - K_H c_w \right) \tag{C-5}$$

where K_g is the overall gas phase mass transfer coefficient (m s^{-1}), which is defined by:

$$\frac{1}{K_g} = \frac{1}{k_g} + \frac{4}{\bar{v}a} + \frac{K_H}{b\ k_w} \tag{C-6}$$

Equation C-5 is in principle the same as equation (5) in the main report where $c_{g,surface} = K_H c_w$.

It should be noted that the flux can be expressed as an overall aqueous phase mass transfer coefficient as well:

$$F = -K_w \left(\frac{c_g}{K_H} - c_w \right) \tag{C-7}$$

where K_w is defined by:

$$\frac{1}{\mathrm{K_w}} = \frac{1}{\mathrm{K_H k_g}} + \frac{4}{\bar{v}a\mathrm{K_H}} + \frac{1}{b\ \mathrm{k_w}} \tag{C-8}$$

Equations (C-7) and (C-8) are aqueous phase equivalents of (C-5) and (C-6).

The terms in (C-6) or (C-8) add like electrical resistances in series, illustrating that the mass transfer is governing by three subsequent transfer processes.

If the mass accommodation coefficient is greater than of the order of 1×10^{-4}, i.e. that the more than 1 out of 10000 gas molecules are absorbed when they hit the water surface the transport through the interface is so fast that it does not limit the overall transfer (Schwartz, 1992). The mass accommodation coefficient has only been determined for a limited number of more common atmospheric gases that have a low molecular weight (Seinfeld and Pandis, 1998) and not at all for pesticides. So it cannot be excluded that for some pesticides the transport through the interface is so slow that it limits the overall mass transfer. In the following, we will assume that the mass transfer coefficient of pesticides is so high that the second term in (C-6) and (C-4) can be neglected. If this is not correct, the mass transfer will occur at a lower rate than predicted with the simplified forms of (C-6) and (C-4).

In the following the effect of chemical reactions is also neglected and it is hence assumed that $\beta = 1$. In reality, however, reactions can be important for some pesticides, especially those that e.g. dissociate very fast in water.

If there is no reaction and no resistance at the interface (i.e. the mass accomodation coefficient is large enough) (C-6) becomes:

$$\frac{1}{K_g} = \frac{1}{k_g} + \frac{K_H}{k_w} \qquad \text{(C-9)}$$

There is in that case a critical Henry's law coefficient $K_{H,crit}$ for which the gas and aqueous phase mass transfer coefficients are equal:

$$K_{H,crit} \equiv \frac{k_w}{k_g} \qquad \text{(C-10)}$$

If $K_H >> K_{H,crit}$ the overall mass transfer is controlled by transfer in the aqueous phase and for $K_H << K_{H,crit}$ the overall mass transfer is controlled by the transfer gas phase.

The approach in this section is the engineering approach. The mass transfer coefficient in the gas phase k_g covers in fact the transport from a certain reference height in a part of the turbulent atmosphere, then through the stagnant or intermittently mixed boundary layer to the interface/surface. In the engineering approach the concentration in the bulk air phase is the same everywhere. Atmospheric scientists have a different approach and allow a vertical concentration gradient in the bulk air that is caused by dry deposition.

Meteorologists use the following equation for the flux:

$$F = \frac{1}{r_a + r_b + r_c}\left(c_{g,r} - c_{g,i}\right) \qquad \text{(C-11)}$$

where (see section 2.4 of the main report):

r_a = aerodynamic resistance (s m^{-1})
r_b = laminar boundary layer resistance (s m^{-1})
r_c = surface resistance (s m^{-1})
$c_{g,r}$ = concentration in the gas phase at reference height (kg m^{-3})

Comparing (C-11) for the situation where r_c is zero with (C-2) describing the same situation leads to the following equation:

$$r_a + r_b = \frac{1}{k_g} \tag{C-12}$$

Comparing (C-11) with (C-5) with the K_g value from (C-9) leads to the equation for the surface resistance:

$$r_c = \frac{K_H}{k_w} \tag{C-13}$$

This relation shows that r_c increases with K_H and decreases with the mass transfer coefficient in the aqueous phase, which is a measure of how fast the compound is transported away from the interface into the bulk water. The molecules that have been transported away from the surface can then again be replaced by "fresh" molecules that reach the interface from the gas phase. It is equation C-13 that we will use in the main report to calculate r_c.

It should be noted here that the model not only describes dry deposition to water surfaces, but also emission from water surfaces, e.g. emission that can occur due to spills of chemicals.

References

Schwartz, S.E. (1992). Factors governing dry deposition of gases to surface water. In: Schwartz, S.E. and Slinn, W.G.N. Precipitation scavenging and atmosphere-surface exchange. Hemisphere Publishing Corporation, Washington D.C., USA, 789-801.

Schwarzenbach, R.P., Gschwend, P.M., Imboden, D.M. (1993). Environmental organic chemistry. John Wiley, New York, USA.

Seinfeld, J.H., Pandis, S.N. (1998) Atmospheric chemistry and physics. John Wiley, New York, USA.

1 Experimental values of aqueous phase mass transfer coefficients

In the following information is given on all data on the measurements of the aqueous phase mass transfer coefficient of CO_2 at 20°C in freshwater k(600) as a function of the wind speed at 10 m height (u(10)) used in this report. The values were either found in tables in the publications, derived from figures and sometimes aqueous phase mass transfer coefficients for other gases and conditions were converted to k(600) values.

1.1 Rockland Lake

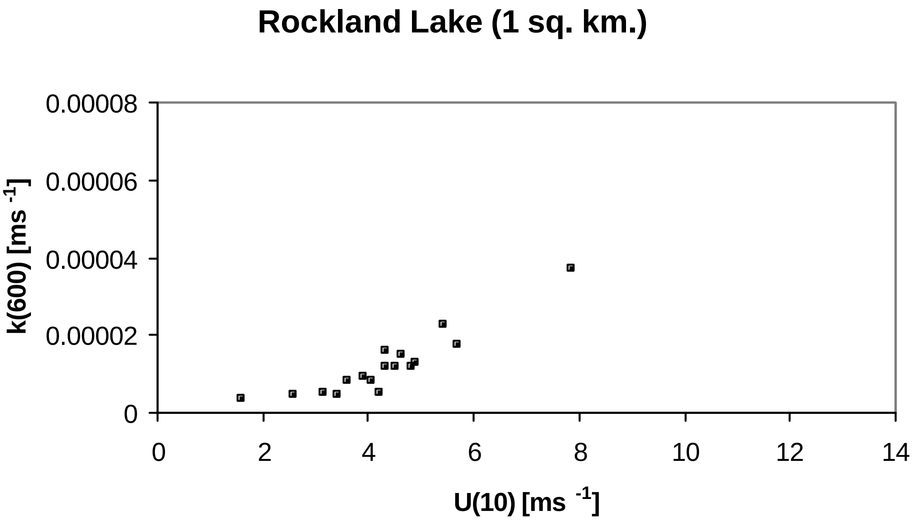

Figure D-1. Relation between k(600) and u(10) for Rockland Lake (1 km^2)(Wanninkhof et al., 1995).
Figur D-1. Forhold mellem k(600) og u(10) for Rockland Lake (1 km^2)(Wanninkhof et al., 1995).

Table D-1. Measurements of u(10) and k(600) for Rockland Lake.
Table D-1. Målinger af u(10) og k(600) for Rockland Lake.

u(10) (m s^{-1})	k(600) (m s^{-1})
1.61	3.47×10^{-6}
2.58	4.81×10^{-6}
3.14	5.14×10^{-6}
3.4	4.39×10^{-6}
3.62	8.44×10^{-6}
3.89	9.42×10^{-6}
4.06	8.44×10^{-6}
4.2	5.14×10^{-6}
4.32	1.19×10^{-5}
4.32	1.59×10^{-5}
4.52	1.17×10^{-5}
4.61	1.49×10^{-5}
4.83	1.17×10^{-5}
4.89	1.29×10^{-5}
5.43	2.28×10^{-5}
5.68	1.75×10^{-5}
7.87	3.69×10^{-5}

1.2 Lake 302 N

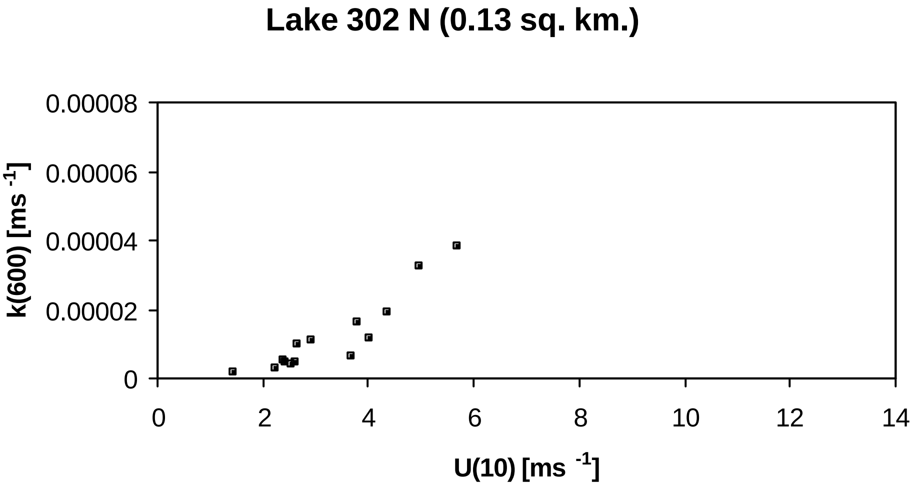

Figure D-2. Relation between k(600) and u(10) for Lake 302 N (0.13 km^2) (Crucius and Wanninkhof, 1990).
Figur D-2. Forhold mellem k(600) og u(10) for Lake 302 N (0.13 km^2) (Crucius and Wanninkhof, 1990).

Table D-2. Measurements of u(10) and k(600) for Lake 302 N.
Tabel D-2. Målinger af u(10) og k(600) for Lake 302 N.

u(10) (m s^{-1})	k(600) (m s^{-1})
1.43	1.97×10^{-6}
2.25	2.97×10^{-6}
2.38	5.28×10^{-6}
2.44	4.47×10^{-6}
2.54	4.14×10^{-6}
2.60	4.47×10^{-6}
2.67	9.75×10^{-6}
2.92	1.13×10^{-5}
3.68	6.28×10^{-6}
3.81	1.64×10^{-5}
4.03	1.18×10^{-5}
4.38	1.92×10^{-5}
4.98	3.22×10^{-5}
5.68	3.83×10^{-5}

1.3 Pyramid Lake

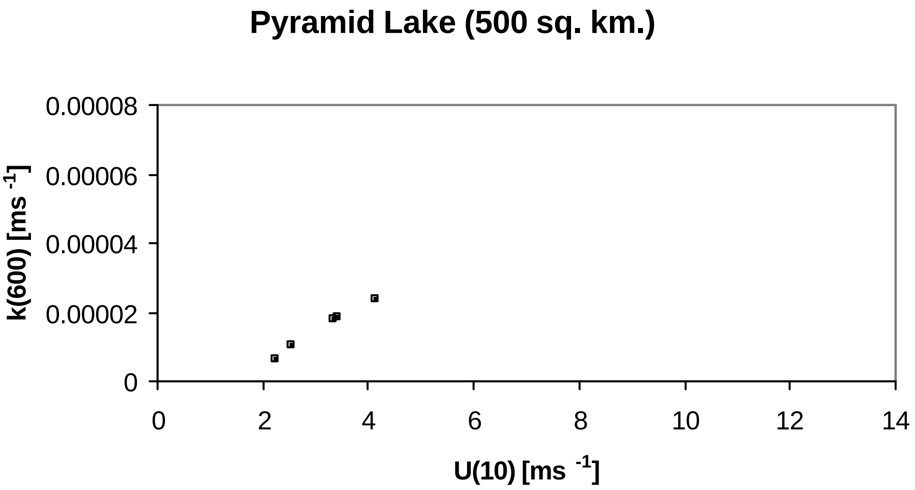

Figure D-3. Relation between k(600) and u(10) for Pyramid Lake (500 km^2) (Peng and Broecker, 1990).
Figur D-3. Forhold mellem k(600) og u(10) for Pyramid Lake (500 km^2) (Peng og Broecker, 1990).

Table D-3. Measurements of u(10) and k(600) for Pyramid Lake.
Tabel D-3. Målinger af u(10) og k(600) for Pyramid Lake.

u(10) (m s^{-1})	k(600) (m s^{-1})
2.22	6.44×10^{-6}
2.54	1.04×10^{-5}
3.33	1.77×10^{-5}
3.43	1.84×10^{-5}
4.13	2.38×10^{-5}

1.4 Crowley Lake

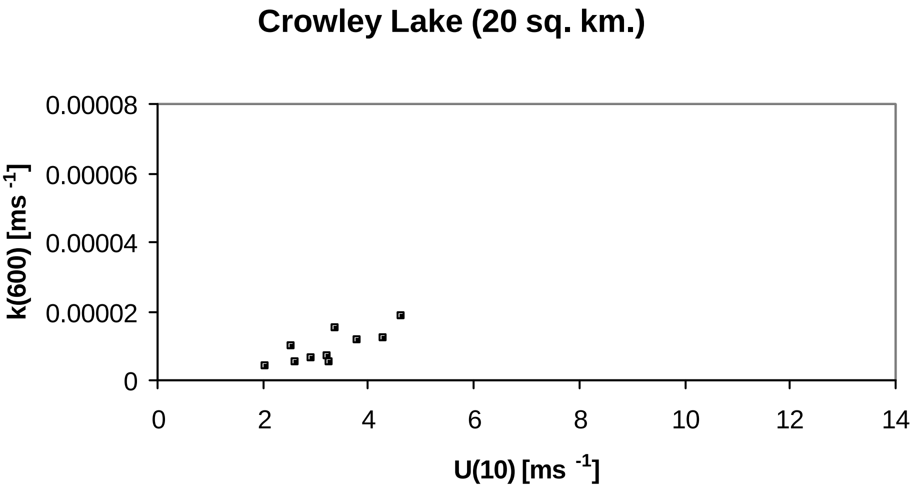

Figure D-4. Relation between k(600) and u(10) for Crowley Lake (20 km^2) (Wanninkhof et al., 1991a).
Figur D-4. Forhold mellem k(600) og u(10) for Crowley Lake (20 km^2) (Wanninkhof et al., 1991a).

Table D-4. Measurements of u(10) and k(600) for Crowley Lake.
Tabel D-4. Målinger af u(10) og k(600) for Crowley Lake.

u(10) (m s^{-1})	k(600) (m s^{-1})
2.06	4.31×10^{-6}
2.54	9.58×10^{-6}
2.63	5.28×10^{-6}
2.92	6.11×10^{-6}
3.23	6.78×10^{-6}
3.27	5.44×10^{-6}
3.37	1.52×10^{-5}
3.81	1.14×10^{-5}
4.29	1.21×10^{-5}
4.62	1.83×10^{-5}

1.5 Mono Lake

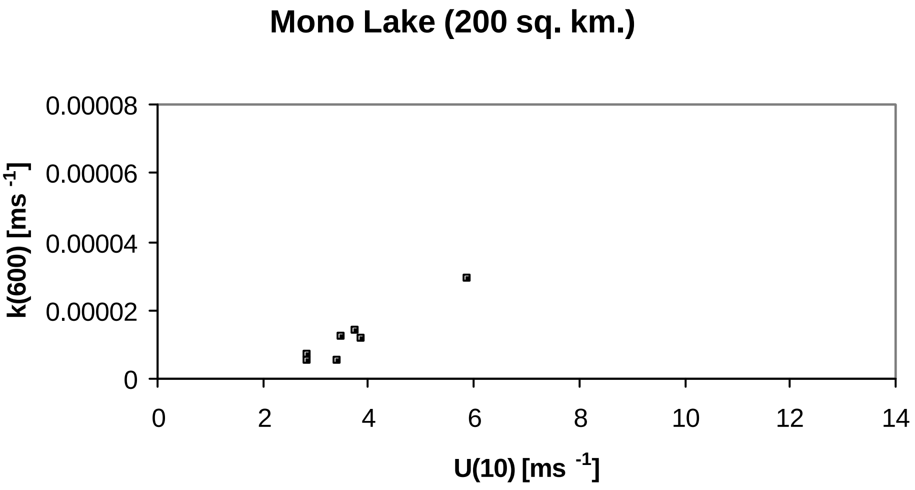

Figure D-5. Relation between k(600) and u(10) for Mono Lake (200 km^2) (Wanninkhof et al., 1991a).
Figur D-5. Forhold mellem k(600) og u(10) for Mono Lake (200 km^2) (Wanninkhof et al., 1991a).

Table D-5. Measurements of u(10) and k(600) for Mono Lake.
Tabel D-5. Målinger af u(10) og k(600) for Mono Lake.

u(10) (m s^{-1})	k(600) (m s^{-1})
2.83	4.97×10^{-6}
2.86	7.28×10^{-6}
3.43	4.97×10^{-6}
3.49	1.20×10^{-5}
3.75	1.39×10^{-5}
3.87	1.19×10^{-5}
5.87	2.94×10^{-5}

1.6 Siblyback Lake

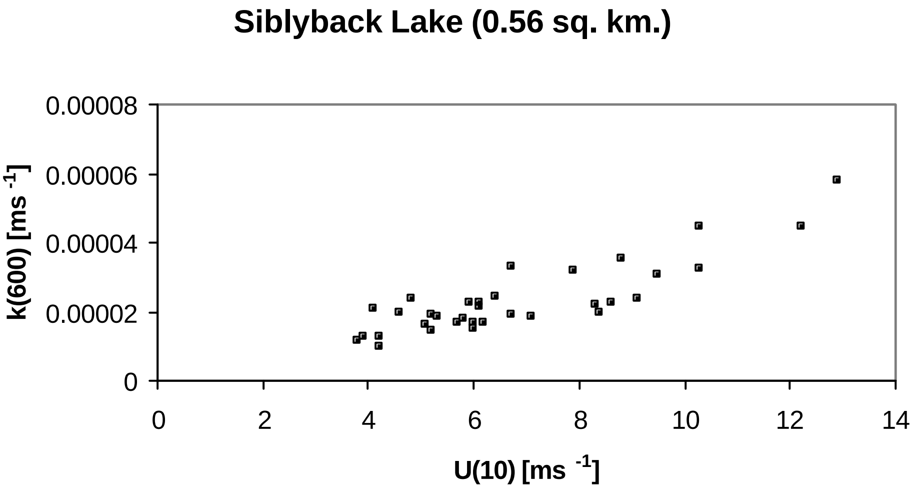

Figure D-6. Relation between u(10) and k(600) for Siblyback Lake (0.56 km^2) (Upstill-Goddard et al., 1990).
Figur D-7. Forhold mellem u(10) og k(600) for Siblyback Lake (0.56 km^2) (Upstill-Goddard et al., 1990).

Table D-6. Measurements of u(10) and k(600) for Siblyback Lake.
Tabel D-6. Målinger af u(10) og k(600) for Siblyback Lake.

u(10) (m s^{-1})	k(600) (m s^{-1})
3.8	1.17×10^{-5}
3.9	1.25×10^{-5}
4.1	2.11×10^{-5}
4.2	1.00×10^{-5}
4.2	1.25×10^{-5}
4.6	1.97×10^{-5}
4.8	2.39×10^{-5}
5.1	1.61×10^{-5}
5.2	1.44×10^{-5}
5.2	1.89×10^{-5}
5.3	1.83×10^{-5}
5.7	1.69×10^{-5}
5.8	1.78×10^{-5}
5.9	2.25×10^{-5}
6.0	1.53×10^{-5}
6.0	1.67×10^{-5}
6.1	2.17×10^{-5}
6.1	2.25×10^{-5}
6.2	1.69×10^{-5}
6.4	2.44×10^{-5}
6.7	1.92×10^{-5}

6.7	3.28×10^{-5}
7.1	1.83×10^{-5}
7.9	3.17×10^{-5}
8.3	2.19×10^{-5}
8.4	1.97×10^{-5}
8.6	2.25×10^{-5}
8.8	3.56×10^{-5}
9.1	2.36×10^{-5}
9.5	3.08×10^{-5}
10.3	3.25×10^{-5}
10.3	4.47×10^{-5}
12.2	4.47×10^{-5}
12.9	5.81×10^{-5}

1.7 Dozmary Pool

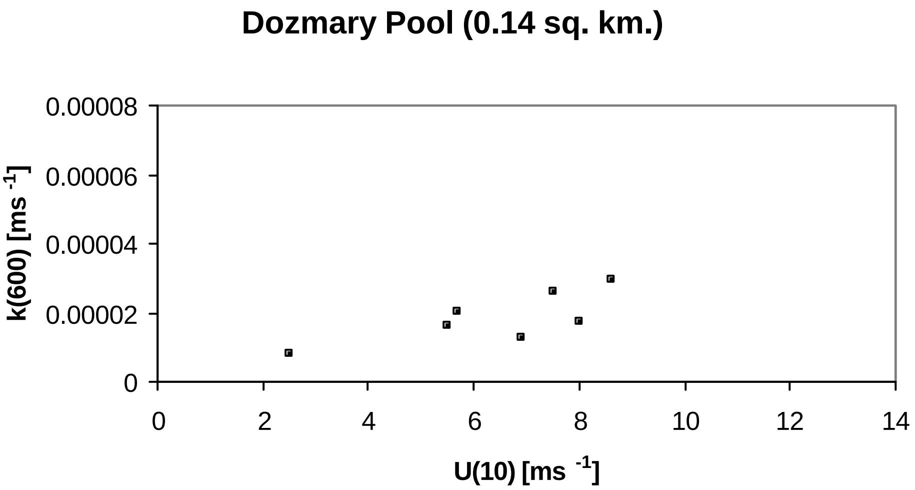

Figure D-7. Relation between k(600) and u(10) for Dozmary Pool (0.14 km^2) (Upstill-Goddard et al., 1990).
Figur D-7. Forhold mellem k(600) og u(10) for Dozmary Pool (0.14 km^2) (Upstill-Goddard et al., 1990).

Table D-7. Measurements of u(10) and k(600) for Dozmary Pool.
Tabel D-7. Målinger af u(10) og k(600) for Dozmary Pool.

u(10) (m s^{-1})	k(600) (m s^{-1})
2.5	8.06×10^{-6}
5.5	1.61×10^{-5}
5.7	2.06×10^{-5}
6.9	1.28×10^{-5}
7.5	2.61×10^{-5}
8.0	1.75×10^{-5}
8.6	2.97×10^{-5}

Figure 10 in the main part of this report gives the relation between k(600) and u(10) for all lakes.

1.8 Relations between u(10) and k(600) for sea areas

In the following tables information is shown on the experimentally determined relations between u(10) and k(600) for sea areas.

Table D-8. Measurements of u(10) and k(600) for the North Sea (Watson et al., 1991).
Table D-8. Målinger af u(10) og k(600) for Nordsøen (Watson et al, 1991).

u(10) (m s^{-1})	k(600) (m s^{-1})
11.7	4.72×10^{-5}
11.9	4.94×10^{-5}
12.1	6.03×10^{-5}
17.5	1.51×10^{-4}

Table D-9. Average values of u(10) and k(600) for the Atlantic and Pacific Ocean (Peng et al., 1979; published in Hartman and Hammond (1985).
Tabel D-9. Gennemsnitlige værdier af u(10) og k(600) for Atlanterhavet og Stillehavet (Peng et al, 1979; offentligtgjort i Hartman og Hammond (1985).

u(10) (m s^{-1})	k(600) (m s^{-1})
8	4.14×10^{-5}

Table D-10. Measurements of u(10) and k(600) for the North Pacific (Peng et al., 1979) published in Hartman and Hammond (1985).
Tabel D-10. Målinger af u(10) og k(600) for den nordlige del af Stillehavet (Peng et al, 1979; offentligtgjort i Hartman og Hammond (1985).
.

u(10) (m s^{-1})	k(600) (m s^{-1})
12	8.44×10^{-5}

Table D-11. Measurements of u(10) and k(600) for the Atlantic Ocean (Broecker and Peng, 1971) published in Hartman and Hammond (1985).
Tabel D-11. Målinger af u(10) og k(600) for Atlanterhavet (Peng et al, 1979; offentligtgjort i Hartman og Hammond (1985).
.

u(10) (m s^{-1})	k(600) (m s^{-1})
7	2.52×10^{-5}

Table D-12.Average u(10) and k(600) for the Antarctic Ocean (Peng et al., 1979) published in Hartman and Hammond (1985).
Tabel D-12. Gennemsnitlige værdier af u(10) og k(600) for Atlanterhavet (Peng et al, 1979; offentligtgjort i Hartman og Hammond (1985).
.

u(10) (m s^{-1})	k(600) (m s^{-1})
10.1	6.06×10^{-5}

Table D-13. Measurements of u(10) and k(600) for the NE Atlantic Ocean (Kromer and Roether, 1983).
Tabel D-13. Målinger af u(10) og k(600) for den nordøstlige del af Atlanterhavet (Kromer og Roether, 1983).

u(10) (m s^{-1})	k(600) (m s^{-1})
6	2.97×10^{-5}
8	8.00×10^{-5}

Table D-14. Measurements of u(10) and k(600) for the Equatorial Atlantic Ocean (Kromer and Roether, 1983; published in Hartman and Hammond, 1985).
Tabel D-14. Målinger af u(10) og k(600) for den tropiske del af Atlanterhavet (Kromer og Roether, 1983; offentligtgjort i Hartman og Hammond, 1985).

u(10) (m s^{-1})	k(600) (m s^{-1})
5	1.63×10^{-5}
7	1.18×10^{-5}
7	1.92×10^{-5}

Table D-15. Measurements of u(10) and k(600) for the Equatorial Pacific Ocean (Nightingale et al., 2000).
Tabel D-15. Målinger af u(10) og k(600) for den tropiske del af Stillehavet (Nightingale et al., 2000).

u(10) (m s^{-1})	k(600) (m s^{-1})
6.05	3.69×10^{-5}
6.65	2.72×10^{-5}
7.15	3.08×10^{-5}
7.15	3.17×10^{-5}

Table D-16. Measurements of u(10) and k(600) for George Banks (Wanninkhof et al., 1993).
Tabel D-16. Målinger af u(10) og k(600) for George Banks (Wanninkhof et al., 1993).

u(10) [ms^{-1}]	k(600) (m s^{-1})
4.54	1.69×10^{-5}
5.69	3.25×10^{-5}
8.80	6.54×10^{-5}
11.5	7.74×10^{-5}

Table D-17. Measurements of u(10) and k(600) for the southern North Sea (Nightingale et al., 2000).
Tabel D-17. Målinger af u(10) og k(600) for den sydlige del af Norsøen (Nightingale et al., 2000).

u(10) (m s^{-1})	k(600) (m s^{-1})
5.9	1.99×10^{-5}
7.6	6.00×10^{-5}
8.2	4.00×10^{-5}
10.0	6.89×10^{-5}
10.1	5.25×10^{-5}
10.6	5.50×10^{-5}
11.4	1.16×10^{-4}
12.5	7.36×10^{-5}
14.7	1.72×10^{-4}

Figure 12 in the main part of this report gives the relation between k(600) and u(10) for all sea areas.

1.9 Estuaries

The following measurements are made in estuaries.

Table D-18. Measurements of u(10) and k(600) for San Francisco Bay (Hartman and Hammond, 1984).
Tabel D-18. Målinger af u(10) og k(600) for San Francisco Bay (Hartman og Hammond, 1984).

U(10) (m s^{-1})	k(600) (m s^{-1})
3.2	6.94×10^{-6}
3.8	1.85×10^{-5}
4.1	1.88×10^{-5}
4.9	1.39×10^{-5}
5.0	2.26×10^{-5}
5.5	2.03×10^{-5}
6.4	2.66×10^{-5}

Table D-19. Measurements of u(10) and k(600) for the Potomac (Hartman and Hammond, 1985).
Tabel D-19. Målinger af u(10) og k(600) for Potomac (Hartman og Hammond, 1985).

u(10) (m s^{-1})	k(600) (m s^{-1})
4	8.28×10^{-6}

Figure 8 gives an overview of the relation between k(600) and u(10) for estuaries.

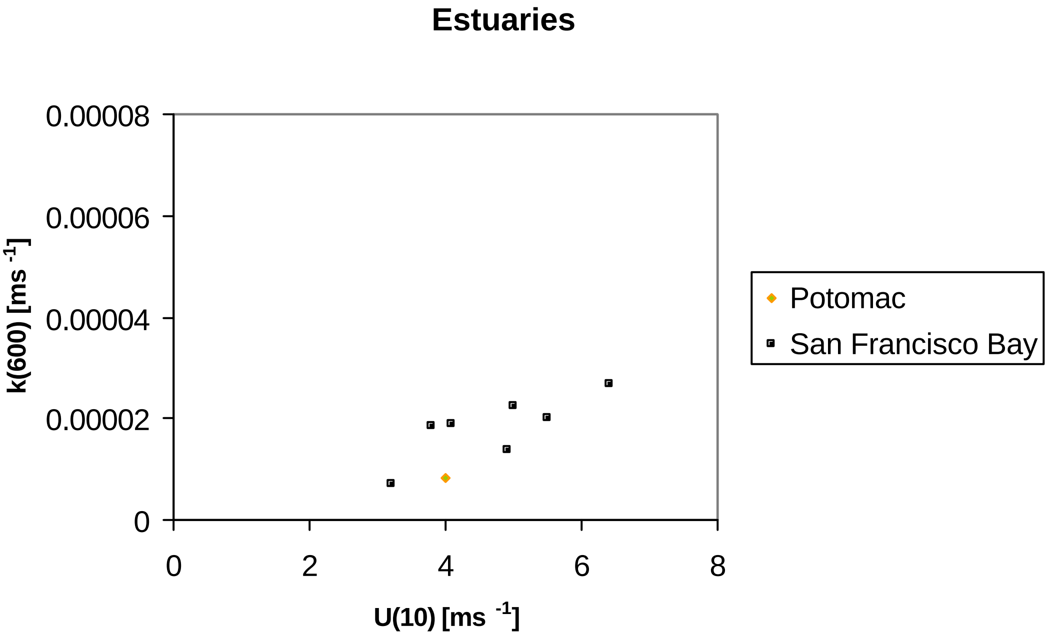

Figure D-7. Relation between k(600) and u(10) for all estuaries.
Figur D-7. Forhold mellem k(600) og u(10) for alle flodmundinger.

1.10 Wind tank

Figure 9 gives the results of experiments in a wind-water tank (Wanninkhof et al., 1991b). The wind speed at 10 m (u(10)) was calculated using the following correlation betwen A(0) and u(10): log (u(10)) = (log(a) – log(c) + b A(0))/d, where a = 72.75, b= 0.0730 (Wanninkhof et al., 1991b), c=0.45 and d = 1.6 (MacIntyre et al., 1995).

Figure D-8. Relation mellem k(600) og u(10) for wind tank experiments (Wanninkhof et al., 1991b).
Figur D-8. Forhold mellem k(600) og u(10) for vindtankeksperimenter (Wanninkhof et al., 1991b).

Table D-20. Measurements of u(10) and k(600) in wind tanks.
Tabel D-20. Målinger af u(10) og k(600) i vindtanke.

u(10) (m s^{-1})	k(600) (m s^{-1})
2.64	8.58×10^{-6}
3.65	1.75×10^{-5}
5.82	2.81×10^{-5}
8.26	4.11×10^{-5}
8.68	6.17×10^{-5}
10.3	6.17×10^{-5}
11.2	7.08×10^{-5}
11.2	7.78×10^{-5}
11.2	8.53×10^{-5}
13.3	1.32×10^{-4}
14.2	1.44×10^{-4}
14.2	1.51×10^{-4}
15.6	2.20×10^{-4}

References

Broecker, W.S., Peng, T.H. (1971) The vertical distribution of radon in the BOMEX area. Earth Planet. Sci. Lett. 11, 99-108

Crucius, J., Wanninkhof, R. (1990) A gas exchange- wind speed relationship measured on Lake 302N with SF6. EOS 71, 1234.

Hartman, B., Hammond, D.E. (1984) Gas exchange rates across the sediment-water and air-water interface in south San Francisco Bay. J. Geophys. Res. 89. 3593-3603.

Hartman, B., Hammond, D.E. (1985): Gas exchange in San Francisco Bay. Hydrobiologia 129, 59-68

Kromer, B., Roether W. (1983) Field measurements of air-sea gas exchange by the radon deficit method during JASIN 1978 and FGGE 1979. Meteor-Forsch. Ergebn. A24, 55-75.

Liss, P.S., Merlivat, L. (1986) Air-sea gas exchange rates: Introduction and synthesis. In: Buat-Ménard, P. (ed.) The role of air-sea exchange in geochemical cycling. Reidel, Dordrecht, The Netherlands, 113-127.

Macintyre, S., Wanninkhof, R., Chanton, J.P. (1995) Tracer gas exchange across the air-water interface in freshwater and coastal marine environments. In: Matson, P.A., Harriss, R.C. (eds.): Biogenic trace gases: measuring emissions from soil and water, Blackwell Science, Oxford, UK, 52-97.

Nightingale, P.D., Liss, P.S., Schlosser, P. (2000): Measurements of air-sea gas exchange during an open ocean algal bloom. Geoph. Res. Lett. 27, 2117-2120.

Nightingale, P.D, Malin, G., Law, C.S., Watson, A.J., Liss, P.S. Liddicoat, M.I., Boutin, J., Upstill-Goddard, R.C. (2000) In situ evaluation of air-sea gas exchange parameterizations using novel conservative and volatile tracers. Global Biogeochemical Cycles 14, 373-387.

Peng ,T.H., Takahashi, T., Broecker, W.S. (1974) Surface radon measurements in the north Pacific Ocean station PAPA. J. Geophys. Res. 79, 1772-1780

Peng, T.H., Broecker, W.S., Mathieu, G.G., Li ,Y.H. Bainbridge, A.E. (1979): Radon evasion rates in the Atlantic and Pacific Oceans as determined during the GEOSECS program. J. Geophys. Res. 79, 2471-2486

Peng, T.H., Broecker, W. (1980) Gas exchange rates for three closed basin lakes. Limnol. Ocean. 25, 789-796

Upstill-Goddard, R.C., Watson, A.J., Liss, P.S., Liddicoat, M.I. (1990) Gas transfer velocities in lakes measured with SF6, Tellus 42B, 364-377

Wanninkhof, R., Bliven, L.F., Glover, D.M. (1991b) Transfer velocities and radar backscatter. International symposium on gas transfer at water surfaces, p 294-308.

Wanninkhof, R., Ledwell, J.R., Broecker, W.S. (1985) Gas exchange-wind speed relation measured with sulfur hexfluoride on a Lake. Science, 227,1224-1226.

Wanninkhof, R., Ledwell, J.R., Crucius, J. (1991a): Gas exchange on Mono Lake and Crowley Lake,California. J. Geophys. Res., 92, 14567-14580

Wannikhof R., Asher W., Weppernig R., Chen H., Schlosser P., Langdon C., Sambrotto, R. (1993): Gas transfer experiment on George Banks using two volatile deliberate tracers. J. Geophys. Res. 98, 20237-20248.

Watson, A.J., Upstill-Goddard, R.C., Liss, P.S. (1991) Air-sea gas exchange in rough and stormy seas measured by a dual-tracer technique. Nature 349,145-147

1 Example model runs

Example model runs were made for volatilisation and transport of pesticides to a river. The runs was made for all pesticides for which the physico-chemical properties were given by Smit et al. (1997) with a very few additions (316 pesticides at all).

The model runs were made for widths of non-spray zones and water bodies as defined by the FOCUS group for winter cereals (Table E-1).

Table E-1. Dimensions of the non-spray zone and the water bodies used in the model runs.
Tabel E-1. Størrelse af bufferzonen og vandløb/søer i modelkørslerne.

Water body	width non-spray zone (m)	width water body (m)
Stream	1.5	1.5
Pond	3.5	30.0
Ditch	1.0	1.0

In the model runs it has been assumed that the upwind area onto which pesticide was applied is 100 m. This assumption has some influence on the results, as the upwind length of the field has an effect on the shape of the vertical concentration profile.

The temperature of the air, the crop, the soil and the water body are assumed to be 15°C. It is also assumed that the water body does not contain pesticide, i.e. that the flux to the water body is not reduced by the presence of pesticide in the water body.

The model runs for rivers (streams) are made for the situations:

- A situation with a small surface resistance (r_c). A flow velocity of 0.52 m s^{-1}, a depth of 1.37 m and a slope of 7.4×10^{-3} m m^{-1} were adopted. This gives a reaeration coefficient K_{2d} of about 44 day^{-1} with the Thyssen and Erlandsen (1987) parameterisation. This is a rather large value and this leads to a rather small surface resistance, leading to an upper estimate of the dry deposition to the river.
- A situation with a relatively large surface resistance (r_c). A flow velocity of 0.06 m s^{-1}, a depth of 0.12 m and a slope of 3×10^{-4} m m^{-1} were adopted. This gives a reaeration coefficient K_{2d} of about 1 day^{-1} with the Thyssen and Erlandsen (1987) parameterisation. This is a rather low value and this leads to a rather high surface resistance, leading to an lower estimate of the dry deposition to the river.
- A situation for a pond at a wind speed of 5 m s^{-1}.
- A situation for a ditch at a wind speed of 5 m s^{-1}.

It is assumed that the mass accommodation coefficient of the pesticide is so large that it will not have any influence on the uptake rate by water (see Appendix C). It is also assumed that the are no reaction of the pesticide in water. If there is a fast reaction in the water the surface resistance r_c will become lower and the flux larger.

The vapour pressure needed to calculate the accumulated emission from crops is found from the actual temperature using equation (A-16) in appendix A and assuming a heat of evaporation of 95000 J mol^{-1}.

The Henry's law coefficient needed to calculate the accumulated emission from normal to moist fallow soil is found from the actual temperature and equation (A-20) in appendix A, assuming a heat of dissolution at constant temperature and pressure of –68000 J mol^{-1}.

For the situation of emission from crops a surface roughness length z_{0m} of 0.1 m and a friction velocity u_* of 0.386 m s^{-1} is taken. For the situation from emission from fallow soil a z_{0m} of 0.01 m is taken and a u_* of 0.284 m s^{-1}. These values will give the average wind speed in Denmark at 60 m height (Appendix G).

Some pesticides are applied to crops, others are applied to (almost) fallow soil. This difference will lead to differences in the volatilisation, due to different parameterisations of volatilisation from crops or from fallow soil. In the examples presented here emission is modelled either from crops or from fallow soil, although usually only one type of application is used. This is done because otherwise information had to be collected on the use of the pesticide in the real world.

In the calculations of the volatilisation from the soil K_d is calculated from K_{ow} for all pesticides assuming that the pesticide is adsorbed at the organic matter in the soil (see Appendix A for a description of the method). This is done because otherwise information had to be collected on the adsorption of each pesticide, which was not possible within this project. Not all pesticides are, however, adsorbed to the organic matter in the soil and this may lead to errors.

So the user of these tables has to check which assumption on the volatilisation (from crop or from fallow soil) is most realistic and has to use the most likely results. Moreover, the user should not use the results presented here if the pesticide is not adsorbed to the organic matter in the soil but e.g. to minerals.

For some pesticides the parameterisation of the accumulated emission from crops will lead to a volatilisation of more than 100% of the dose. This is of course not correct. In that case the volatilisation is set to 100%. This is not necessarily correct either, but should be used as a first guess and an indication that the accumulated emission is rather large. The parameterisation of the accumulated emission from normal to moist soil has a maximum of 95.1%.

Table E-2 gives an overview of the model runs made and the associated tables.

Table E-2. Overview of model runs made.

Tabel E-2. Oversigt over modelkørslerne.

Table wit results of run	Emission from	Water body
E-3	crops	river, r_c = small
E-4	crops	river, r_c = large
E-5	crops	pond
E-6	crops	ditch
E-7	soil	river, r_c = small

The results of the model runs are presented in Tables E-3 to E-7 give the following information:

1. Name of the compound.
2. Accumulated emission of the pesticide (in % of the dose).
3. Accumulated flux of the pesticide (kg m^{-2}) to the water expressed as a percentage of the accumulated emission flux (kg m^{-2}). This is the average flux over the whole width of the water body.
4. Accumulated flux of the pesticide (kg m^{-2}) to the water expressed as a percentage of the dose flux (kg m^{-2}). This is the average flux over the whole width of the water body. This number can be compared directly to the spray drift flux.

The results for abamectine 1a in Table E-3 show e.g. that if 1 kg m^{-2} abamectine 1a is applied, 0.03% of that amount has been dry deposited per m^{-2} of water surface, i.e. 3×10^{-4} kg m^{-2}.

Comparing the results for the deposition flux of pesticides emitted from crops to rivers with a small and a large surface resistance r_c (Tables E-3 and E-4) shows that the results are often the same. This is because for most compounds the dry deposition flux is limited by the laminar boundary layer resistance r_b and different surface resistances caused by different stream parameters have no influence on the dry deposition flux. Only for compounds with Henry's law coefficient k_H (c_g/c_w) of the order of 2×10^{-3} and larger dry deposition flux is limited by the surface resistance, which is a function of the stream parameters. In that case a difference will be found between the results of the two runs.

The deposition flux of pesticides to ponds caused by pesticides emitted from crops is lower than to streams with a large surface resistance r_c. This is mainly caused by the fact that the width of the non-spray zone and the width of the water body is larger for the pond than for the stream. Due to the average longer distance to the emission area in the case of ponds, the pesticide is more mixed up in the vertical and the average concentration will be lower than in case of the streams. Moreover, there is an effect due to the difference in r_c values for streams and ponds.

Comparing the results for deposition flux of pesticides emitted from crops to ponds and ditches, shows that the average deposition flux to ditches is almost a factor two higher than to ponds. This difference is caused by differences in the width of the non-spray zone and the water body.

The accumulated emission from crops and the accumulated emission from soil are quite different, which results in difference deposition fluxes (compare Table E-3 and E-7)

Table E-3. Volatilisation from crops and accumulated flux to a river with a low r_c. Note: the numbers are given much more accurately than they actually are known.

Tabel E-3. Fordampning fra afgrøder og akkumuleret fluks til et vandløb med en lav r_c-værdi. Bemærk at tallene vises i flere decimaler end de er kendte.

Compound	% of the dose that volatilises	Accumulated flux to water (kg m^{-2}) as % of the emission in the field (kg m^{-2})	Accumulated flux to water (kg m^{-2}) as % of the dose in the field (kg m^{-2})
abamectine 1a	0.40	7.86	0.03
acephate	10.64	13.19	1.40
aclonifen	3.58	11.71	0.42
acrinathrin (acrinate)	0.47	9.25	0.04
alachlor	24.48	11.64	2.85
aldicarb	81.32	13.03	10.60
alloxydim-sodium	7.09	10.73	0.76
aminocarb	31.12	12.66	3.94
amitraz	11.13	11.32	1.26
amitrol	5.64	16.90	0.95
ancymidol	3.54	11.83	0.42
anilazine	0.90	11.56	0.10
asulam	24.61	12.25	3.02
atrazine	3.98	12.51	0.50
azaconazole	2.68	11.24	0.30
azinphos-methyl	4.80	11.04	0.53
azocyclotin	0.01	9.94	0.00
benazolin	0.34	12.03	0.04
benazolin-ethyl	11.42	11.61	1.33
bendiocarb	37.33	12.38	4.62
benfuracarb	4.54	10.14	0.46
benodanil	0.12	10.97	0.01
benomyl	0.08	11.36	0.01
bensultap	10.52	9.97	1.05
bentazone	17.14	12.08	2.07
bifenox	7.95	10.76	0.86
bifenthrin	3.71	10.03	0.37
bitertanol-A	0.02	10.82	0.00
brodifacoum	4.05	9.35	0.38
bromacil	4.10	11.76	0.48
bromofenoxim	0.84	9.76	0.08
bromophos-ethyl	31.40	10.01	3.14
bromopropylate	3.01	10.00	0.30
bromoxynil	24.61	11.54	2.84
buminaphos	100.00	10.70	10.70
bupirimate	6.21	11.05	0.69
buprofezin	20.14	11.16	2.25
butocarboxim	73.95	13.03	9.64
butoxycarboxim	13.28	12.39	1.65
captafol	0.84	10.69	0.09
captan	2.22	11.23	0.25
carbaryl	8.20	12.80	1.05
carbendazim	0.28	13.01	0.04
carbetamide	0.00	12.15	0.00
carbophenothion	18.97	10.71	2.03
carbofuran	6.51	12.41	0.81
carboxin	3.19	12.17	0.39
chlorbromuron	5.37	11.32	0.61
chlorfenvinphos	18.15	10.59	1.92
chloridazon	2.88	12.41	0.36
chlormequat	2.88	13.83	0.40
chlorothalonil	5.46	11.69	0.64
chlorotoluron	2.72	12.57	0.34
chloroxuron	0.54	11.36	0.06
chlorpropham	24.61	12.55	3.09
chlorpyriphos-ethyl	28.83	10.65	3.07
chlorpyrifos-methyl	40.50	10.95	4.43
chlorthal-dimethyl (DCPA)	8.77	10.87	0.95
clodinafop-propargyl	1.25	10.69	0.13
clofentezine	0.28	11.20	0.03

cloquintoceet-mexyl (CGA 185072)	1.58	10.83	0.17
coumatetralyl	0.11	11.34	0.01
cyanamide	100.00	20.94	20.94
cyanazine	0.48	12.08	0.06
cycloate	100.00	12.50	12.50
cycloxydim	2.88	10.94	0.31
cyfluthrin	1.19	9.93	0.12
cyhalotrin	0.98	0.00	0.00
cyhexatin	0.00	10.35	0.00
cymoxanil	5.59	12.86	0.72
cypermethrin (cis)	0.45	10.09	0.05
cypermethrin (trans)	0.45	10.09	0.05
alpha-cypermethrin	4.24	10.01	0.42
cyproconazole	5.13	11.34	0.58
cyprofuram	1.75	11.50	0.20
cyromazine	0.50	13.61	0.07
2,4-D (pH soil > 5)	24.61	12.42	3.06
dalapon	2.88	14.29	0.41
daminozide	0.84	13.78	0.12
dazomet	16.06	13.72	2.20
deltamethrin	2.42	8.44	0.20
demeton-S-methylsulfon	1.79	11.74	0.21
desmedipham	0.47	11.24	0.05
desmetryn	9.61	12.56	1.21
diallate	73.30	11.61	8.51
dial.dichl.aceetamid(cdaa)	100.00	13.42	13.42
diazinon	64.86	11.18	7.25
dicamba	36.58	12.42	4.54
dicamba dimethylammonium	1.48	11.69	0.17
dichlobenil	100.00	13.41	13.41
dichlofluanid	4.07	10.86	0.44
1,3-dichloropropene	100.00	6.74	6.74
cis-dichloropropene	100.00	5.91	5.91
dichlorprop	2.88	12.17	0.35
dichlorprop-P	6.74	12.17	0.82
dichlorvos	100.00	12.41	12.41
dicloran	10.48	12.68	1.33
dicofol (op)	5.37	10.49	0.56
dicofol (pp)	5.37	10.49	0.56
dieldrin	16.06	10.32	1.66
dienochlor	20.51	9.66	1.98
diethatyl-ethyl	9.12	11.10	1.01
diethofencarb	66.35	11.66	7.74
difenoconazole	0.15	10.17	0.02
difenoxuron	0.04	11.41	0.00
diflubenzuron	0.27	11.11	0.03
diflufenican	3.91	10.27	0.40
dikegulac-sodium	0.82	11.29	0.09
dimefuron	8.42	10.80	0.91
dimethachlor	34.78	11.84	4.12
dimethoate	18.97	12.27	2.33
dimethomorph (E-isomer)	0.72	10.33	0.07
dimethomorph (Z-isomer)	0.73	10.33	0.07
dinocap	2.14	10.54	0.23
dinoseb	44.03	12.08	5.32
dinoseb-acetate	0.00	11.47	0.00
dinoterb	99.40	11.97	11.90
diquat-dibromide	0.00	10.75	0.00
dithianon	5.11	11.28	0.58
diuron	2.04	12.20	0.25
DNOC	62.08	12.86	7.99
dodemorph	17.48	11.48	2.01
2,4-D-propylene glycolbutyl ether ester	24.61	12.42	3.06
endosulfan	3.13	10.17	0.32
EPTC	100.00	12.95	12.95
esfenvalerate	0.88	10.05	0.09
ethephon	2.88	14.24	0.41
ethiofencarb	16.96	12.34	2.09
ethofumesate	14.85	11.41	1.70

ethoprophos	100.00	12.05	12.05
etofenprox	2.52	5.32	0.13
etridiazole	81.32	11.96	9.73
etrimfos	67.08	11.33	7.60
fenaminosulf	0.00	11.91	0.00
fenamiphos	4.62	11.20	0.52
fenarimol	3.49	10.88	0.38
fenbutatinoxide	0.04	7.38	0.00
fenchlorazole-ethyl	0.93	10.20	0.10
fenfuram	3.98	12.80	0.51
fenitrothion	19.02	11.53	2.19
fenoprop-butoxypropyl ester (2,4,5-TP)	2.47	11.64	0.29
fenoxaprop-ethyl	1.43	10.57	0.15
fenoxaprop-P-ethyl	0.73	10.57	0.08
fenoxycarb	0.93	11.22	0.10
fenpiclonil	0.03	12.14	0.00
fenpropathrin	18.23	10.65	1.94
fenpropidin	67.95	11.58	7.87
fenpropimorph	36.28	11.18	4.06
fentin-acetate	3.75	10.15	0.38
fentin-hydroxide	1.10	10.52	0.12
fenvalerate	0.88	10.05	0.09
ferbam	0.00	10.09	0.00
fluazifop-butyl	6.37	10.92	0.70
fluazifop-p-butyl	5.02	10.37	0.52
flucycloxuron	49.09	0.48	0.23
flurenol(-butyl)	7.01	11.47	0.80
flurochloridon	3.99	11.10	0.44
fluroxypyr	0.07	11.85	0.01
fluroxypyr 1-methylheptylester	1.13	10.52	0.12
flusilazole	4.00	11.06	0.44
flutolanil	32.11	10.96	3.52
fluvalinate	2.12	9.31	0.20
folpet	27.81	11.24	3.13
fonofos	85.74	11.97	10.26
formothion	9.61	11.82	1.14
fosetyl-aluminium	2.47	10.64	0.26
fuberidazol	0.05	13.17	0.01
furalaxyl	7.13	11.22	0.80
furathiocarb	1.37	10.38	0.14
gluphosinate-amm.	0.00	12.86	0.00
glyphosate	0.00	13.54	0.00
glyphosate-trimesium (glyph,part)	4.05	12.00	0.49
glyphosate-trimesium (trim,part)	4.05	12.00	0.49
haloxyfop ethoxyethyl	0.14	9.96	0.01
heptachlor	100.00	3.57	3.57
heptenophos	100.00	11.92	11.92
hexaconazole	2.88	11.07	0.32
hexazinone	3.37	11.89	0.40
hexythiazox	1.23	10.66	0.13
hymexazol	100.00	16.05	16.05
imazalil	10.42	11.27	1.17
imazamethabenz-methyl (m-isomer)	1.02	11.39	0.12
imazamethabenz-methyl (p-isomer)	1.02	11.39	0.12
imazapyr	0.37	11.76	0.04
imidacloprid	0.46	11.84	0.06
ioxynil	24.61	10.48	2.58
iprodione	0.53	10.89	0.06
isofenphos	16.06	10.73	1.72
isoproturon	1.72	12.70	0.22
isoxaben	4.62	10.87	0.50
kasugamycine	0.08	10.41	0.01
lambda-cyhalothrin	0.46	9.84	0.05
lenacil	0.34	12.18	0.04
lindane	54.93	11.33	6.22

linuron	31.12	11.94	3.72
malathion	24.61	10.89	2.68
maleine-hydrazide	0.00	15.44	0.00
mancozeb	0.00	10.89	0.00
maneb	0.00	11.70	0.00
MCPA	4.24	12.81	0.54
mecoprop	14.26	12.54	1.79
mecoprop-P	16.06	12.54	2.01
mefluidide	0.00	11.12	0.00
mepiquat.chloride	0.00	14.08	0.00
metalaxyl	15.87	11.51	1.83
metaldehyde	0.00	13.36	0.00
metam-sodium	0.00	14.76	0.00
metamitron	0.92	12.78	0.12
metazachlor	6.04	11.53	0.70
methabenzthiazuron	2.25	12.41	0.28
methamidophos	36.28	14.35	5.20
methidathion	12.50	11.21	1.40
methiocarb	3.48	12.34	0.43
methomyl	44.03	13.72	6.04
methylbromide	100.00	2.17	2.17
methylisothiocyanate	100.00	14.15	14.15
metiram	0.00	7.30	0.00
metobromuron	16.06	11.79	1.89
metolachlor	35.34	11.45	4.05
metoxuron	48.56	12.28	5.96
metribuzin	6.53	12.54	0.82
metsulfuron-methyl	0.02	10.39	0.00
mevinphos	92.15	12.36	11.39
mexacarbate	100.00	11.02	11.02
monolinuron	93.45	12.53	11.71
myclobutanil	8.77	11.38	1.00
nitrapyrin	100.00	12.06	12.06
nitrothal-isopropyl	2.88	11.30	0.33
nuarimol	1.15	11.07	0.13
omethoate	42.93	12.56	5.39
oxamyl	89.91	12.45	11.19
oxycarboxim	1.62	11.67	0.19
oxydemeton-methyl	46.40	11.99	5.56
paclobutrazol	0.98	11.32	0.11
paraquat	0.00	11.82	0.00
parathion	23.31	11.35	2.64
parathion-methyl	33.99	11.73	3.99
penconazole	11.89	11.44	1.36
pencycuron	0.03	10.91	0.00
pendimethalin	34.62	11.32	3.92
pentachlorophenol	45.61	11.69	5.33
permethrin	0.93	10.30	0.10
phenmedipham	0.03	11.24	0.00
phosalone	6.11	10.51	0.64
phosmet	5.08	11.03	0.56
phosphamidon	26.21	11.24	2.95
picloram	3.17	12.06	0.38
picloram-potassium salt	0.17	11.50	0.02
piperonylbutoxide	9.06	7.98	0.72
pirimicarb	25.79	12.12	3.13
pirimiphos-methyl	33.99	11.17	3.80
pp-DDT	4.41	10.49	0.46
prochloraz	10.17	10.43	1.06
procymidon	83.24	11.37	9.46
prometon	14.17	12.34	1.75
prometryn	7.84	12.07	0.95
propachlor	100.00	12.59	12.59
propamocarb	16.36	12.35	2.02
propaquizafop	0.01	9.88	0.00
propazine	1.86	12.26	0.23
propetamphos	33.19	11.48	3.81
profenofos	6.86	10.46	0.72
propiconazole	4.74	10.76	0.51
propoxur	27.81	12.64	3.51
propyzamide	4.82	11.84	0.57

prosulfocarb	5.22	11.91	0.62
pyrazophos	7.22	10.46	0.75
pyrethrins	0.84	10.89	0.09
pyridate	0.38	10.41	0.04
pyridathioben (pyridaben)	12.90	9.86	1.27
pyrifenox	23.24	11.30	2.63
quinmerac	2.88	12.41	0.36
quintozeen	59.32	9.91	5.88
quizalofop-ethyl	0.04	10.47	0.00
quizalofop-P-ethyl	0.35	10.47	0.04
rimsulfuron	0.88	9.97	0.09
sethoxydim	3.00	10.92	0.33
simazine	1.20	12.79	0.15
sulfotep	84.18	10.93	9.20
TCA	0.00	13.14	0.00
tebuconazole	1.11	11.15	0.12
teflubenzuron	0.04	10.39	0.00
tefluthrin	64.86	4.01	2.60
temephos	2.07	9.71	0.20
terbufos	94.63	11.30	10.69
terbutryn	10.03	12.07	1.21
terbutylazine	7.50	12.26	0.92
tetrachloorvinphos	2.20	10.53	0.23
tetradifon	0.20	10.63	0.02
thiabendazole	0.00	12.80	0.00
thifensulfuron-methyl	0.11	10.33	0.01
thiocyclam hydrogen oxalate	18.55	11.61	2.15
thiodicarb	55.38	10.64	5.89
thiofanate-methyl	2.88	10.76	0.31
thiofanox	77.60	12.47	9.67
thiometon	100.00	11.98	11.98
thiram	26.75	12.08	3.23
tolclofos-methyl	100.00	8.45	8.45
tolylfluanid	3.58	10.71	0.38
toxaphene	17.82	10.11	1.80
2,4,5-T-propylene glycolbutyl ether ester	0.68	10.51	0.07
tri-allate	74.55	11.11	8.28
triadimefon	1.36	11.32	0.15
triadimenol	0.22	11.29	0.03
triazophos	8.72	11.08	0.97
trichlorfon	11.89	11.82	1.41
trichloronaat	33.99	10.85	3.69
triclopyr	8.57	11.83	1.01
tridemorph	58.45	11.25	6.58
triflumizole	8.29	10.73	0.89
trifluralin	64.10	10.32	6.62
triforine	3.37	9.95	0.34
vinclozolin	3.58	11.42	0.41
warfarin	19.49	11.14	2.17
zineb	2.88	11.55	0.33
ziram	2.79	11.17	0.31

Table E-4. Volatilisation from crops and accumulated flux to the river with a high r_c. Note: the numbers are given much more accurately than they actually are known.

Tabel E-4. Fordampning fra afgrøder og akkumuleret fluks til et vandløb med en lav r_c-værdi. Bemærk at tallene vises i flere decimaler end de er kendte.

Compound	% of the dose that volatilises	Accumulated flux to water (kg m^{-2}) as % of the emission in the field (kg m^{-2})	Accumulated flux to water (kg m^{-2}) as % of the dose in the field (kg m^{-2})
abamectine 1a	0.40	7.86	0.03
acephate	10.64	13.19	1.40
aclonifen	3.58	11.58	0.41
acrinathrin (acrinate)	0.47	9.12	0.04
alachlor	24.48	11.60	2.84
aldicarb	81.32	13.01	10.58
alloxydim-sodium	7.09	10.73	0.76
aminocarb	31.12	12.64	3.93
amitraz	11.13	9.85	1.10
amitrol	5.64	16.90	0.95
ancymidol	3.54	11.83	0.42
anilazine	0.90	11.56	0.10
asulam	24.61	12.25	3.02
atrazine	3.98	12.51	0.50
azaconazole	2.68	11.24	0.30
azinphos-methyl	4.80	11.02	0.53
azocyclotin	0.01	9.94	0.00
benazolin	0.34	12.03	0.04
benazolin-ethyl	11.42	11.57	1.32
bendiocarb	37.33	11.93	4.45
benfuracarb	4.54	10.09	0.46
benodanil	0.12	10.97	0.01
benomyl	0.08	11.36	0.01
bensultap	10.52	7.81	0.82
bentazone	17.14	12.08	2.07
bifenox	7.95	9.24	0.73
bifenthrin	3.71	8.17	0.30
bitertanol-A	0.02	10.82	0.00
brodifacoum	4.05	9.33	0.38
bromacil	4.10	11.76	0.48
bromofenoxim	0.84	9.74	0.08
bromophos-ethyl	31.40	0.88	0.28
bromopropylate	3.01	9.68	0.29
bromoxynil	24.61	11.45	2.82
buminaphos	100.00	7.33	7.33
bupirimate	6.21	11.02	0.68
buprofezin	20.14	6.85	1.38
butocarboxim	73.95	13.03	9.64
butoxycarboxim	13.28	12.39	1.65
captafol	0.84	10.69	0.09
captan	2.22	11.22	0.25
carbaryl	8.20	12.79	1.05
carbendazim	0.28	13.01	0.04
carbetamide	0.00	12.15	0.00
carbophenothion	18.97	4.07	0.77
carbofuran	6.51	12.41	0.81
carboxin	3.19	12.17	0.39
chlorbromuron	5.37	11.31	0.61
chlorfenvinphos	18.15	10.56	1.92
chloridazon	2.88	12.41	0.36
chlormequat	2.88	13.83	0.40
chlorothalonil	5.46	11.33	0.62
chlorotoluron	2.72	12.57	0.34
chloroxuron	0.54	11.35	0.06
chlorpropham	24.61	12.45	3.06
chlorpyriphos-ethyl	28.83	4.99	1.44
chlorpyrifos-methyl	40.50	5.31	2.15
chlorthal-dimethyl (DCPA)	8.77	9.08	0.80
clodinafop-propargyl	1.25	10.68	0.13
clofentezine	0.28	10.96	0.03

cloquintoceet-mexyl (CGA 185072)	1.58	10.79	0.17
coumatetralyl	0.11	11.34	0.01
cyanamide	100.00	20.94	20.94
cyanazine	0.48	12.08	0.06
cycloate	100.00	7.37	7.37
cycloxydim	2.88	10.94	0.31
cyfluthrin	1.19	4.88	0.06
cyhalotrin	0.98	0.00	0.00
cyhexatin	0.00	10.35	0.00
cymoxanil	5.59	12.86	0.72
cypermethrin (cis)	0.45	9.43	0.04
cypermethrin (trans)	0.45	9.43	0.04
alpha-cypermethrin	4.24	2.36	0.10
cyproconazole	5.13	11.34	0.58
cyprofuram	1.75	11.50	0.20
cyromazine	0.50	13.61	0.07
2,4-D (pH soil > 5)	24.61	12.41	3.05
dalapon	2.88	14.29	0.41
daminozide	0.84	13.78	0.12
dazomet	16.06	13.72	2.20
deltamethrin	2.42	0.20	0.00
demeton-S-methylsulfon	1.79	11.74	0.21
desmedipham	0.47	11.24	0.05
desmetryn	9.61	12.56	1.21
diallate	73.30	7.48	5.48
dial.dichl.aceetamid(cdaa)	100.00	12.90	12.90
diazinon	64.86	9.93	6.44
dicamba	36.58	12.41	4.54
dicamba dimethylammonium	1.48	11.69	0.17
dichlobenil	100.00	5.03	5.03
dichlofluanid	4.07	10.65	0.43
1,3-dichloropropene	100.00	0.03	0.03
cis-dichloropropene	100.00	0.02	0.02
dichlorprop	2.88	12.17	0.35
dichlorprop-P	6.74	12.17	0.82
dichlorvos	100.00	11.20	11.20
dicloran	10.48	12.44	1.30
dicofol (op)	5.37	9.95	0.53
dicofol (pp)	5.37	9.95	0.53
dieldrin	16.06	2.79	0.45
dienochlor	20.51	9.33	1.91
diethatyl-ethyl	9.12	11.09	1.01
diethofencarb	66.35	8.95	5.94
difenoconazole	0.15	10.17	0.02
difenoxuron	0.04	11.41	0.00
diflubenzuron	0.27	11.10	0.03
diflufenican	3.91	7.71	0.30
dikegulac-sodium	0.82	11.29	0.09
dimefuron	8.42	10.72	0.90
dimethachlor	34.78	11.83	4.11
dimethoate	18.97	12.27	2.33
dimethomorph (E-isomer)	0.72	10.33	0.07
dimethomorph (Z-isomer)	0.73	10.33	0.07
dinocap	2.14	10.53	0.23
dinoseb	44.03	11.56	5.09
dinoseb-acetate	0.00	11.47	0.00
dinoterb	99.40	2.47	2.45
diquat-dibromide	0.00	10.75	0.00
dithianon	5.11	10.67	0.55
diuron	2.04	12.20	0.25
DNOC	62.08	12.45	7.73
dodemorph	17.48	11.42	2.00
2,4-D-propylene glycolbutyl ether ester	24.61	12.34	3.04
endosulfan	3.13	9.76	0.31
EPTC	100.00	3.14	3.14
esfenvalerate	0.88	6.96	0.06
ethephon	2.88	14.24	0.41
ethiofencarb	16.96	12.34	2.09
ethofumesate	14.85	11.35	1.69

ethoprophos	100.00	11.77	11.77
etofenprox	2.52	0.03	0.00
etridiazole	81.32	9.79	7.96
etrimfos	67.08	9.29	6.23
fenaminosulf	0.00	11.91	0.00
fenamiphos	4.62	11.20	0.52
fenarimol	3.49	10.87	0.38
fenbutatinoxide	0.04	7.38	0.00
fenchlorazole-ethyl	0.93	10.18	0.09
fenfuram	3.98	12.80	0.51
fenitrothion	19.02	11.26	2.14
fenoprop-butoxypropyl ester (2,4,5-TP)	2.47	11.64	0.29
fenoxaprop-ethyl	1.43	10.54	0.15
fenoxaprop-P-ethyl	0.73	10.56	0.08
fenoxycarb	0.93	11.22	0.10
fenpiclonil	0.03	12.14	0.00
fenpropathrin	18.23	3.95	0.72
fenpropidin	67.95	11.44	7.77
fenpropimorph	36.28	7.05	2.56
fentin-acetate	3.75	10.15	0.38
fentin-hydroxide	1.10	10.52	0.12
fenvalerate	0.88	6.96	0.06
ferbam	0.00	10.09	0.00
fluazifop-butyl	6.37	10.58	0.67
fluazifop-p-butyl	5.02	10.14	0.51
flucycloxuron	49.09	0.00	0.00
flurenol(-butyl)	7.01	11.45	0.80
flurochloridon	3.99	11.09	0.44
fluroxypyr	0.07	11.85	0.01
fluroxypyr 1-methylheptylester	1.13	10.32	0.12
flusilazole	4.00	11.05	0.44
flutolanil	32.11	9.04	2.90
fluvalinate	2.12	1.14	0.02
folpet	27.81	4.76	1.32
fonofos	85.74	7.48	6.42
formothion	9.61	11.82	1.14
fosetyl-aluminium	2.47	10.64	0.26
fuberidazol	0.05	13.17	0.01
furalaxyl	7.13	11.22	0.80
furathiocarb	1.37	10.38	0.14
gluphosinate-amm.	0.00	12.86	0.00
glyphosate	0.00	13.54	0.00
glyphosate-trimesium (glyph,part)	4.05	12.00	0.49
glyphosate-trimesium (trim,part)	4.05	12.00	0.49
haloxyfop ethoxyethyl	0.14	9.96	0.01
heptachlor	100.00	0.01	0.01
heptenophos	100.00	11.17	11.17
hexaconazole	2.88	11.06	0.32
hexazinone	3.37	11.89	0.40
hexythiazox	1.23	10.62	0.13
hymexazol	100.00	16.05	16.05
imazalil	10.42	11.26	1.17
imazamethabenz-methyl (m-isomer)	1.02	11.39	0.12
imazamethabenz-methyl (p-isomer)	1.02	11.39	0.12
imazapyr	0.37	11.76	0.04
imidacloprid	0.46	11.84	0.06
ioxynil	24.61	10.23	2.52
iprodione	0.53	10.89	0.06
isofenphos	16.06	10.52	1.69
isoproturon	1.72	12.70	0.22
isoxaben	4.62	10.60	0.49
kasugamycine	0.08	10.41	0.01
lambda-cyhalothrin	0.46	9.26	0.04
lenacil	0.34	12.18	0.04
lindane	54.93	6.16	3.38
linuron	31.12	11.74	3.65

malathion	24.61	10.80	2.66
maleine-hydrazide	0.00	15.44	0.00
mancozeb	0.00	10.89	0.00
maneb	0.00	11.70	0.00
MCPA	4.24	12.81	0.54
mecoprop	14.26	12.53	1.79
mecoprop-P	16.06	12.53	2.01
mefluidide	0.00	11.12	0.00
mepiquat.chloride	0.00	14.08	0.00
metalaxyl	15.87	11.51	1.83
metaldehyde	0.00	13.36	0.00
metam-sodium	0.00	14.76	0.00
metamitron	0.92	12.78	0.12
metazachlor	6.04	11.52	0.70
methabenzthiazuron	2.25	12.41	0.28
methamidophos	36.28	14.35	5.20
methidathion	12.50	11.20	1.40
methiocarb	3.48	12.33	0.43
methomyl	44.03	13.72	6.04
methylbromide	100.00	0.01	0.01
methylisothiocyanate	100.00	0.18	0.18
metiram	0.00	7.30	0.00
metobromuron	16.06	11.78	1.89
metolachlor	35.34	11.41	4.03
metoxuron	48.56	12.22	5.93
metribuzin	6.53	12.54	0.82
metsulfuron-methyl	0.02	10.39	0.00
mevinphos	92.15	12.36	11.39
mexacarbate	100.00	0.25	0.25
monolinuron	93.45	12.33	11.52
myclobutanil	8.77	11.37	1.00
nitrapyrin	100.00	1.74	1.74
nitrothal-isopropyl	2.88	11.00	0.32
nuarimol	1.15	11.06	0.13
omethoate	42.93	12.56	5.39
oxamyl	89.91	12.45	11.19
oxycarboxim	1.62	11.67	0.19
oxydemeton-methyl	46.40	11.99	5.56
paclobutrazol	0.98	11.32	0.11
paraquat	0.00	11.82	0.00
parathion	23.31	10.46	2.44
parathion-methyl	33.99	11.37	3.86
penconazole	11.89	11.41	1.36
pencycuron	0.03	10.91	0.00
pendimethalin	34.62	1.74	0.60
pentachlorophenol	45.61	11.67	5.32
permethrin	0.93	8.87	0.08
phenmedipham	0.03	11.24	0.00
phosalone	6.11	10.31	0.63
phosmet	5.08	11.02	0.56
phosphamidon	26.21	11.24	2.95
picloram	3.17	12.06	0.38
picloram-potassium salt	0.17	11.50	0.02
piperonylbutoxide	9.06	0.08	0.01
pirimicarb	25.79	12.11	3.12
pirimiphos-methyl	33.99	8.99	3.06
pp-DDT	4.41	1.60	0.07
prochloraz	10.17	10.37	1.05
procymidon	83.24	3.12	2.60
prometon	14.17	12.34	1.75
prometryn	7.84	12.04	0.94
propachlor	100.00	12.30	12.30
propamocarb	16.36	12.35	2.02
propaquizafop	0.01	9.88	0.00
propazine	1.86	12.25	0.23
propetamphos	33.19	11.29	3.75
profenofos	6.86	10.43	0.72
propiconazole	4.74	10.76	0.51
propoxur	27.81	12.63	3.51
propyzamide	4.82	11.82	0.57
prosulfocarb	5.22	11.88	0.62

pyrazophos	7.22	10.26	0.74
pyrethrins	0.84	6.26	0.05
pyridate	0.38	10.41	0.04
pyridathioben (pyridaben)	12.90	0.37	0.05
pyrifenox	23.24	11.25	2.61
quinmerac	2.88	12.41	0.36
quintozeen	59.32	0.20	0.12
quizalofop-ethyl	0.04	10.47	0.00
quizalofop-P-ethyl	0.35	10.46	0.04
rimsulfuron	0.88	9.97	0.09
sethoxydim	3.00	10.92	0.33
simazine	1.20	12.79	0.15
sulfotep	84.18	4.18	3.52
TCA	0.00	13.14	0.00
tebuconazole	1.11	11.15	0.12
teflubenzuron	0.04	10.39	0.00
tefluthrin	64.86	0.02	0.01
temephos	2.07	6.45	0.13
terbufos	94.63	2.76	2.61
terbutryn	10.03	12.01	1.20
terbutylazine	7.50	12.19	0.91
tetrachloorvinphos	2.20	10.52	0.23
tetradifon	0.20	10.62	0.02
thiabendazole	0.00	12.80	0.00
thifensulfuron-methyl	0.11	10.33	0.01
thiocyclam hydrogen oxalate	18.55	11.61	2.15
thiodicarb	55.38	8.89	4.92
thiofanate-methyl	2.88	10.73	0.31
thiofanox	77.60	12.45	9.66
thiometon	100.00	10.91	10.91
thiram	26.75	11.56	3.09
tolclofos-methyl	100.00	0.09	0.09
tolylfluanid	3.58	10.49	0.38
toxaphene	17.82	8.14	1.45
2,4,5-T-propylene glycolbutyl ether ester	0.68	10.51	0.07
tri-allate	74.55	3.03	2.26
triadimefon	1.36	11.32	0.15
triadimenol	0.22	11.29	0.03
triazophos	8.72	11.06	0.96
trichlorfon	11.89	11.82	1.41
trichloronaat	33.99	10.36	3.52
triclopyr	8.57	11.83	1.01
tridemorph	58.45	7.09	4.14
triflumizole	8.29	10.73	0.89
trifluralin	64.10	0.52	0.33
triforine	3.37	9.93	0.33
vinclozolin	3.58	11.36	0.41
warfarin	19.49	10.77	2.10
zineb	2.88	11.54	0.33
ziram	2.79	11.17	0.31

Table E-5 Volatilisation from crops and accumulated flux to a pond at a wind speed of 5 m s^{-1}. Note: the numbers are given much more accurately than they actually are known.

Tabel E-5. Fordampning fra afgrøder og akkumuleret fluks til en sø ved en vindhastighed på 5 m s^{-1}. Bemærk at tallene vises i flere decimaler end de er kendte.

Compound	% of the dose that volatilises	Accumulated flux to water (kg m^{-2}) as % of the emission in the field (kg m^{-2})	Accumulated flux to water (kg m^{-2}) as % of the dose in the field (kg m^{-2})
abamectine 1a	0.40	4.26	0.02
acephate	10.64	6.92	0.74
aclonifen	3.58	6.18	0.22
acrinathrin (acrinate)	0.47	4.96	0.02
alachlor	24.48	6.16	1.51
aldicarb	81.32	6.84	5.56
alloxydim-sodium	7.09	5.71	0.40
aminocarb	31.12	6.66	2.07
amitraz	11.13	5.89	0.66
amitrol	5.64	8.66	0.49
ancymidol	3.54	6.26	0.22
anilazine	0.90	6.12	0.06
asulam	24.61	6.46	1.59
atrazine	3.98	6.59	0.26
azaconazole	2.68	5.96	0.16
azinphos-methyl	4.80	5.86	0.28
azocyclotin	0.01	5.31	0.00
benazolin	0.34	6.35	0.02
benazolin-ethyl	11.42	6.14	0.70
bendiocarb	37.33	6.49	2.42
benfuracarb	4.54	5.41	0.25
benodanil	0.12	5.83	0.01
benomyl	0.08	6.02	0.01
bensultap	10.52	5.15	0.54
bentazone	17.14	6.38	1.09
bifenox	7.95	5.61	0.45
bifenthrin	3.71	5.21	0.19
bitertanol-A	0.02	5.75	0.00
brodifacoum	4.05	5.02	0.20
bromacil	4.10	6.22	0.25
bromofenoxim	0.84	5.22	0.04
bromophos-ethyl	31.40	2.29	0.72
bromopropylate	3.01	5.32	0.16
bromoxynil	24.61	6.10	1.50
buminaphos	100.00	5.38	5.38
bupirimate	6.21	5.86	0.36
buprofezin	20.14	5.49	1.11
butocarboxim	73.95	6.84	5.06
butoxycarboxim	13.28	6.53	0.87
captafol	0.84	5.69	0.05
captan	2.22	5.96	0.13
carbaryl	8.20	6.72	0.55
carbendazim	0.28	6.83	0.02
carbetamide	0.00	6.41	0.00
carbophenothion	18.97	4.73	0.90
carbofuran	6.51	6.54	0.43
carboxin	3.19	6.42	0.20
chlorbromuron	5.37	6.00	0.32
chlorfenvinphos	18.15	5.64	1.02
chloridazon	2.88	6.54	0.19
chlormequat	2.88	7.22	0.21
chlorothalonil	5.46	6.16	0.34
chlorotoluron	2.72	6.62	0.18
chloroxuron	0.54	6.02	0.03
chlorpropham	24.61	6.60	1.62
chlorpyriphos-ethyl	28.83	4.96	1.43
chlorpyrifos-methyl	40.50	5.13	2.08
chlorthal-dimethyl (DCPA)	8.77	5.64	0.49
clodinafop-propargyl	1.25	5.69	0.07

clofentezine	0.28	5.93	0.02
cloquintoceet-mexyl (CGA 185072)	1.58	5.76	0.09
coumatetralyl	0.11	6.01	0.01
cyanamide	100.00	10.47	10.47
cyanazine	0.48	6.37	0.03
cycloate	100.00	6.05	6.05
cycloxydim	2.88	5.82	0.17
cyfluthrin	1.19	4.69	0.06
cyhalotrin	0.98	0.00	0.00
cyhexatin	0.00	5.52	0.00
cymoxanil	5.59	6.76	0.38
cypermethrin (cis)	0.45	5.34	0.02
cypermethrin (trans)	0.45	5.34	0.02
alpha-cypermethrin	4.24	3.78	0.16
cyproconazole	5.13	6.01	0.31
cyprofuram	1.75	6.09	0.11
cyromazine	0.50	7.12	0.04
2,4-D (pH soil > 5)	24.61	6.54	1.61
dalapon	2.88	7.44	0.21
daminozide	0.84	7.20	0.06
dazomet	16.06	7.17	1.15
deltamethrin	2.42	0.71	0.02
demeton-S-methylsulfon	1.79	6.21	0.11
desmedipham	0.47	5.96	0.03
desmetryn	9.61	6.61	0.64
diallate	73.30	5.75	4.21
dial.dichl.aceetamid(cdaa)	100.00	6.99	6.99
diazinon	64.86	5.84	3.79
dicamba	36.58	6.54	2.39
dicamba dimethylammonium	1.48	6.18	0.09
dichlobenil	100.00	5.82	5.82
dichlofluanid	4.07	5.76	0.23
1,3-dichloropropene	100.00	0.12	0.12
cis-dichloropropene	100.00	0.10	0.10
dichlorprop	2.88	6.42	0.18
dichlorprop-P	6.74	6.42	0.43
dichlorvos	100.00	6.45	6.45
dicloran	10.48	6.65	0.70
dicofol (op)	5.37	5.55	0.30
dicofol (pp)	5.37	5.55	0.30
dieldrin	16.06	4.09	0.66
dienochlor	20.51	5.15	1.06
diethatyl-ethyl	9.12	5.89	0.54
diethofencarb	66.35	5.94	3.94
difenoconazole	0.15	5.43	0.01
difenoxuron	0.04	6.05	0.00
diflubenzuron	0.27	5.90	0.02
diflufenican	3.91	5.26	0.21
dikegulac-sodium	0.82	5.99	0.05
dimefuron	8.42	5.74	0.48
dimethachlor	34.78	6.26	2.18
dimethoate	18.97	6.47	1.23
dimethomorph (E-isomer)	0.72	5.51	0.04
dimethomorph (Z-isomer)	0.73	5.51	0.04
dinocap	2.14	5.62	0.12
dinoseb	44.03	6.34	2.79
dinoseb-acetate	0.00	6.07	0.00
dinoterb	99.40	4.25	4.22
diquat-dibromide	0.00	5.72	0.00
dithianon	5.11	5.94	0.30
diuron	2.04	6.44	0.13
DNOC	62.08	6.73	4.18
dodemorph	17.48	6.08	1.06
2,4-D-propylene glycolbutyl ether ester	24.61	6.53	1.61
endosulfan	3.13	5.40	0.17
EPTC	100.00	4.89	4.89
esfenvalerate	0.88	5.09	0.04
ethephon	2.88	7.42	0.21
ethiofencarb	16.96	6.50	1.10

ethofumesate	14.85	6.04	0.90
ethoprophos	100.00	6.34	6.34
etofenprox	2.52	0.11	0.00
etridiazole	81.32	6.14	5.00
etrimfos	67.08	5.84	3.92
fenaminosulf	0.00	6.29	0.00
fenamiphos	4.62	5.94	0.27
fenarimol	3.49	5.78	0.20
fenbutatinoxide	0.04	4.01	0.00
fenchlorazole-ethyl	0.93	5.44	0.05
fenfuram	3.98	6.73	0.27
fenitrothion	19.02	6.09	1.16
fenoprop-butoxypropyl ester (2,4,5-TP)	2.47	6.16	0.15
fenoxaprop-ethyl	1.43	5.63	0.08
fenoxaprop-P-ethyl	0.73	5.63	0.04
fenoxycarb	0.93	5.95	0.06
fenpiclonil	0.03	6.40	0.00
fenpropathrin	18.23	4.67	0.85
fenpropidin	67.95	6.12	4.16
fenpropimorph	36.28	5.53	2.01
fentin-acetate	3.75	5.42	0.20
fentin-hydroxide	1.10	5.61	0.06
fenvalerate	0.88	5.09	0.04
ferbam	0.00	5.39	0.00
fluazifop-butyl	6.37	5.78	0.37
fluazifop-p-butyl	5.02	5.51	0.28
flucycloxuron	49.09	0.01	0.00
flurenol(-butyl)	7.01	6.07	0.43
flurochloridon	3.99	5.89	0.23
fluroxypyr	0.07	6.26	0.00
fluroxypyr 1-methylheptylester	1.13	5.59	0.06
flusilazole	4.00	5.87	0.23
flutolanil	32.11	5.67	1.82
fluvalinate	2.12	2.59	0.06
folpet	27.81	5.09	1.42
fonofos	85.74	5.88	5.04
formothion	9.61	6.25	0.60
fosetyl-aluminium	2.47	5.67	0.14
fuberidazol	0.05	6.90	0.00
furalaxyl	7.13	5.95	0.42
furathiocarb	1.37	5.53	0.08
gluphosinate-amm.	0.00	6.76	0.00
glyphosate	0.00	7.08	0.00
glyphosate-trimesium (glyph,part)	4.05	6.34	0.26
glyphosate-trimesium (trim,part)	4.05	6.34	0.26
haloxyfop ethoxyethyl	0.14	5.32	0.01
heptachlor	100.00	0.06	0.06
heptenophos	100.00	6.24	6.24
hexaconazole	2.88	5.88	0.17
hexazinone	3.37	6.28	0.21
hexythiazox	1.23	5.67	0.07
hymexazol	100.00	8.27	8.27
imazalil	10.42	5.98	0.62
imazamethabenz-methyl (m-isomer)	1.02	6.03	0.06
imazamethabenz-methyl (p-isomer)	1.02	6.03	0.06
imazapyr	0.37	6.22	0.02
imidacloprid	0.46	6.26	0.03
ioxynil	24.61	5.57	1.37
iprodione	0.53	5.79	0.03
isofenphos	16.06	5.70	0.91
isoproturon	1.72	6.68	0.11
isoxaben	4.62	5.76	0.27
kasugamycine	0.08	5.55	0.00
lambda-cyhalothrin	0.46	5.22	0.02
lenacil	0.34	6.43	0.02
lindane	54.93	5.43	2.98

linuron	31.12	6.30	1.96
malathion	24.61	5.78	1.42
maleine-hydrazide	0.00	7.98	0.00
mancozeb	0.00	5.79	0.00
maneb	0.00	6.19	0.00
MCPA	4.24	6.73	0.29
mecoprop	14.26	6.60	0.94
mecoprop-P	16.06	6.60	1.06
mefluidide	0.00	5.90	0.00
mepiquat.chloride	0.00	7.34	0.00
metalaxyl	15.87	6.09	0.97
metaldehyde	0.00	7.00	0.00
metam-sodium	0.00	7.66	0.00
metamitron	0.92	6.72	0.06
metazachlor	6.04	6.10	0.37
methabenzthiazuron	2.25	6.54	0.15
methamidophos	36.28	7.47	2.71
methidathion	12.50	5.95	0.74
methiocarb	3.48	6.50	0.23
methomyl	44.03	7.17	3.16
methylbromide	100.00	0.03	0.03
methylisothiocyanate	100.00	0.68	0.68
metiram	0.00	3.96	0.00
metobromuron	16.06	6.23	1.00
metolachlor	35.34	6.06	2.14
metoxuron	48.56	6.47	3.14
metribuzin	6.53	6.60	0.43
metsulfuron-methyl	0.02	5.54	0.00
mevinphos	92.15	6.51	6.00
mexacarbate	100.00	0.88	0.88
monolinuron	93.45	6.58	6.15
myclobutanil	8.77	6.03	0.53
nitrapyrin	100.00	3.64	3.64
nitrothal-isopropyl	2.88	5.97	0.17
nuarimol	1.15	5.88	0.07
omethoate	42.93	6.61	2.84
oxamyl	89.91	6.55	5.89
oxycarboxim	1.62	6.18	0.10
oxydemeton-methyl	46.40	6.33	2.94
paclobutrazol	0.98	6.00	0.06
paraquat	0.00	6.25	0.00
parathion	23.31	5.95	1.39
parathion-methyl	33.99	6.18	2.10
penconazole	11.89	6.06	0.72
pencycuron	0.03	5.80	0.00
pendimethalin	34.62	3.53	1.22
pentachlorophenol	45.61	6.18	2.82
permethrin	0.93	5.38	0.05
phenmedipham	0.03	5.96	0.00
phosalone	6.11	5.59	0.34
phosmet	5.08	5.86	0.30
phosphamidon	26.21	5.97	1.56
picloram	3.17	6.37	0.20
picloram-potassium salt	0.17	6.09	0.01
piperonylbutoxide	9.06	0.30	0.03
pirimicarb	25.79	6.39	1.65
pirimiphos-methyl	33.99	5.75	1.95
pp-DDT	4.41	3.26	0.14
prochloraz	10.17	5.56	0.56
procymidon	83.24	4.51	3.75
prometon	14.17	6.50	0.92
prometryn	7.84	6.37	0.50
propachlor	100.00	6.61	6.61
propamocarb	16.36	6.51	1.06
propaquizafop	0.01	5.28	0.00
propazine	1.86	6.46	0.12
propetamphos	33.19	6.07	2.01
profenofos	6.86	5.57	0.38
propiconazole	4.74	5.73	0.27
propoxur	27.81	6.65	1.85
propyzamide	4.82	6.26	0.30

prosulfocarb	5.22	6.29	0.33
pyrazophos	7.22	5.56	0.40
pyrethrins	0.84	5.30	0.04
pyridate	0.38	5.55	0.02
pyridathioben (pyridaben)	12.90	1.24	0.16
pyrifenox	23.24	5.99	1.39
quinmerac	2.88	6.54	0.19
quintozeen	59.32	0.73	0.43
quizalofop-ethyl	0.04	5.58	0.00
quizalofop-P-ethyl	0.35	5.58	0.02
rimsulfuron	0.88	5.33	0.05
sethoxydim	3.00	5.80	0.17
simazine	1.20	6.72	0.08
sulfotep	84.18	4.83	4.06
TCA	0.00	6.89	0.00
tebuconazole	1.11	5.92	0.07
teflubenzuron	0.04	5.54	0.00
tefluthrin	64.86	0.07	0.04
temephos	2.07	4.88	0.10
terbufos	94.63	4.30	4.07
terbutryn	10.03	6.36	0.64
terbutylazine	7.50	6.46	0.48
tetrachloorvinphos	2.20	5.61	0.12
tetradifon	0.20	5.66	0.01
thiabendazole	0.00	6.73	0.00
thifensulfuron-methyl	0.11	5.51	0.01
thiocyclam hydrogen oxalate	18.55	6.15	1.14
thiodicarb	55.38	5.53	3.06
thiofanate-methyl	2.88	5.72	0.16
thiofanox	77.60	6.56	5.09
thiometon	100.00	6.25	6.25
thiram	26.75	6.34	1.70
tolclofos-methyl	100.00	0.34	0.34
tolylfluanid	3.58	5.69	0.20
toxaphene	17.82	5.24	0.93
2,4,5-T-propylene glycolbutyl ether ester	0.68	5.60	0.04
tri-allate	74.55	4.40	3.28
triadimefon	1.36	6.00	0.08
triadimenol	0.22	5.99	0.01
triazophos	8.72	5.88	0.51
trichlorfon	11.89	6.25	0.74
trichloronaat	33.99	5.74	1.95
triclopyr	8.57	6.25	0.54
tridemorph	58.45	5.56	3.25
triflumizole	8.29	5.71	0.47
trifluralin	64.10	1.60	1.03
triforine	3.37	5.32	0.18
vinclozolin	3.58	6.05	0.22
warfarin	19.49	5.89	1.15
zineb	2.88	6.12	0.18
ziram	2.79	5.93	0.17

Table E-6. Volatilisation from crops and accumulated flux to a ditch at a wind speed of 5 m s^{-1}. Note: the numbers are given much more accurately than they actually are known.

Tabel E-6. Fordampning fra afgrøder og akkumuleret fluks til en kanal ved en vindhastighed på 5 m s^{-1}. Bemærk at tallene vises i flere decimaler end de er kendte.

Compound	% of the dose that volatilises	Accumulated flux to water (kg m^{-2}) as % of the emission in the field (kg m^{-2})	Accumulated flux to water (kg m^{-2}) as % of the dose in the field (kg m^{-2})
abamectine 1a	0.40	8.27	0.03
acephate	10.64	13.88	1.48
aclonifen	3.58	12.30	0.44
acrinathrin (acrinate)	0.47	9.72	0.05
alachlor	24.48	12.24	3.00
aldicarb	81.32	13.71	11.15
alloxydim-sodium	7.09	11.30	0.80
aminocarb	31.12	13.32	4.14
amitraz	11.13	11.67	1.30
amitrol	5.64	17.78	1.00
ancymidol	3.54	12.45	0.44
anilazine	0.90	12.16	0.11
asulam	24.61	12.89	3.17
atrazine	3.98	13.17	0.52
azaconazole	2.68	11.83	0.32
azinphos-methyl	4.80	11.61	0.56
azocyclotin	0.01	10.46	0.00
benazolin	0.34	12.66	0.04
benazolin-ethyl	11.42	12.21	1.39
bendiocarb	37.33	12.96	4.84
benfuracarb	4.54	10.66	0.48
benodanil	0.12	11.55	0.01
benomyl	0.08	11.96	0.01
bensultap	10.52	10.11	1.06
bentazone	17.14	12.72	2.18
bifenox	7.95	11.08	0.88
bifenthrin	3.71	10.25	0.38
bitertanol-A	0.02	11.38	0.00
brodifacoum	4.05	9.84	0.40
bromacil	4.10	12.38	0.51
bromofenoxim	0.84	10.27	0.09
bromophos-ethyl	31.40	4.34	1.36
bromopropylate	3.01	10.48	0.32
bromoxynil	24.61	12.13	2.99
buminaphos	100.00	10.60	10.60
bupirimate	6.21	11.62	0.72
buprofezin	20.14	10.81	2.18
butocarboxim	73.95	13.71	10.14
butoxycarboxim	13.28	13.04	1.73
captafol	0.84	11.26	0.10
captan	2.22	11.82	0.26
carbaryl	8.20	13.47	1.11
carbendazim	0.28	13.69	0.04
carbetamide	0.00	12.79	0.00
carbophenothion	18.97	9.22	1.75
carbofuran	6.51	13.06	0.85
carboxin	3.19	12.80	0.41
chlorbromuron	5.37	11.91	0.64
chlorfenvinphos	18.15	11.14	2.02
chloridazon	2.88	13.06	0.38
chlormequat	2.88	14.56	0.42
chlorothalonil	5.46	12.25	0.67
chlorotoluron	2.72	13.23	0.36
chloroxuron	0.54	11.95	0.06
chlorpropham	24.61	13.19	3.25
chlorpyriphos-ethyl	28.83	9.71	2.80
chlorpyrifos-methyl	40.50	10.07	4.08
chlorthal-dimethyl (DCPA)	8.77	11.14	0.98
clodinafop-propargyl	1.25	11.25	0.14

clofentezine	0.28	11.75	0.03
cloquintoceet-mexyl (CGA 185072)	1.58	11.39	0.18
coumatetralyl	0.11	11.93	0.01
cyanamide	100.00	22.03	22.03
cyanazine	0.48	12.71	0.06
cycloate	100.00	12.01	12.01
cycloxydim	2.88	11.52	0.33
cyfluthrin	1.19	9.16	0.11
cyhalotrin	0.98	0.00	0.00
cyhexatin	0.00	10.90	0.00
cymoxanil	5.59	13.53	0.76
cypermethrin (cis)	0.45	10.52	0.05
cypermethrin (trans)	0.45	10.52	0.05
alpha-cypermethrin	4.24	7.28	0.31
cyproconazole	5.13	11.94	0.61
cyprofuram	1.75	12.10	0.21
cyromazine	0.50	14.32	0.07
2,4-D (pH soil > 5)	24.61	13.06	3.22
dalapon	2.88	15.03	0.43
daminozide	0.84	14.49	0.12
dazomet	16.06	14.43	2.32
deltamethrin	2.42	1.32	0.03
demeton-S-methylsulfon	1.79	12.36	0.22
desmedipham	0.47	11.83	0.06
desmetryn	9.61	13.22	1.27
diallate	73.30	11.37	8.33
dial.dichl.aceetamid(cdaa)	100.00	14.05	14.05
diazinon	64.86	11.57	7.50
dicamba	36.58	13.07	4.78
dicamba dimethylammonium	1.48	12.30	0.18
dichlobenil	100.00	11.50	11.50
dichlofluanid	4.07	11.40	0.46
1,3-dichloropropene	100.00	0.23	0.23
cis-dichloropropene	100.00	0.18	0.18
dichlorprop	2.88	12.81	0.37
dichlorprop-P	6.74	12.81	0.86
dichlorvos	100.00	12.87	12.87
dicloran	10.48	13.31	1.39
dicofol (op)	5.37	10.96	0.59
dicofol (pp)	5.37	10.96	0.59
dieldrin	16.06	7.91	1.27
dienochlor	20.51	10.12	2.08
diethatyl-ethyl	9.12	11.68	1.06
diethofencarb	66.35	11.78	7.82
difenoconazole	0.15	10.71	0.02
difenoxuron	0.04	12.01	0.01
diflubenzuron	0.27	11.69	0.03
diflufenican	3.91	10.34	0.40
dikegulac-sodium	0.82	11.88	0.10
dimefuron	8.42	11.36	0.96
dimethachlor	34.78	12.46	4.33
dimethoate	18.97	12.91	2.45
dimethomorph (E-isomer)	0.72	10.87	0.08
dimethomorph (Z-isomer)	0.73	10.87	0.08
dinocap	2.14	11.10	0.24
dinoseb	44.03	12.64	5.57
dinoseb-acetate	0.00	12.07	0.00
dinoterb	99.40	8.23	8.18
diquat-dibromide	0.00	11.31	0.00
dithianon	5.11	11.78	0.60
diuron	2.04	12.84	0.26
DNOC	62.08	13.47	8.36
dodemorph	17.48	12.07	2.11
2,4-D-propylene glycolbutyl ether ester	24.61	13.05	3.21
endosulfan	3.13	10.64	0.33
EPTC	100.00	9.56	9.56
esfenvalerate	0.88	9.98	0.09
ethephon	2.88	14.98	0.43
ethiofencarb	16.96	12.98	2.20

ethofumesate	14.85	12.00	1.78
ethoprophos	100.00	12.64	12.64
etofenprox	2.52	0.20	0.01
etridiazole	81.32	12.21	9.93
etrimfos	67.08	11.57	7.77
fenaminosulf	0.00	12.53	0.00
fenamiphos	4.62	11.79	0.54
fenarimol	3.49	11.45	0.40
fenbutatinoxide	0.04	7.77	0.00
fenchlorazole-ethyl	0.93	10.73	0.10
fenfuram	3.98	13.47	0.54
fenitrothion	19.02	12.10	2.30
fenoprop-butoxypropyl ester (2,4,5-TP)	2.47	12.25	0.30
fenoxaprop-ethyl	1.43	11.12	0.16
fenoxaprop-P-ethyl	0.73	11.12	0.08
fenoxycarb	0.93	11.81	0.11
fenpiclonil	0.03	12.77	0.00
fenpropathrin	18.23	9.10	1.66
fenpropidin	67.95	12.17	8.27
fenpropimorph	36.28	10.90	3.95
fentin-acetate	3.75	10.68	0.40
fentin-hydroxide	1.10	11.07	0.12
fenvalerate	0.88	9.98	0.09
ferbam	0.00	10.62	0.00
fluazifop-butyl	6.37	11.45	0.73
fluazifop-p-butyl	5.02	10.88	0.55
flucycloxuron	49.09	0.01	0.00
flurenol(-butyl)	7.01	12.06	0.85
flurochloridon	3.99	11.68	0.47
fluroxypyr	0.07	12.47	0.01
fluroxypyr 1-methylheptylester	1.13	11.04	0.12
flusilazole	4.00	11.64	0.47
flutolanil	32.11	11.21	3.60
fluvalinate	2.12	4.93	0.10
folpet	27.81	9.98	2.78
fonofos	85.74	11.64	9.98
formothion	9.61	12.44	1.20
fosetyl-aluminium	2.47	11.20	0.28
fuberidazol	0.05	13.86	0.01
furalaxyl	7.13	11.81	0.84
furathiocarb	1.37	10.92	0.15
gluphosinate-amm.	0.00	13.54	0.00
glyphosate	0.00	14.25	0.00
glyphosate-trimesium (glyph,part)	4.05	12.63	0.51
glyphosate-trimesium (trim,part)	4.05	12.63	0.51
haloxyfop ethoxyethyl	0.14	10.48	0.02
heptachlor	100.00	0.10	0.10
heptenophos	100.00	12.43	12.43
hexaconazole	2.88	11.65	0.34
hexazinone	3.37	12.52	0.42
hexythiazox	1.23	11.21	0.14
hymexazol	100.00	16.88	16.88
imazalil	10.42	11.86	1.24
imazamethabenz-methyl (m-isomer)	1.02	11.98	0.12
imazamethabenz-methyl (p-isomer)	1.02	11.98	0.12
imazapyr	0.37	12.37	0.05
imidacloprid	0.46	12.46	0.06
ioxynil	24.61	11.00	2.71
iprodione	0.53	11.46	0.06
isofenphos	16.06	11.26	1.81
isoproturon	1.72	13.36	0.23
isoxaben	4.62	11.40	0.53
kasugamycine	0.08	10.95	0.01
lambda-cyhalothrin	0.46	10.26	0.05
lenacil	0.34	12.82	0.04
lindane	54.93	10.70	5.88
linuron	31.12	12.54	3.90

malathion	24.61	11.45	2.82
maleine-hydrazide	0.00	16.24	0.00
mancozeb	0.00	11.47	0.00
maneb	0.00	12.31	0.00
MCPA	4.24	13.48	0.57
mecoprop	14.26	13.19	1.88
mecoprop-P	16.06	13.19	2.12
mefluidide	0.00	11.70	0.00
mepiquat.chloride	0.00	14.81	0.00
metalaxyl	15.87	12.11	1.92
metaldehyde	0.00	14.06	0.00
metam-sodium	0.00	15.53	0.00
metamitron	0.92	13.45	0.12
metazachlor	6.04	12.13	0.73
methabenzthiazuron	2.25	13.06	0.29
methamidophos	36.28	15.09	5.48
methidathion	12.50	11.80	1.47
methiocarb	3.48	12.98	0.45
methomyl	44.03	14.44	6.36
methylbromide	100.00	0.05	0.05
methylisothiocyanate	100.00	1.26	1.26
metiram	0.00	7.68	0.00
metobromuron	16.06	12.41	1.99
metolachlor	35.34	12.04	4.26
metoxuron	48.56	12.91	6.27
metribuzin	6.53	13.20	0.86
metsulfuron-methyl	0.02	10.93	0.00
mevinphos	92.15	13.01	11.99
mexacarbate	100.00	1.64	1.64
monolinuron	93.45	13.16	12.30
myclobutanil	8.77	11.98	1.05
nitrapyrin	100.00	7.00	7.00
nitrothal-isopropyl	2.88	11.85	0.34
nuarimol	1.15	11.65	0.13
omethoate	42.93	13.22	5.68
oxamyl	89.91	13.10	11.78
oxycarboxim	1.62	12.28	0.20
oxydemeton-methyl	46.40	12.62	5.85
paclobutrazol	0.98	11.91	0.12
paraquat	0.00	12.44	0.00
parathion	23.31	11.80	2.75
parathion-methyl	33.99	12.29	4.18
penconazole	11.89	12.04	1.43
pencycuron	0.03	11.48	0.00
pendimethalin	34.62	6.77	2.35
pentachlorophenol	45.61	12.30	5.61
permethrin	0.93	10.60	0.10
phenmedipham	0.03	11.83	0.00
phosalone	6.11	11.03	0.67
phosmet	5.08	11.61	0.59
phosphamidon	26.21	11.83	3.10
picloram	3.17	12.70	0.40
picloram-potassium salt	0.17	12.10	0.02
piperonylbutoxide	9.06	0.56	0.05
pirimicarb	25.79	12.75	3.29
pirimiphos-methyl	33.99	11.38	3.87
pp-DDT	4.41	6.25	0.28
prochloraz	10.17	10.97	1.12
procymidon	83.24	8.76	7.29
prometon	14.17	12.98	1.84
prometryn	7.84	12.69	0.99
propachlor	100.00	13.21	13.21
propamocarb	16.36	13.00	2.13
propaquizafop	0.01	10.40	0.00
propazine	1.86	12.90	0.24
propetamphos	33.19	12.05	4.00
profenofos	6.86	11.00	0.75
propiconazole	4.74	11.33	0.54
propoxur	27.81	13.30	3.70
propyzamide	4.82	12.45	0.60
prosulfocarb	5.22	12.53	0.65

pyrazophos	7.22	10.98	0.79
pyrethrins	0.84	10.41	0.09
pyridate	0.38	10.96	0.04
pyridathioben (pyridaben)	12.90	2.31	0.30
pyrifenox	23.24	11.88	2.76
quinmerac	2.88	13.06	0.38
quintozeen	59.32	1.35	0.80
quizalofop-ethyl	0.04	11.02	0.00
quizalofop-P-ethyl	0.35	11.02	0.04
rimsulfuron	0.88	10.50	0.09
sethoxydim	3.00	11.49	0.34
simazine	1.20	13.46	0.16
sulfotep	84.18	9.43	7.94
TCA	0.00	13.83	0.00
tebuconazole	1.11	11.73	0.13
teflubenzuron	0.04	10.94	0.00
tefluthrin	64.86	0.13	0.08
temephos	2.07	9.56	0.20
terbufos	94.63	8.33	7.89
terbutryn	10.03	12.69	1.27
terbutylazine	7.50	12.89	0.97
tetrachloorvinphos	2.20	11.08	0.24
tetradifon	0.20	11.18	0.02
thiabendazole	0.00	13.47	0.00
thifensulfuron-methyl	0.11	10.88	0.01
thiocyclam hydrogen oxalate	18.55	12.22	2.27
thiodicarb	55.38	10.90	6.04
thiofanate-methyl	2.88	11.32	0.33
thiofanox	77.60	13.12	10.18
thiometon	100.00	12.44	12.44
thiram	26.75	12.64	3.38
tolclofos-methyl	100.00	0.62	0.62
tolylfluanid	3.58	11.24	0.40
toxaphene	17.82	10.30	1.83
2,4,5-T-propylene glycolbutyl ether ester	0.68	11.07	0.07
tri-allate	74.55	8.54	6.37
triadimefon	1.36	11.91	0.16
triadimenol	0.22	11.88	0.03
triazophos	8.72	11.66	1.02
trichlorfon	11.89	12.44	1.48
trichloronaat	33.99	11.35	3.86
triclopyr	8.57	12.45	1.07
tridemorph	58.45	10.97	6.41
triflumizole	8.29	11.29	0.94
trifluralin	64.10	3.00	1.92
triforine	3.37	10.47	0.35
vinclozolin	3.58	12.01	0.43
warfarin	19.49	11.67	2.27
zineb	2.88	12.16	0.35
ziram	2.79	11.76	0.33

Table E-7. Volatilisation from fallow soil and accumulated flux to the river with a low r_c. Notes:the numbers are given much more accurately than they actually are known. A value of "-" is given in the third column when the accumulated emission is exactly 0, because it is then not possible to divide by the accumulated emission. There are small values for the accumulated emission that are rounded off to 0.00. For these values it is possible to give a number in the third column.

Tabel E-7. Fordampning fra jord og akkumuleret fluks til floden med en lav r_c-værdi. Bemærkninger: tallene vises i flere decimaler end de er kendte. I den tredje kolonne gives en værdi "-" hvis fluksen er helt præcist 0, fordi i det tilfælde er det ikke muligt at dividere med den akkumulerede emission. Der eksisterer små værdier af den akkumulerede emission, som er afrundet til 0.00. For disse stoffer er det muligt at give en værdi i den tredje kolonne.

Compound	% of the dose that volatilises	Accumulated flux to water (kg m^{-2}) as % of the emission in the field (kg m^{-2})	Accumulated flux to water (kg m^{-2}) as % of the dose in the field (kg m^{-2})
abamectine 1a	0.00	-	0.00
acephate	0.00	-	0.00
aclonifen	23.04	13.78	3.18
acrinathrin (acrinate)	24.67	11.00	2.71
alachlor	16.73	13.70	2.29
aldicarb	14.00	15.25	2.14
alloxydim-sodium	0.00	-	0.00
aminocarb	11.96	14.84	1.78
amitraz	36.24	13.34	4.84
amitrol	0.00	-	0.00
ancymidol	0.00	-	0.00
anilazine	0.00	-	0.00
asulam	1.85	14.39	0.27
atrazine	4.22	14.68	0.62
azaconazole	0.00	-	0.00
azinphos-methyl	11.65	13.02	1.52
azocyclotin	0.00	-	0.00
benazolin	0.00	-	0.00
benazolin-ethyl	16.84	13.67	2.30
bendiocarb	29.26	14.52	4.25
benfuracarb	19.04	12.01	2.29
benodanil	0.00	-	0.00
benomyl	0.00	-	0.00
bensultap	39.39	11.82	4.65
bentazone	9.21	14.20	1.31
bifenox	36.79	12.72	4.68
bifenthrin	38.40	11.89	4.57
bitertanol-A	0.00	-	0.00
brodifacoum	16.73	11.12	1.86
bromacil	0.00	-	0.00
bromofenoxim	15.22	11.58	1.76
bromophos-ethyl	57.79	11.94	6.90
bromopropylate	28.77	11.85	3.41
bromoxynil	21.06	13.59	2.86
buminaphos	41.91	12.65	5.30
bupirimate	14.64	13.03	1.91
buprofezin	43.48	13.16	5.72
butocarboxim	3.09	15.25	0.47
butoxycarboxim	0.00	-	0.00
captafol	8.12	12.64	1.03
captan	10.73	13.24	1.42
carbaryl	6.45	14.99	0.97
carbendazim	0.00	-	0.00
carbetamide	0.00	-	0.00
carbophenothion	48.32	12.67	6.12
carbofuran	0.00	-	0.00
carboxin	0.00	-	0.00
chlorbromuron	11.15	13.34	1.49
chlorfenvinphos	16.78	12.52	2.10
chloridazon	0.00	-	0.00
chlormequat	0.00	-	0.00

chlorothalonil	28.48	13.76	3.92
chlorotoluron	0.00	-	0.00
chloroxuron	0.00	-	0.00
chlorpropham	21.65	14.72	3.19
chlorpyriphos-ethyl	46.48	12.60	5.86
chlorpyrifos-methyl	46.13	12.93	5.97
chlorthal-dimethyl (DCPA)	37.67	12.84	4.84
clodinafop-propargyl	6.37	12.63	0.80
clofentezine	26.70	13.21	3.53
cloquintoceet-mexyl (CGA 185072)	18.37	12.79	2.35
coumatetralyl	0.00	-	0.00
cyanamide	0.00	-	0.00
cyanazine	0.00	-	0.00
cycloate	43.93	14.67	6.44
cycloxydim	4.84	12.92	0.62
cyfluthrin	46.06	11.78	5.42
cyhalotrin	95.10	0.00	0.00
cyhexatin	0.00	-	0.00
cymoxanil	0.00	-	0.00
cypermethrin (cis)	32.51	11.96	3.89
cypermethrin (trans)	32.51	11.96	3.89
alpha-cypermethrin	51.83	11.89	6.16
cyproconazole	4.00	13.37	0.53
cyprofuram	0.00	-	0.00
cyromazine	0.00	-	0.00
2,4-D (pH soil > 5)	10.22	14.57	1.49
dalapon	0.00	-	0.00
daminozide	0.00	-	0.00
dazomet	0.00	-	0.00
deltamethrin	65.29	10.38	6.78
demeton-S-methylsulfon	0.00	-	0.00
desmedipham	0.00	-	0.00
desmetryn	2.28	14.73	0.34
diallate	42.81	13.68	5.86
dial.dichl.aceetamid(cdaa)	29.57	15.68	4.64
diazinon	35.44	13.19	4.68
dicamba	3.35	14.57	0.49
dicamba dimethylammonium	0.00	-	0.00
dichlobenil	48.29	15.68	7.57
dichlofluanid	25.96	12.82	3.33
1,3-dichloropropene	76.92	9.50	7.31
cis-dichloropropene	77.99	8.51	6.64
dichlorprop	0.00	-	0.00
dichlorprop-P	0.00	-	0.00
dichlorvos	34.59	14.57	5.04
dicloran	25.84	14.86	3.84
dicofol (op)	31.14	12.40	3.86
dicofol (pp)	31.14	12.40	3.86
dieldrin	50.90	12.24	6.23
dienochlor	29.16	11.47	3.35
diethatyl-ethyl	9.71	13.09	1.27
diethofencarb	39.81	13.73	5.47
difenoconazole	0.00	-	0.00
difenoxuron	0.00	-	0.00
diflubenzuron	8.97	13.11	1.17
diflufenican	40.29	12.16	4.90
dikegulac-sodium	0.00	-	0.00
dimefuron	21.25	12.76	2.71
dimethachlor	10.61	13.93	1.48
dimethoate	0.00	-	0.00
dimethomorph (E-isomer)	0.00	-	0.00
dimethomorph (Z-isomer)	0.00	-	0.00
dinocap	13.69	12.47	1.71
dinoseb	30.20	14.20	4.29
dinoseb-acetate	0.00	-	0.00
dinoterb	52.60	14.10	7.42
diquat-dibromide	0.00	-	0.00
dithianon	31.48	13.30	4.19
diuron	0.00	-	0.00
DNOC	28.62	15.06	4.31

dodemorph	18.99	13.52	2.57
2,4-D-propylene glycolbutyl ether ester	20.29	14.57	2.96
endosulfan	29.93	12.04	3.60
EPTC	51.49	15.19	7.82
esfenvalerate	41.78	11.92	4.98
ethephon	0.00	-	0.00
ethiofencarb	2.98	14.48	0.43
ethofumesate	19.43	13.45	2.61
ethoprophos	27.03	14.16	3.83
etofenprox	75.66	7.36	5.57
etridiazole	38.23	14.06	5.38
etrimfos	38.20	13.36	5.10
fenaminosulf	0.00	-	0.00
fenamiphos	0.00	-	0.00
fenarimol	10.91	12.85	1.40
fenbutatinoxide	4.87	8.87	0.43
fenchlorazole-ethyl	12.85	12.08	1.55
fenfuram	1.28	14.99	0.19
fenitrothion	27.10	13.58	3.68
fenoprop-butoxypropyl ester (2,4,5-TP)	0.00	-	0.00
fenoxaprop-ethyl	16.26	12.50	2.03
fenoxaprop-P-ethyl	9.46	12.50	1.18
fenoxycarb	0.52	13.23	0.07
fenpiclonil	0.00	-	0.00
fenpropathrin	48.51	12.60	6.11
fenpropidin	23.75	13.64	3.24
fenpropimorph	43.11	13.19	5.69
fentin-acetate	7.51	12.02	0.90
fentin-hydroxide	6.84	12.44	0.85
fenvalerate	41.78	11.92	4.98
ferbam	0.00	-	0.00
fluazifop-butyl	28.54	12.90	3.68
fluazifop-p-butyl	26.77	12.27	3.29
flucycloxuron	89.07	0.79	0.70
flurenol(-butyl)	13.02	13.51	1.76
flurochloridon	3.19	13.09	0.42
fluroxypyr	0.00	-	0.00
fluroxypyr 1-methylheptylester	26.07	12.44	3.24
flusilazole	5.55	13.05	0.72
flutolanil	38.08	12.94	4.93
fluvalinate	55.94	11.12	6.22
folpet	47.38	13.27	6.29
fonofos	43.19	14.07	6.08
formothion	0.00	-	0.00
fosetyl-aluminium	0.00	-	0.00
fuberidazol	0.00	-	0.00
furalaxyl	5.43	13.23	0.72
furathiocarb	2.74	12.28	0.34
gluphosinate-amm.	0.00	-	0.00
glyphosate	0.00	-	0.00
glyphosate-trimesium (glyph,part)	0.00	-	0.00
glyphosate-trimesium (trim,part)	0.00	-	0.00
haloxyfop ethoxyethyl	0.00	-	0.00
heptachlor	79.07	5.25	4.15
heptenophos	32.16	14.01	4.51
hexaconazole	8.97	13.06	1.17
hexazinone	0.00	-	0.00
hexythiazox	16.75	12.60	2.11
hymexazol	3.41	18.55	0.63
imazalil	10.70	13.29	1.42
imazamethabenz-methyl (m-isomer)	0.00	-	0.00
imazamethabenz-methyl (p-isomer)	0.00	-	0.00
imazapyr	0.00	-	0.00
imidacloprid	0.00	-	0.00
ioxynil	27.35	12.40	3.39

iprodione	0.00	-	0.00
isofenphos	26.29	12.68	3.33
isoproturon	0.00	-	0.00
isoxaben	27.36	12.83	3.51
kasugamycine	0.00	-	0.00
lambda-cyhalothrin	31.92	11.67	3.72
lenacil	0.00	-	0.00
lindane	44.93	13.36	6.00
linuron	25.25	14.04	3.55
malathion	21.68	12.86	2.79
maleine-hydrazide	0.00	-	0.00
mancozeb	0.00	-	0.00
maneb	0.00	-	0.00
MCPA	0.00	-	0.00
mecoprop	5.16	14.70	0.76
mecoprop-P	5.87	14.70	0.86
mefluidide	0.00	-	0.00
mepiquat.chloride	0.00	-	0.00
metalaxyl	0.00	-	0.00
metaldehyde	0.00	-	0.00
metam-sodium	0.00	-	0.00
metamitron	0.00	-	0.00
metazachlor	0.08	13.57	0.01
methabenzthiazuron	0.00	-	0.00
methamidophos	0.00	-	0.00
methidathion	10.49	13.22	1.39
methiocarb	7.01	14.48	1.02
methomyl	0.00	-	0.00
methylbromide	84.49	3.44	2.90
methylisothiocyanate	68.66	17.34	11.91
metiram	0.00	-	0.00
metobromuron	11.64	13.87	1.62
metolachlor	17.07	13.48	2.30
metoxuron	19.17	14.42	2.76
metribuzin	0.00	-	0.00
metsulfuron-methyl	0.00	-	0.00
mevinphos	0.00	-	0.00
mexacarbate	65.41	13.38	8.75
monolinuron	25.24	14.70	3.71
myclobutanil	8.52	13.41	1.14
nitrapyrin	54.78	14.22	7.79
nitrothal-isopropyl	27.68	13.32	3.69
nuarimol	0.00	-	0.00
omethoate	0.00	-	0.00
oxamyl	0.00	-	0.00
oxycarboxim	0.00	-	0.00
oxydemeton-methyl	0.00	-	0.00
paclobutrazol	0.00	-	0.00
paraquat	0.00	-	0.00
parathion	33.39	13.37	4.47
parathion-methyl	28.49	13.80	3.93
penconazole	16.45	13.48	2.22
pencycuron	0.00	-	0.00
pendimethalin	54.46	13.39	7.29
pentachlorophenol	13.68	13.75	1.88
permethrin	36.72	12.19	4.48
phenmedipham	0.00	-	0.00
phosalone	26.18	12.43	3.25
phosmet	13.06	13.02	1.70
phosphamidon	0.00	-	0.00
picloram	0.00	-	0.00
picloram-potassium salt	0.00	-	0.00
piperonylbutoxide	70.66	10.24	7.24
pirimicarb	3.24	14.23	0.46
pirimiphos-methyl	38.71	13.17	5.10
pp-DDT	54.56	12.45	6.80
prochloraz	19.81	12.34	2.44
procymidon	50.73	13.42	6.81
prometon	5.45	14.48	0.79
prometryn	13.95	14.18	1.98
propachlor	26.95	14.76	3.98

propamocarb	0.00	-	0.00
propaquizafop	0.00	-	0.00
propazine	8.81	14.40	1.27
propetamphos	25.26	13.52	3.41
profenofos	15.34	12.37	1.90
propiconazole	4.21	12.72	0.54
propoxur	7.95	14.82	1.18
propyzamide	12.75	13.92	1.77
prosulfocarb	14.38	14.00	2.01
pyrazophos	26.01	12.37	3.22
pyrethrins	44.31	12.87	5.70
pyridate	0.27	12.32	0.03
pyridathioben (pyridaben)	62.48	11.89	7.43
pyrifenox	18.89	13.32	2.52
quinmerac	0.00	-	0.00
quintozeen	66.05	12.12	8.01
quizalofop-ethyl	0.00	-	0.00
quizalofop-P-ethyl	6.00	12.38	0.74
rimsulfuron	0.00	-	0.00
sethoxydim	0.00	-	0.00
simazine	0.00	-	0.00
sulfotep	48.26	12.92	6.24
TCA	0.00	-	0.00
tebuconazole	0.00	-	0.00
teflubenzuron	0.00	-	0.00
tefluthrin	77.90	5.78	4.50
temephos	42.46	11.52	4.89
terbufos	51.53	13.34	6.88
terbutryn	18.58	14.18	2.63
terbutylazine	20.06	14.40	2.89
tetrachloorvinphos	9.01	12.45	1.12
tetradifon	7.65	12.56	0.96
thiabendazole	0.00	-	0.00
thifensulfuron-methyl	0.00	-	0.00
thiocyclam hydrogen oxalate	0.00	-	0.00
thiodicarb	37.67	12.57	4.74
thiofanate-methyl	17.36	12.72	2.21
thiofanox	12.67	14.62	1.85
thiometon	34.11	14.09	4.81
thiram	30.16	14.19	4.28
tolclofos-methyl	70.25	10.78	7.58
tolylfluanid	26.54	12.66	3.36
toxaphene	38.69	11.97	4.63
2,4,5-T-propylene glycolbutyl ether ester	0.00	-	0.00
tri-allate	50.79	13.13	6.67
triadimefon	0.00	-	0.00
triadimenol	0.00	-	0.00
triazophos	14.97	13.07	1.96
trichlorfon	0.00	-	0.00
trichloronaat	30.53	12.82	3.91
triclopyr	0.00	-	0.00
tridemorph	43.13	13.27	5.72
triflumizole	0.00	-	0.00
trifluralin	60.91	12.36	7.53
triforine	14.35	11.79	1.69
vinclozolin	18.97	13.45	2.55
warfarin	28.85	13.14	3.79
zineb	10.87	13.60	1.48
ziram	0.93	13.17	0.12

References

Smit, A.A.M.F.R., van den Berg, F., Leistra, M. (1997) Estimation method for the volatilization of pesticides from fallow soil. Report Environmental Planning Bureau Series 2, DLO Winand Staring Centre, Wageningen, the Netherlands.

Thyssen, N., Erlandsen, M. (1987) Reaeration of oxygen in shallow, macrophyte rich streams: II. Relationship between the reaeration rate coefficient and hydraulic properties. Int. Revue. ges. Hydrobiol. 72, 575-597.

1 Parameters necessary to calculate the drop temperature and the ventilation coefficient for water vapour

1.1 Latent heat of evaporation of water

The latent heat of evaporation of water L (J kg^{-1})between –40°C and 40°C (J kg^{-1}) is given by:

$$L = 2.5008\times10^{6}\left(\frac{273.15}{T_w}\right)^{\left(0.167+3.67\times10^{-4}\,T_w\right)} \qquad \text{(F-1)}$$

where T_w is the water temperature (K).

1.2 Diffusivity of water vapour in air

The diffusivity of water vapour in air D_{wa} ($m^2\ s^{-1}$) is given by (Pruppacher and Klett, 1997):

$$D_{wa} = 2.5007\times10^{-5}\left(\frac{T_w}{298.15}\right)^{1.94}\left(\frac{P}{1}\right) \qquad \text{(F-2)}$$

where:
T_w = water temperature (K)
P = pressure (atm)

1.3 Thermal conductivity of air

The thermal conductivity of moist air k_a (J $m^{-1}\ s^{-1}\ K^{-1}$) is almost the same as the thermal conductivity of dry air. The thermal conductivity of dry air (J $m^{-1}\ s^{-1}\ K^{-1}$) is given by (Pruppacher and Klett, 1997):

$$k_a = 2.38228\times10^{-2} + 7.11756\times10^{-5}\,ta \qquad \text{(F-3)}$$

where ta is the air temperature (C).

1.4 Saturation pressure of water vapour

The saturation pressure of water vapour above liquid water p_{sat} (N m^{-2}) between -50°C and 50°C is given by (Pruppacher and Klett, 1997):

$$p_{sat} = a_0 + a_1 tw + a_2 tw^2 + a_3 tw^3 + a_4 tw^4 + a_5 tw^5 + a_6 tw^6 \qquad \text{(F-4)}$$

where:

a_0 = 6.107799961×10^2
a_1 = 4.436518521×10^1
a_2 = 1.428945805
a_3 = $2.650648471 \times 10^{-2}$
a_4 = $3.031240396 \times 10^{-4}$
a_5 = $2.034080948 \times 10^{-6}$
a_6 = $6.136820929 \times 10^{-9}$
tw = water temperature (C)

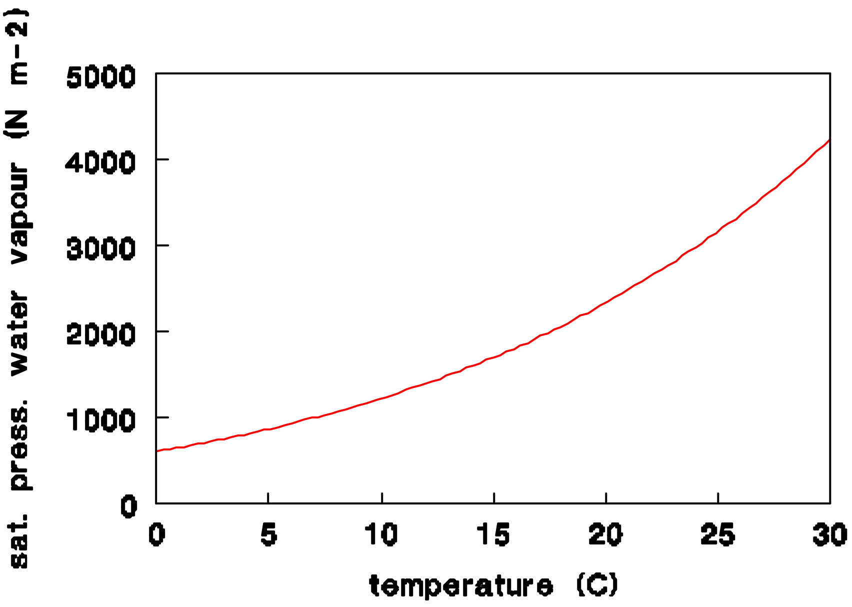

Figure F-1. Saturation pressure of water vapour as a function of temperature.
Figur F-1. Vanddamps mætningstryk som funktion af temperatur.

References

Pruppacher, H.R., Klett, J.D. (1997) Microphysics of clouds and precipitation. Kluwer, Dordrecht, The Netherlands.

1 Documentation of PESTDEP

In this appendix the different processes of the PESTDEP model are described as well as the way they are integrated. For each process the input parameters are given as well as the output parameters. Moreover, it is indicated which equations from this report are used in the calculations. It should be noted here, that the version of the model discussed here is the version that is integrated in the model-based tool for evaluation of exposure and effects of pesticides in surface water being developed by DHI Water & Environment. As this model has to be used by people that are not familiar with atmospheric sciences in the approval procedure for pesticides to describe generalised situations, the number of parameters that can be chosen freely is limited.

In the model the wind direction (x direction) is always perpendicular to the water body (y direction). The deposition is assumed to be the same everywhere in the y direction along the river (in the model the river and the emission field are indefinitely long in this direction). The z direction is the vertical. The wind is always blowing from the emission area to the water body. Although this sounds unrealistic, it is in fact not so unrealistic because there are usually fields on both sides of the water body. Part of the time the wind will be blowing along the water body. This situation is not taken into account. In this way a maximum dry deposition to the water body is calculated.

The model version described here is made for streams and small ponds, not for large water bodies, such as seas.

1.1 Emission

In the input file the indicator indicvol indicates the type of volatilisation calculation that has to be made:

- If indicvol = 1, the accumulated emission after application to crops during 7 days is calculated. In that case the parameters necessary for the calculation of the accumulated emission after application to normal moist fallow soil are read, but not used.
- If indicvol = 2, the accumulated emission after application to normal moist fallow soil during 21 days is calculated. In that case the parameters necessary for the calculation of the accumulated emission after application to crops are read, but not used. If the fraction of the pesticide in the gas phase in the soil is outside the range for which the accumulated emission can be calculated a value of 0 is given (otherwise e.g. negative emissions will be generated).

The length of the emission zone in the x direction (downwind direction, perpendicular to the water body) is needed to calculate the absolute emission for the whole emission zone.

1.1.1 Emission from crops

Input data:

- Dose (kg active ingredient ha^{-1}).
- Vapour pressure at a reference temperature (Pa).
- Reference temperature vapour pressure (K).
- Actual temperature of the crop (K). It is set to the actual air temperature that is read in the input file.

Output data:

- Accumulated emission during 7 days (% of the dose).

The accumulated emission of pesticides during 7 days after application to crops is calculated with equation (1) in the main report. The vapour pressure is calculated for the actual temperature using equation (A-16) in Appendix A and assuming a heat of evaporation of 95000 J mol^{-1}. For some pesticides the parameterisation of the accumulated emission from crops will lead to an emission of more than 100% of the dose. This is of course not correct. In that case the emission is set to 100%. This is not necessarily correct either, but should be used as a first guess and an indication that the accumulated emission is rather large.

1.1.2 Emission from normal moist fallow soil

Input data:

- Dose (kg active ingredient ha^{-1}).
- Henry's law coefficient (c_{gas}/c_{water}) at a reference temperature (dimensionless).
- Reference temperature Henry's law coefficient (K).
- Soil temperature (K).
- Dry bulk density soil (kg solid/m^3 soil).
- Content of organic matter of the soil (%).
- Volumetric moisture content of the soil (%).
- Soil-liquid partitioning coefficient K_d (kg kg^{-1} solid/kg m^{-3} liquid).

Output data:

- Accumulated emission during 21 days (% of the dose).

The accumulated emission of pesticides during 21 days after application to normal moist fallow soil is calculated with equation (2) in the main report. The fraction of the pesticide in the gas phase in the soil needed in this equation is calculated with equations A-1 to A-10 in Appendix A. The Henry's law coefficient at the actual temperature is calculated with equation (A-20) in Appendix A, assuming a heat of dissolution at constant temperature and pressure of –68000 J mol^{-1}. It should be noted that the organic matter content is not used here to calculated the adsorption to the soil, but to find the density of the soil needed to calculate the volume fraction of air in the soil (see Appendix A). The parameterisation of the accumulated emission from normal to moist soil has a maximum of 95.1%.

1.2 Dry deposition

In the model there are 3 zones (see Figure 1):

- Emission zone.
- Non-spray zone.
- Water body.

In an emission zone no dry deposition occurs. In the model the dry deposition velocity in the non-spray zone is set to zero. This is done for two reasons. The first reason is that no information is available on the dry deposition of pesticides to vegetation. The second reason is that in this way the maximum dry deposition to the water body will be estimated.

The flux to the water body is calculated assuming that the concentration of the pesticide in the water body is zero. This is done, because normally the concentration in the water body will be highly variable in time and often been unknown during the emission periods (water bodies are not often sampled). In that way a maximum dry deposition is obtained. The following input and output data are used for the dry deposition velocity:

Input data:

- Friction velocity (m s^{-1}).
- Henry's law coefficient (c_{gas}/c_{water}) at a reference temperature (dimensionless).
- Reference temperature Henry's law coefficient (K).
- Actual temperature of the water body (K).
- Molecular weight pesticide (g mol^{-1}).
- Average depth water body (m).
- Width of the non-spray zone in the x direction (downwind direction).
- Width of the water body in the x direction (downwind direction).
- Length of the water body (y direction, perpendicular to the wind direction) (m)
- Average aeration coefficient (day^{-1}). This coefficient is calculated by DHI Water & Environment using the hydraulic MIKE 11 model that uses the Thyssen and Erlandsen parameterization (equation 25 in the main report).

The laminar boundary layer resistance (for rivers and lakes) is found from equation (11) in the main report.

The surface resistance for rivers is found from equation (14), (21) and (25) in the main report (for rivers) and from equation (14), (27) and (28) in the main report (for lakes). The calculation of K_{2d} with equation (25) in the main report is made by DHI using stream parameters derived with one of their models. In equation (21) and 28 in the main report the diffusivity of the pesticide in water is used, which is calculated from the molecular mass and corrected for the actual water temperature using equations (B-6) and (B-7) in Appendix B.

At last the dry deposition velocity is found from these resistances and equations (5), (6) and (7) in the main report.

Two combinations of surface roughness length (z_{0m}) and friction velocity (u_*) are used:

- For emission from crops: z_{0m} = 0.1 m and u_* = 0.386 m s^{-1}.
- For emission from fallow soil: z_{0m} = 0.01 m and u_* = 0.284 m s^{-1}.

These combinations are chosen in such a way that they give the average wind speed at 60 m height in Denmark. This average wind speed is calculated from the measured average wind speed at Kastrup Airport (near Copenhagen) for the period 1974-1983 at 10 m of 5.4 m s^{-1} using the local surface roughness length of 0.03 m.

The combinations of z_{0m} and u_* mentioned above are also used describe atmospheric diffusion.

Output data (not visible for the user; used as input to calculate the dry deposition):

- Dry deposition velocity (m s^{-1}):

- For streams k_w in equation (21) is derived from the aeration coefficient provided by DHI Water & Environment and equation (30).
- For stagnant water bodies k_w in equation (17) is derived from equations (37) using equations (35) and (36).

1.3 Atmospheric diffusion

Input data:

- Surface roughness length (m)
- Friction velocity (m s^{-1}).

Output data (not visible for the user):

- Wind speed as a function of height (m s^{-1}) calculated with equation (3) in the main report.
- Vertical exchange (eddy diffusivity) (m^2 s^{-1}) calculated with equation (4) in the main report.

For a choice of values for the surface roughness length and the friction velocity see the previous section of this appendix.

1.4 Integration of processes in the PESTDEP model

The PESTDEP model is a two-dimensional steady state K-model, which integrates all above mentioned processes and is based on the following equation (Asman, 1998):

$$u(z)\frac{\partial c_g(x,z)}{\partial z} = \frac{\partial}{\partial z}\left[K_{Heat}(z)\frac{\partial c_g(x,z)}{\partial z}\right] + Q(x,z) - S(x,z) \qquad \text{(G-1)}$$

where:
x = downwind distance (m).

z = height (m).
u(z) = wind speed at height z (m s^{-1}).
$c_g(x,z)$ = concentration of the pesticide in the gas phase (kg m^{-3}).
$K_{Heat}(x,z)$ = eddy diffusivity (m^2 s^{-1}).
Q(x,z) = flux into the atmosphere (kg m^{-1} s^{-1}). This is equal to the emission rate.
S(x,z) = flux out of the atmosphere (kg m^{-1} s^{-1}). This is equal to the dry deposition rate given by equation (13).

1.5 Example of an input file.

Value	Name parameter	Meaning, units and what parameter is used for
bentazon	namecomp	Name compound (40 characters)
5	dose	Dose active ingredient (kg a.i. ha^{-1})
1	indicvol	Indicator volatilisation 1= from crops, 2 = from soil
1	indicdep	Indicator deposition 1=stream, 2=lake
2.e-4	Henrygref	Henry's law coefficient (c_g/c_w) at reference temperature (dimensionless) [volatilisation from soil, surface resistance water]
298.15	TKwHenrygref	Reference temperature Henry's law coefficient (K) [volatilisation from soil, surface resistance water]
1.e-4	Vpref	Vapour pressure at reference temperature (Pa) [volatilisation from crops]
293.15	TKVpref	Reference temperature vapour pressure (K) [volatilisation from crops]
283.15	Tksoil	Actual temperature soil (K) [volatilisation from soil]
1400	denssoil	Dry bulk density of the soil (kg solid/m^3 soil) [volatilisation from soil]
4.7	orgmatproc	Content of organic matter of the soil material (%) [volatilisation from the soil]
20	moistureproc	Volumetric moisture content of the soil (%) [volatilisation from soil]
2.4e-3	Kd	Soil-liquid partitioning coefficient (kg kg^{-1} solid)/(kg m^{-3} liquid) [volatilisation from soil]
293.15	Tka	Actual temperature air (K) [laminar boundary layer resistance]
224.5	molw	Molecular weight (g mol^{-1}) [laminar boundary layer resistance, surface resistance water body]
294.15	TKw	Temperature of the stream (K) [surface resistance water body]
1.2	depthw	Average depth water (m). [surface resistance stream]
4.47	k2_dhi	Average aeration coefficient stream calculated by DHI (day^{-1})

		[surface resistance stream]
100	dxemission	Upwind length of the emission area (m) [concentration in the air]
10	dxns1	Upwind length of the non-spray area before the water body (m) [concentration in the air]
5	dxwater	Upwind length of the water body (m) [concentration in the air]
5000	dywater	Length of the water body perpendicular to the wind direction (m)

References

Asman, W.A.H. (1998) Factors influencing dry deposition of gases with special reference to ammonia. Atmospheric Environment 12, 415-421.